Dynamic interplay between standard and non-standard retinal pathways in the early thalamocortical visual system

Carlos Carvajal

UNIVERSITÉ DE LORRAINE

IAEM Lorraine Graduate School

Dynamic interplay between standard and non-standard retinal pathways in the early thalamocortical visual system: A modeling study

THESIS

submitted and defended publicly on December the 17th, 2014
in partial fulfillment of the requirements for the degree of

Doctor of Science
Specialized in Computer Science

by

Carlos Carvajal

Thesis Committee

Advisor	Dr. Frédéric Alexandre	Inria Bordeaux Sud-Ouest
Co-advisor	Dr. Thierry Viéville	Inria Sophia Antipolis Méditerranée
Reviewers	Dr. Lionel Nowak	CNRS
	Dr. Hélène Paugam-Moisy	Université Lyon 2
Examiners	Dr. Benoît Miramond	Université Cergy-Pontoise
	Dr. Sylvain Contassot-Vivier	Université de Lorraine
	Dr. Adrián Palacios	Universidad de Valparaíso

Inria Bordeaux Sud-Ouest Research Center
Institut of Neurodegenerative Diseases – UMR 5293
Inria Nancy Grand-Est Research Center
Lorraine Research Laboratory in Computer Science and its Applications – UMR 7503

UNIVERSITÉ DE LORRAINE

École Doctorale IAEM Lorraine

Interaction dynamique entre les voies rétiniennes standard et non-standard dans le système visuel thalamocortical précoce : Une étude de modélisation

THÈSE

présentée et soutenue publiquement le 17 Décembre 2014

pour l'obtention du

Doctorat en Sciences

Spécialité Informatique

par

Carlos Carvajal

Comité de thèse

Directeur	Dr. Frédéric Alexandre	Inria Bordeaux Sud-Ouest
Co-directeur	Dr. Thierry Viéville	Inria Sophia Antipolis Méditerranée
Rapporteurs	Dr. Lionel Nowak	CNRS
	Dr. Hélène Paugam-Moisy	Université Lyon 2
Examinateurs	Dr. Benoît Miramond	Université Cergy-Pontoise
	Dr. Sylvain Contassot-Vivier	Université de Lorraine
	Dr. Adrián Palacios	Universidad de Valparaíso

Centre de Recherche Inria Bordeaux Sud-Ouest
Institut des Maladies Neurodégénératives – UMR 5293
Centre de Recherche Inria Nancy Grand-Est
Laboratoire Lorrain de Recherche en Informatique et ses Applications – UMR 7503

"Twenty years from now you will be more disappointed by the things that you didn't do than by the ones you did do. So throw off the bowlines. Sail away from the safe harbor. Catch the trade winds in your sails. Explore. Dream. Discover."

Mark Twain

Acknowledgements

I would like to thank everybody with whom I have shared this PhD experience. Too many names to write them all, but you are all in my heart one way or another.

I would like to start the personal thanks with my advisors, M. Frédéric Alexandre and M. Thierry Viéville, for allowing me to live this PhD experience the way it went professionally, for their guidance, advises, discussions and all the nice moments we shared along the way.

I would also like to thank M. Nicolas Rougier, who at quite a few times was there to share a precise advise, and the people from KEOpS, specially Mme. María-José Escobar, and M. Adrián Palacions, without whom I would have never started working in computational neuroscience, or research.

I thank the reviewers of this manuscript, Mme. Hélène Paugam-Moisy and M. Lionel Nowak, as well as the examiners, M. Benoît Miramond, M. Sylvain Contassot-Vivier and M. Adrián Palacios, for accepting to review my work, and for their constructive feedback.

I cannot forget to thank all the people at Loria, Inria Nancy, IMN and Inria Bordeaux, specially the team assistants of Cortex and Mnemosyne, who had more than one headache dealing with my paperwork... Mme. Laurence Benini, Mme. Anne-Laure Gauthier, M. Nicolas Jahier, and Mme. Chrystel Plumejeau.

I met so many people and lived so many things during these three years... I thank my officemates in Nancy, specially Georgios; the people that allowed me to participate in so many scientific outreach activities when in Bordeaux, particularly Mlle. Lola Kovacic; the people who trusted me with special responsibilities, despite being my initiative to be there, particularly the people in the committee of the center, SO News, and the AFoDIB; the people from the different sportive activities funded by AGOS (and AGOS too): football, foosball and climbing; and all the beautiful people at the Inria Bordeaux Sud-Ouest Research Center for always being so nice to me.

I cannot allow myself not to mention my close friends... Flo, Fred, Arnaud and Anca, Polina, and Marinette. Thanks for being there for me, for trusting me, for sharing trips, musical evenings, secrets, moments of joy and sadness, and the beauty of life in general.

I also thank my family. My mother, Isabel; my father, Carlos; and my "little" brother, Camilo. Despite a great geographical distance separating us at the moment, I know you are there for me.

Abstract

Understanding the behavior of the retino-thalamo-cortico-collicular (i.e. early) visual system in a natural images situation is of utmost importance to understand what further happens in the brain. To understand these behaviors, neuroscientists have looked at the standard Parvocellular and Magnocellular pathways for decades. However, there is also the non-standard Koniocellular pathway, which plays an important modulating role in the local, global, and intermingled processing carried out to achieve such behaviors. Particularly, the standard motion analysis carried out by the Magno pathway is alternated with rapid reactions, like fleeing or approaching to specific motions, which are hard-wired in the Konio pathway. In addition, studying a fixation task in a real situation, e.g., when a predator slowly approaches its prey, not only involves a motion mechanism, but also requires the use of the Parvo pathway, analyzing, at least, the image contrast. Here, we study in a bio-inspired computational neural model how these pathways can be modeled with a minimal set of parameters, in order to provide robust numerical results when doing a real task. This model is based upon an important study to integrate biological elements about the architecture of the circuits, the time constants and the operating characteristics of the different neurons. Our results show that our model, despite operating via local computations, globally shows a good network behavior in terms of space and time, and allows to analyze and propose interpretations to the interplay between thalamus and cortex. At a more macroscopic scale, the behaviors emerging from the model are reproducible and can be qualitatively compared to human-made fixation measurements. This is also true when using natural images, where just a few parameters are slightly modified, keeping the qualitatively human-like results. Robustness results show that the precise values of the parameters are not critical, but their order of magnitude matters. Numerical instability occurs only after a 100% variation of a parameter. We thus can conclude that such a reduced systemic approach is able to represent attentional shifts using natural images, while also being algorithmically robust. This study gives us as well a possible interpretation about the role of the Konio pathway, while at the same time allowing us to participate in the debate between low and high-roads in the attentional and emotional streams. Nevertheless, other information, such as color, is also present in the early visual system, and should be addressed together with more complex cortical mechanisms in a sequel of this work.

Keywords: Early visual system, Behavior, Neural modeling, Thalamocortical pathways, Computational Neuroscience, Visual attention.

Résumé

Comprendre le comportement du système visuel rétino-thalamo-cortico-colliculaire (i.e. précoce) dans une situation d'images naturelles est d'une importance capitale pour comprendre ce qui se passe ensuite dans le cerveau. Pour comprendre ces comportements, les neurobiologistes ont étudié les voies standard, Parvocellulaires et Magnocellulaires, depuis des décennies. Cependant, il y a aussi la voie non-standard, ou Koniocellulaire, qui joue un rôle modulateur important dans les traitements local, global, et entremêlé, pour atteindre de tels comportements. Particulièrement, l'analyse standard du mouvement réalisée par la voie Magno est alternée avec des réactions rapides, comme la fuite ou l'approche à des mouvements spécifiques, qui sont pré-câblés dans la voie Konio. De plus, l'étude d'une tâche de fixation dans une situation réelle, par exemple quand un prédateur s'approche lentement de sa proie, implique non seulement un mécanisme de mouvement, mais nécessite également l'utilisation de la voie Parvo, qui analyse, au moins, le contraste de l'image. Ici, nous étudions dans un modèle neuronal de calcul bio-inspiré comment ces voies peuvent être modélisées avec un ensemble minimal de paramètres, afin de fournir des résultats numériques robustes lors d'une tâche réelle. Ce modèle repose sur une étude approfondie pour intégrer des éléments biologiques dans l'architecture des circuits, les constantes de temps et les caractéristiques de fonctionnement des neurones. Nos résultats montrent que notre modèle, bien que fonctionnant via des calculs locaux, montre globalement un bon comportement de réseau en termes d'espace et de temps, et permet d'analyser et de proposer des interprétations de l'interaction entre le thalamus et le cortex. À une échelle plus macroscopique, les comportements du modèle sont reproductibles et peuvent être qualitativement comparés à des mesures de fixation oculaire chez l'homme. Cela est également vrai lorsque l'on utilise des images naturelles, où quelques paramètres sont légèrement modifiés, en gardant des résultats qualitativement humains. Les résultats de robustesse montrent que les valeurs précises des paramètres ne sont pas critiques, mais leur ordre de grandeur l'est. Une instabilité numérique ne se produit qu'après une variation de 100% d'un paramètre. Nous pouvons donc conclure que cette approche systémique est capable de représenter les changements de l'attention en utilisant des images naturelles, tout en étant algorithmiquement robuste. Cette étude nous donne ainsi une interprétation possible sur le rôle de la voie Konio, tandis qu'en même temps elle nous permet de participer au débat sur les low et high-roads des flux attentionnel et émotionnel. Néanmoins, d'autres informations, comme la couleur, sont également présentes dans le système visuel précoce, et pourraient être prises en considération, ainsi que des mécanismes corticaux plus complexes, dans les perspectives de ce travail.

Mots clés : Système visuel précoce, Comportement, Modélisation neuronale, Voies thalamocorticales, Neuroscience computationnelle, Attention visuelle.

Symbols

BG	Basal Ganglia
DANA	Distributed Asynchronous Numerical and Adaptive computing framework
DoG	Difference of Gaussians
DNF	Dynamic Neural Field
dSC	Deep Superior Colliculus
FEF	Frontal Eye Field
GC	Ganglion Cell
IF	Integrate and Fire
IT	Inferior Temporal Cortex
LGN	Lateral Geniculate Nucleus
LIP	Lateral Intraparietal Cortex
MST	Medial Superior Temporal Area
Pdm	Dorsomedial Pulvinar
PI	Inferior Pulvinar
PL	Lateral Pulvinar
RF	Receptive Field
SC	Superior Colliculus
sSC	Superficial Superior Colliculus
SVM	Support Vector Machine
TRN	Thalamic Reticular Nucleus
V1	Primary Visual Cortex

Contents

Acknowledgements i

Abstract iii

Résumé v

Symbols vii

Contents ix

List of Figures xiv

List of Tables xvi

Introduction xviii

Introduction (Français) xxi

1 Neuroscience of the early visual system of primates 1

1.1 Introduction: Overview of the early visual system 3

1.2 The retina: The smart front-end 5

1.2.1 The notion of receptive field . . . 9
1.2.2 Standard ganglion cells . . . 11
1.2.3 Non-standard ganglion cells . . . 11
1.2.4 Projections of ganglion cells: The birth of visual pathways . . . 13
1.3 The cortex: The adaptable mainframe . . . 15
1.4 The thalamus: The collaborative harmonizer . . . 20
1.4.1 Properties of thalamic structures . . . 24
1.4.2 The complex relay: the lateral geniculate nucleus . . . 26
1.4.3 Konio pathway and its projections . . . 27
1.4.4 The inhibition center: the thalamic reticular nucleus . . . 29
1.4.5 The higher-order thalamic nucleus: briefing of the pulvinar . . . 29
1.5 The superior colliculus: The early sensory-motor hookup . . . 30
1.6 The amygdala: The mnesic and emotional muscle . . . 31
1.6.1 A few facts about the amygdala . . . 31
1.6.2 Amygdala and perception: attention and (un)awareness . . . 31
1.7 Temporal aspects of the early visual system . . . 33
1.8 Summary: A circuit of loops and interacting flows . . . 34

2 Bio-inspired dynamical systems and algorithms 38
2.1 Implementing populations of neurons: the notion of minimal model . . . 41
2.1.1 Spike vs rate models: why we have made the standard choice . . . 41
2.1.2 Driver/Modulator considerations . . . 46
2.1.3 Specification and validation of parameter values . . . 50
2.1.4 Filters and information processing . . . 51
2.1.5 Dynamic Neural Fields . . . 53
2.2 Functional view of the neural system: the systemic level . . . 54
2.2.1 Functional interpretation of retinal mechanisms: non-local filtering . 54
2.2.2 Functional interpretation of retinal mechanisms: visual event detection 56
2.2.3 Functional interpretation of thalamic mechanisms . . . 59
2.2.4 Assembling populations into networks . . . 60
2.2.5 Implementation details . . . 62
2.3 Conclusion . . . 64

3 Implementing a non-standard early visual system **67**
3.1 Summary of previous sections . . . 69
3.1.1 Architecture of the system . . . 69
3.1.2 Dynamics of the system . . . 70
3.2 Our model of the early visual system: modular view . . . 71
3.2.1 Retina: Standard and non-standard cells . . . 73
3.2.2 Thalamus . . . 75
3.2.3 Primary visual cortex . . . 79
3.2.4 Superior colliculus . . . 79
3.2.5 Summary . . . 82

4 Our minimal model in the real world: Experimental results **84**
4.1 First experimental result: using artificial images . . . 87
4.1.1 Discrimination, selection and tracking . . . 89
4.1.2 Numerical Robustness . . . 89
4.2 Original experimental result: using natural images (M+K) . . . 95
4.2.1 Discrimination, selection and tracking . . . 97
4.2.2 Numerical robustness . . . 102
4.3 Experimental result: using natural images (P+M+K) . . . 104
4.4 About observed emerging properties . . . 116
4.5 Open-access software . . . 116

5 Conclusion **118**

6 Conclusion (Français) **123**

Appendix **128**

Bibliography **135**

List of Figures

1.1 Gross architecture of the early visual system 4
1.2 Diversity of neurons in the retina 6
1.3 The road in the retina 7
1.4 Circuitry in the retina 8
1.5 Receptive fields with irregular shapes 10
1.6 Dendritic morphology of macaque ganglion cells 12
1.7 Different retinal projections 14
1.8 Simplified cortical column 16
1.9 Integration of information through thalamocortical and corticocortical interactions 21
1.10 Overview of thalamic nuclei 22
1.11 Thalamocortical connections and how TRN is involved 23
1.12 Schematic diagram of circuitry for the lateral geniculate nucleus 28
1.13 Cortical and subcortical visual and emotional pathways 32

3.1 Model diagram 72

4.1 Sample of artificial stimuli used 88
4.2 Simulation results for "d" 90
4.3 Simulation results for "Se" 91
4.4 Simulation results for "d" with variations of a_9 92
4.5 Simulation results for "d" with variations of g_9 93
4.6 Simulation results for "d" with variations of $\mathcal{K}$ 94
4.7 Simulation results for "d" with variations of τ_{11} 95
4.8 Sample of naturalistic stimuli used 96

4.9 Overview of results with natural stimuli 98
4.10 Retinal detection (standard) 99
4.11 Retinal detection (non-standard) 100
4.12 TRN and mismatch in action 101
4.13 Simulation results for all three systems with natural images 103
4.14 Variation of the simulation results for g_9 105
4.15 Variation of the simulation results for $\mathcal{Z}$ 106
4.16 Variation of the simulation results for $\mathcal{K}$ 107
4.17 Overview of results with natural stimuli in the P+M+K system 109
4.18 Parasol cells detect motion 110
4.19 Appearance of the fearful stimulus 110
4.20 Focus switch occurs 111
4.21 Parvo and Magno convergence 111
4.22 Parasol cells detect motion, but do not transmit it to LGN 113
4.23 Appearance of the fearful stimulus 113
4.24 Focus switch occurs cortically, but it is not yet reflected collicularly 114
4.25 Convergence of the lesioned system 114
4.26 Simulation results for the P+M+K systems 115

6.1 Overview of simulation using Eli P-jump 130
6.2 Overview of simulation using the video of a puppy dog 131
6.3 Overview of simulation using the video of Signature 132

List of Tables

1.1 Anatomical circuitry and functions of V1 connections 17
1.2 Summary of anatomical circuitry of early thalamocortical loops of mammals 19
1.3 Neural dynamics in the visual system 35

2.1 Forward/Backward connections connections main properties, from [54]. Post-synaptic/modulatory effect is a conjecture, so is assumptions on synapses mechanisms. 48
2.2 Notations used in the different equations 65

3.1 Handpicked values for the computations on Core Thalamus 76
3.2 Handpicked values for the computations on TRN 78
3.3 Handpicked values for the computations on the integrative cortex 80
3.4 Handpicked values for the computations on layer 2a of the superior colliculus 80
3.5 Handpicked values for the computations on layer 2b of the superior colliculus 81
3.6 Handpicked values for the computations on the deep superior colliculus . . 82

4.2 Variations from Magno to Parvo values 108
4.1 Numerical Robustness for parameters used with natural stimuli 117

Introduction

"The beginning is the most important part of the work"
– Plato

Understanding how the brain works is arguably one of the greatest scientific challenges nowadays. There are two particularly massive initiatives trying to approach the challenge: one is the Human Brain Project[1], in Europe; and the other is the BRAIN Initiative, in the US[2]. However, this huge challenge is also attacked by many research labs, beyond such very mediatic consortium, as our team.

Among the processing carried out by the brain, more than a quarter of it is dedicated to vision [174]. And despite decades of research, the mystery of vision [107] remains partially unsolved. One possibility is that the difficulty to understand what happens in the brain is a result of our lack of understanding of the earlier visual stages. This includes what the brain receives, and *how* it is encoded, but also *why* (in terms of functionality) such information has been developed along evolution.

The key point is that, through several studies, researchers have assumed that the retina (in the eye) was practically a simple transducer, while the thalamus (between the eye and the cortex) served as a simple relay of information towards the neocortex. Thus, under these assumptions, almost every task should be accomplished by the cortex, from a processing point of view. However, as scientists have explored these areas, they have found that there is much, much more than previously thought. For example, sophisticated processing such as detection of complex patterns (including motion and color) is already found in the retina. In a coarse way, it provides enough information to guide actions [62]. This (e.g. rapid detection of snakes in the pulvinar [176]), together with multi-modal synchronization

[1] `https://www.humanbrainproject.eu/`
[2] `http://www.braininitiative.nih.gov/`

and regulation of information –among others–, has also been shown for the thalamus [149].

We also have the practical issue of technology: we cannot measure with a higher resolution than that provided by the state of the art equipment. We thus can observe *in vivo* behavior of one neuron or a sub-population of neurons, in detail, thanks to electrode arrays, or mesoscopic or macroscopic aspects of the brain activity at rather higher spatial scale but low temporal precision (e.g., fMRI or optical imaging) or low spatial scale and high temporal resolution (e.g., E.E.G. or M.E.G.). Fortunately, when looking at it from a functional, global perspective, today we can already infer new things that can be tested at more detailed levels, using numerical experiments. With methods related to those used by engineers to design new airplanes, we are now able to simulate some aspects of the central nervous system behavior, and derive some new findings from such experimentation.

This key point is our motivation to investigate further how the early visual system works, how the neurons code information at the scale of neural maps and raise assumptions about how the brain may process such information. We will carefully explain how minimal models are to be worked out in such a paradigm. This does not negate the huge processing power of the different cortical areas. We simply support the trend of showing that certain aspects of this processing are to be made explicit and studied. We also consider that the visual system is really a distributed processing system as far as analyzing the information captured from the visual world is concerned.

This work has been realized under the Franco-Chilean project KEOpS. The goal of the project is to study and model the early visual system, focusing on the non-standard behavior of retinal ganglion cells in natural scenarios. The retina is the first stage in the visual system, and understanding it better is expected to provide more knowledge to understand the following stages of the visual system, and eventually the brain, since they rely not only on "image input", but also on the processing carried out in the visual front-end to the different information flows.

This thesis also contributes to one application of KEOpS, i.e., to incorporate the resulting models into real engineering applications as new dynamic early-visual modules able to process natural image sequences.

Here, standard and non-standard retinal flows are combined, from the retina to the primary visual cortex, including thalamic and collicular structures. The idea is to close the early visual system loop, with a special focus on attentional mechanism. This beautiful mess is analyzed, modeled locally, but always having the systemic view in mind: complex properties are not to be hardwired in the system, but shall instead emerge from the different

interactions between structures and connections.

Since we develop minimal models, but without loss of generality, the amount of parameters, and the mechanisms used to represent the real-world circuits, are simplified and increased in complexity or amount only if really needed. This approach allows us to provide a relatively straightforward tool to analyze the early visual system, where the results qualitatively reproduce human behavior while using sequences of natural images, and at the same time provides robust, stable and easily modifiable modules for each structure involved.

This is, in a nutshell, the work presented in detail in the following sections of this thesis.

Introduction

"Le début est la partie la plus importante du travail"
– Platon

Comprendre comment fonctionne le cerveau est sans doute l'un des plus grands défis scientifiques de nos jours. Il y a deux initiatives particulièrement massives qui tentent d'aborder le défi : l'un est le Human Brain Project[3], en Europe; et l'autre est l'initiative BRAIN, aux États-Unis[4]. Toutefois, ce défi est aussi attaqué par de nombreux laboratoires de recherche, au-delà de ce consortium très médiatique, comme notre équipe.

Parmi les traitements effectués par le cerveau, plus d'un quart d'entre eux est dédié à la vision [174]. Et malgré des décennies de recherche, le mystère de la vision [107] ne reste que partiellement résolu. Une possibilité est que la difficulté à comprendre ce qui se passe dans le cerveau soit le résultat de notre manque de compréhension des étapes visuelles précoces. Cela comprend ce que le cerveau reçoit, et *comment* cette information est codée, mais aussi *pourquoi* (en termes de fonctionnalité) de telles informations ont été développées au cours de l'évolution.

Le point clé est que, à travers plusieurs études, les chercheurs ont considéré la rétine (dans l'oeil) pratiquement comme un transducteur simple, tandis que le thalamus (entre l'oeil et le cortex) comme un simple relais de l'information vers le néocortex. Ainsi, sous ces hypothèses, presque chaque tâche doit être accomplie par le cortex, du point de vue du traitement. Cependant, plus les scientifiques ont exploré ces zones, plus ils ont trouvé qu'il y avait beaucoup, beaucoup plus qu'on ne le pensait. Par exemple, des traitements sophistiqués tels que la détection de motifs complexes (y compris le mouvement et la couleur) sont déjà présents dans la rétine. D'une manière grossière, la rétine fournit suffisamment

[3] `https://www.humanbrainproject.eu/`
[4] `http://www.braininitiative.nih.gov/`

d'informations pour guider des actions [62]. Aussi, le thalamus a été montré capable de réguler les flux d'information que le traversent, ainsi que de synchroniser différentes modalités (audition et vision, par exemple) [149]. Un autre example est pour le thalamus et la détection rapide des serpents dans le pulvinar [176].

Nous avons aussi la question pratique de la technologie : nous ne pouvons pas mesurer avec une résolution supérieure à celle prévue par l'équipement de pointe. Nous pouvons ainsi observer le comportement *in vivo* d'un neurone ou d'une sous-population de neurones, en détail, grâce aux matrices d'électrodes, ou des aspects mésoscopiques ou macroscopiques de l'activité cérébrale à des échelles spatiales plus élevées, mais avec une faible précision temporelle (par exemple, avec les IRMf ou l'imagerie optique) ou une faible échelle spatiale et une haute résolution temporelle (par exemple, avec EEG ou MEG). Heureusement, quand on regarde les choses d'un point de vue global, fonctionnel, aujourd'hui, nous pouvons déjà déduire de nouvelles choses qui peuvent être testées à des niveaux plus détaillés, par des expériences numériques. Avec des méthodes liées à celles utilisées par les ingénieurs pour concevoir de nouveaux avions, nous sommes maintenant en mesure de simuler certains aspects du comportement du système nerveux central, et de dériver, de ces expérimentations, de nouvelles conclusions.

Ce point clé est notre motivation pour étudier plus loin comment fonctionne le système visuel précoce, comment les neurones codent les informations à l'échelle des cartes neurales, et pour proposer des hypothèses sur la façon dont le cerveau peut traiter de telles informations. Nous allons expliquer soigneusement comment les modèles minimaux doivent être travaillés dans un tel paradigme. Cela ne remet pas en cause l'énorme puissance de traitement des différentes aires corticales. Nous tentons simplement de montrer que certains aspects de ce traitement doivent être rendus explicites et étudiés. Nous considérons également que le système visuel est vraiment un système de traitement distribué dès que l'analyse de l'information recueillie à partir du monde visuel est concerné.

Ce travail a été réalisé dans le cadre du projet Franco-Chilien KEOpS. Le but du projet est d'étudier et de modéliser le système visuel précoce, mettant l'accent sur le comportement non-standard des cellules ganglionnaires de la rétine dans des scénarios naturels. La rétine est la première étape dans le système visuel, et mieux la comprendre devrait fournir plus de connaissances pour comprendre les étapes suivantes du système visuel, et, éventuellement, du cerveau, car ces étapes reposent non seulement sur l'image d'entrée, mais également sur le traitement effectué sur les différentes flux d'information dans les différentes structures.

Cette thèse contribue également à une application de KEOpS, c'est-à-dire, à intégrer les modèles qui en résultent dans de réelles applications d'ingénierie en tant que de nouveaux modules dynamiques de vision précoce, capables de traiter des séquences d'images naturelles.

Ici, les flux rétiniens standard et non-standard sont combinés, de la rétine au cortex visuel primaire, y compris des structures thalamiques et colliculaires. L'idée est de fermer la boucle du système visuel précoce, avec un accent particulier sur le mécanisme d'attention. Ce système est analysée et modélisée localement, mais en gardant toujours la vue systémique à l'esprit : les propriétés complexes ne doivent pas être câblées dans le système, mais doivent à la place émerger des différentes interactions entre les structures et les connexions.

Puisque nous développons des modèles minimaux, mais sans perte de généralité, la quantité de paramètres, et les mécanismes utilisés pour représenter les circuits du monde réel, sont simplifiés et augmentés en complexité ou en montant seulement si c'est vraiment nécessaire. Cette approche nous permet de fournir un outil relativement simple –peu de paramètres et très facile à adapter– pour analyser le système visuel précoce, où les résultats reproduisent qualitativement le comportement humain lors de l'utilisation de séquences d'images naturelles, et en même temps fournit des modules robustes, stables et facilement modifiables pour chaque structure impliquée.

C'est, en un mot, le travail présenté en détail dans les sections suivantes de cette thèse.

Chapter 1

Neuroscience of the early visual system of primates

Contents

1.1 Introduction: Overview of the early visual system 3

1.2 The retina: The smart front-end 5

1.2.1 The notion of receptive field 9

1.2.2 Standard ganglion cells 11

1.2.3 Non-standard ganglion cells 11

1.2.4 Projections of ganglion cells: The birth of visual pathways 13

1.3 The cortex: The adaptable mainframe 15

1.4 The thalamus: The collaborative harmonizer 20

1.4.1 Properties of thalamic structures 24

1.4.2 The complex relay: the lateral geniculate nucleus 26

1.4.3 Konio pathway and its projections 27

1.4.4 The inhibition center: the thalamic reticular nucleus 29

1.4.5 The higher-order thalamic nucleus: briefing of the pulvinar 29

1.5 The superior colliculus: The early sensory-motor hookup . . . 30

1.6 The amygdala: The mnesic and emotional muscle 31

1.6.1 A few facts about the amygdala 31

1.6.2 Amygdala and perception: attention and (un)awareness 31

1.7 Temporal aspects of the early visual system 33

1.8 Summary: A circuit of loops and interacting flows 34

Summary

New findings regarding the study of the retina and thalamus, due to increasingly more interest to these structures, have led scientists to review their viewpoint in terms of the functionality of these subcortical structures. One keypoint is that processing usually attributed to the cortex has been in fact also made explicit -in a new but fast form- in these early vision structures. The retina, on the one hand, providing the visual input for the rest of the system, was considered mainly a transductor. However, some processing, such as looming motion detection, has been found to be part of the mechanisms this two-layer structure carries out as a visual front-end. The thalamus, on the other hand, was classically regarded as a simple relay of feedforward information, but there is much more to add to the story. For example, the thalamus receives neither only visual information, nor solely feedforward information from early visual regions, but also information from other modalities (e.g. audition), and feedback information from many cortical areas. In addition, the thalamus boasts inhibitory mechanisms, allowing to regulate, and thus harmonize multi-modal information based on several sources, making it a quite collaborative ensemble.

The goal of this chapter is to gather and present information about the early visual system to establish a ground-base knowledge for further reading of this document, while at the same time teasing the reader on the importance and interest that started this work.

Keywords: Early visual system, Visual pathway, Thalamocortical loops, Neuroscience.

Organization of this chapter:

After a brief introduction of the early visual system, with basic definitions and ideas, its different components are reviewed: the retina, the cortex, the thalamus and the superior colliculus. In addition, we very briefly discuss the amygdala, as understanding further visual processing is crucial for the systemic approach we used to conceive the original work here presented. The chapter is then finished by refreshing and reinforcing the idea that the beautiful mess we here study is a circuit of various loops, where different interacting information flows are the actors, and that these actors work at different time scales, but despite all this, it allows us to marvel at the beauty of the visual world.

1.1 Introduction: Overview of the early visual system

The brain is an amazingly resourceful and complex entity. Arguably, the most demanding sense –in terms of processing in the cortex of primates– is vision. However, vision starts way before the cortex, in what is called the early visual system.

The early visual system has been previously studied sequentially towards the cortex, but nowadays we know that a series of loops and interacting information flows exist prior to the processing carried out by the cortex.

The early visual system, in simple words, is the ensemble formed by the retina (in the eye), the lateral geniculate nucleus and the thalamic reticular nucleus (in the thalamus), the superficial and deep superior colliculus (in the midbrain), and the primary visual cortex. In addition, as if having quite a few structures was not enough, we should consider that all these different structures hold different types of neurons, with different processing capabilities and timing... Here the conclusion is that there is a quite complex system before the cortex, a beautiful mess, called the early visual system, and that in order to understand what information is fed to the brain, one must embark on the adventure and sail the complex ocean of studying it. Here, many scientists have observed what are now called the "standard" information flows, but there is much more to discover when hoisting the sails to explore the "non-standard" information flows.

In order to provide a deeper understanding of how the early visual system works the way it does, other regions, such as other cortical areas, the pulvinar and the amygdala, are also going to be briefly reviewed in this chapter.

The circuitry/architecture of the early visual system is presented in Figure 1.1. Light penetrates our eyes and is transduced by the retina into a train of spikes after being further processed within the retina. These electric signals are then rearranged at the optic chiasm[1] and sent towards further structures. These neuronal structures are mainly the lateral geniculate nucleus (LGN), in the thalamus; and the superior colliculus, in the midbrain. Through LGN, information gets to the primary visual cortex, involving thalamo-cortical loops. Feedforward information is sent to the cortex, and feedback information is sent back to the thalamus by cortical areas. These loops are regulated by a structure called the thalamic reticular nucleus (TRN), which is not present in Figure 1.1. Through the superior colliculus, information arrives to the pulvinar (another structure in the thalamus)

[1] This rearrangement consists in combining the left and right visual fields, or hemifields, of each eye into separated both-left and both-right streams.

and then to the amygdala. The pulvinar also receives and sends information to and from cortical areas, in thalamocortical loops similar to those of LGN, also regulated by TRN.

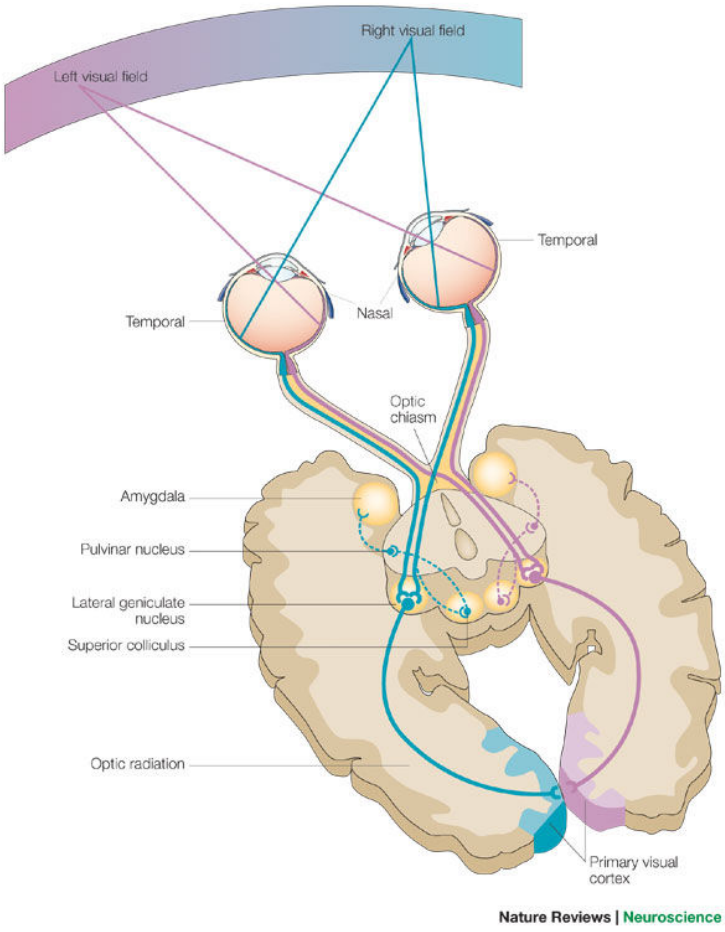

Figure 1.1: Gross architecture of the early visual system. Image taken from [69], itself adapted, with permission from [59].

All these are the primary structures to what is called "vision for behavior", which consists not only in regular visual processing for "perceiving", but also provides the capabilities to act with the environment in close relation to our body, our needs, and our emotions. Or simply said, to properly behave.

In a classical viewpoint, vision architecture is based on the two-streams hypothesis [63]. This hypothesis argues that humans possess two visual systems: the "what" and

the "where/how" pathways, fed by the Parvo and Magno layers of LGN respectively, that themselves receive information from midget and parasol ganglion cells in the retina. The non-standard Konio pathway has been explored more recently, and acts as a modulating stream along the whole early visual system and beyond, thanks to widespread connections to various cortical areas.

Let us describe these structures in more detail.

1.2 The retina: The smart front-end

The retina [45] is the first non-optical stage of the mammalian visual system. It is non-optical in the sense that it is different from the cornea and other parts of the eye, because it transduces light, i.e., converts it into electrical signals.

The mammalian retina is a small tissue located in the back of the eye (Figure 1.3), and is described as a two layered circuit composed by over 50 anatomically different types of cells [105][106](Figure 1.2). These cells are grouped in five categories: the photoreceptors, the bipolar cells, the horizontal cells, the amacrine cells, and the ganglion cells. A connection between neurons is called a synapse, and the connectivity between these different neurons can be seen in Figure 1.4, where colored dots represent excitatory (black) or inhibitory (white) chemical synapses, while electrical synapses (gap-junctions) are represented by those spring-looking symbols, which depict resistors.

Before going deeper in understanding these neurons, one must be reminded a few concepts. We call the retina a two-layered structure (cf. Figure 1.4) for all what happens 1) from photoreceptors to bipolar cells, and 2) from bipolar to ganglion cells. There is a special place in the retina called the fovea, which covers about 3 degrees, and contains the neurons that give us the most detailed view we can have of the visual field (the human visual field is approximately 160 degrees horizontally and 135 degrees vertically). One should as well consider that humans have a blind spot, which is basically the retinal surface where the retinal "output-wire", called the optic nerve, is created, gathering the information of our ganglion cells. We do not notice this blind spot, nor the lesser-quality details outside the fovea, because our eyes move really fast all the time, and also because our brain is able to reconstruct the scene from all these samples, filling gaps when necessary, interpolating, replacing information to make sense of the visual world. And now, let us analyze in more depth the different retinal neurons.

Photoreceptors, as their name suggests, capture photons in the light beam, and com-

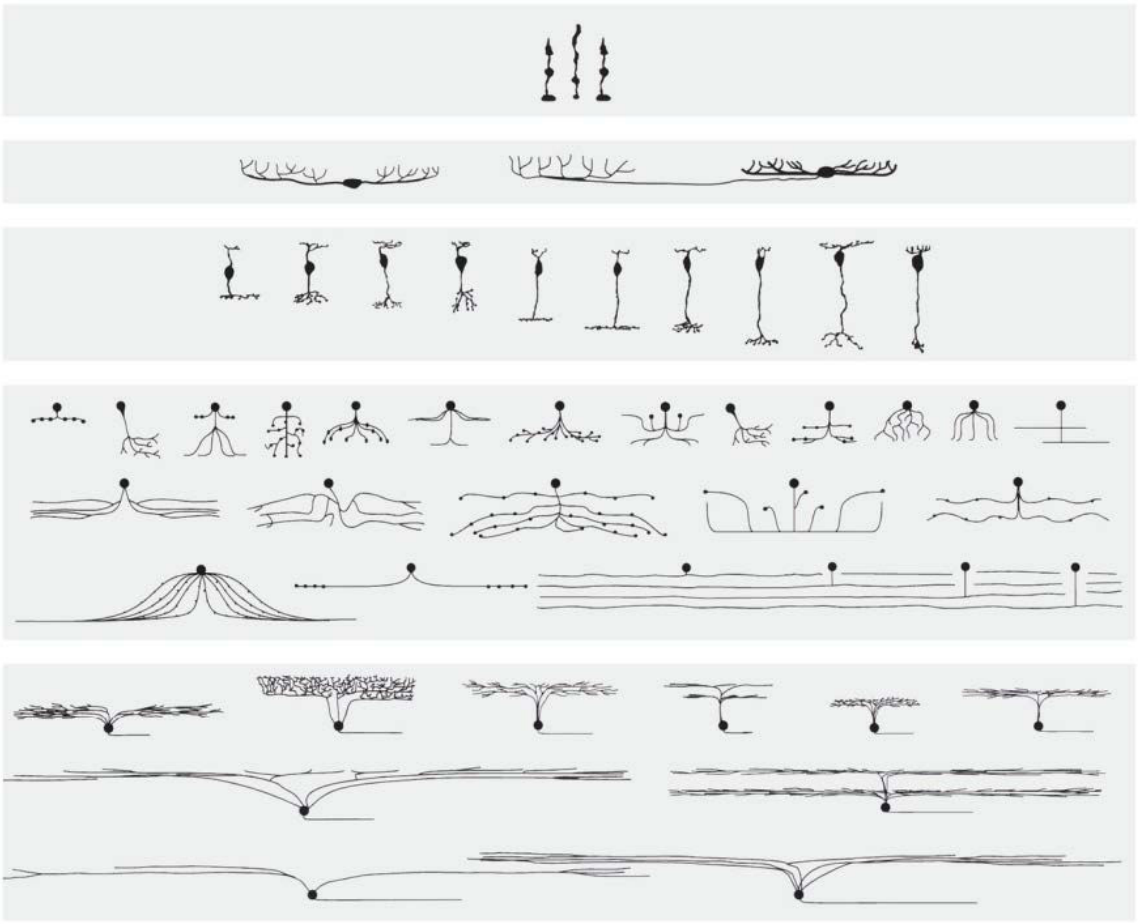

Figure 1.2: Diversity of neurons in the retina. From top to bottom: photoreceptors, horizontal cells, bipolar cells, amacrin cells and ganglion cells. For all these classes, certain types can be identified depending on their morphology and dendritic organization. Image taken from [106].

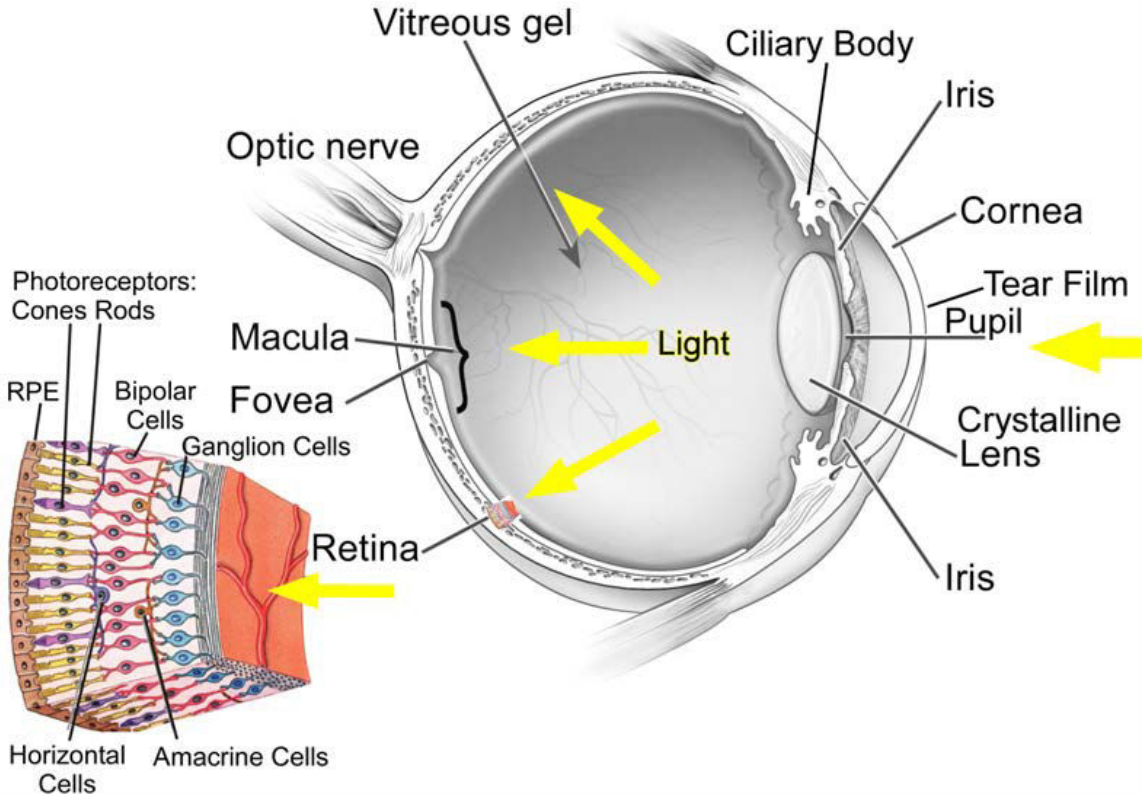

Figure 1.3: The road in the retina. Light enters the eye through the cornea –the transparent cover of our eyes–, to then pass through a chamber full of fluid (called the aqueous humour), in order to reach the iris, which regulates the amount of light that passes through the pupil, the black "spot" on our eyes. Then, the light rays passing through the pupil reach the lens, which turns them upside down and, through another liquid chamber, called the vitreous humour, focuses them into the retina, which is the thin bowl-shaped tissue in the back of the eyeball. Image taken from [56], itself modified from the National Eye Institute, National Institutes of Health.

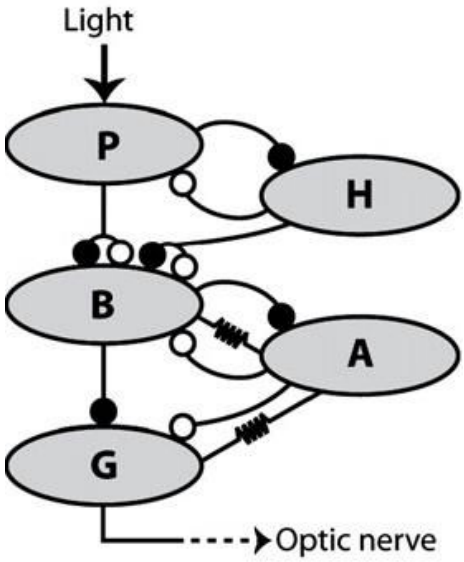

Figure 1.4: Circuitry in the retina, where P = photoreceptors, H = horizontal cells, B = bipolar cells, A = amacrine cells, and G = ganglion cells. The neurons in the retina are connected through chemical synapses that are either sign preserving (excitatory, closed circles) or sign inverting (inhibitory, open circles). In addition, one finds a considerable amount of electrical coupling between cells via gap junctions within all cell classes and across some types of cells (marked by resistor symbols). The input into the network is incident light, which hyperpolarizes the photoreceptors. The connections from photoreceptors to bipolar cells are of either sign, producing both OFF-type and ON-type bipolars. Horizontal cells provide negative feedback and lateral inhibition to photoreceptors and bipolar cells. Bipolar cells are reciprocally connected to amacrine cells with chemical synapses and, for some types, through electrical gap junctions. Ganglion cells represent the output layer of the retina; their axons form the optic nerve. They collect excitation from bipolar cells and mostly inhibition from amacrine cells. In addition, ganglion cells and amacrine cells can be electrically coupled. This general connectivity sets the framework for any specific retinal microcircuit. Image and caption taken from [62].

municate their information to horizontal and bipolar cells. There are two types of photoreceptors: rods and cones. Rods are sensitive to not-so-intense (dim) light in the visual field, and are more numerous as we go away from the fovea, where they are practically non-existent [118]. This makes them really useful in peripheral vision, and as they are more sensitive than cones, our night-vision comes almost completely from rods. Cones, on the other hand, are sensitive to relatively bright light and are most numerous in the fovea, where they are densely packed [118]. They are also really useful to us as they are sensitive to color, but as their numbers diminish as we go further away from the fovea, they are mainly central vision neurons, thus giving central vision the exclusivity of color. Again, we do not notice this because our eyes move really fast all the time, and because the brain reconstructs the visual space from all these samples, filling the gaps when necessary.

Horizontal cells are laterally interconnecting neurons that communicate with photoreceptors and bipolar cells. We owe them the capacity to see properly in environments with bright and dim light, as they integrate and regulate the input from the photoreceptors.

Bipolar cells are versatile cells. Their location is one of the keys to proper retinal function, as they connect with all 4 other types of cells. However, the communication with ganglion cells is only feedforward, i.e., it only outputs to ganglion cells, never receiving any input from them directly. Nevertheless, it could receive information from ganglion cells indirectly, i.e., coming from amacrine cells that communicate with ganglion cells via gap-junctions, which are electrical synapses.

Amacrine cells basically regulate bipolar cells, but they are also the main input to ganglion cells. This is evident when realizing bipolar cells are responsible for about 30% of the input ganglion cells receive, whereas amacrine cells account for the other 70%.

Ganglion cells are the output of the retina. They integrate information from bipolar and amacrine cells, and transmit this integrated information to several structures, such as the superior colliculus or the lateral geniculate nucleus [123]. This communication is one-way, i.e., there are no feedback connections towards the retina, thus making it a fully peripheral structure. Due to their importance –they have the central role in integration of information–, we will analyze them thoroughly in the next sections, but first we need to define receptive fields and their role in information integration.

1.2.1 The notion of receptive field

When we look at the retinal circuit, and how it maps the visual field, one needs to understand the notion of receptive field. The receptive field (RF) of a neuron is simply the region

of visual space that will be mapped by such neuron. As stated before, the retinal output –result of a series of integrations across the different cell types– is ultimately generated by the ganglion cells, thus usually one will speak of the receptive field of a ganglion cell when referring to a retinal receptive field. Classically, RFs were considered circular, and eventually ellipsoidal. Today, this approximation is still used for the geometric simplicity it implies. However, real RFs vary substantially from this description [58]. In fact, they have a fine structure and irregular contours that differ from cell to cell, where neighbors complement each other, as it would happen in a puzzle, meaning that the cell population is spatially coordinated (Figure 1.5) [58].

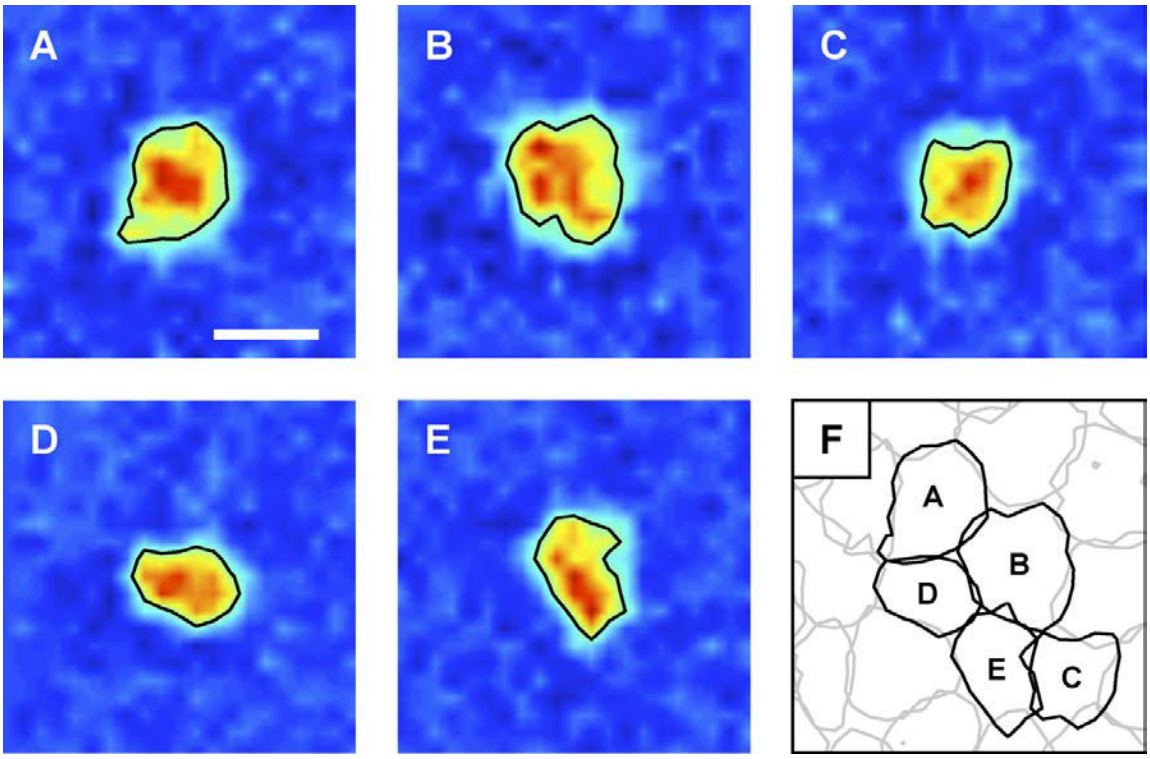

Figure 1.5: Receptive fields with irregular shapes, which allow for a more uniform mapping of the visual space. Image taken from [58].

Another important point about receptive fields is that they usually follow an antagonist center/surround organization. These antagonists are simply called ON and OFF. This means that we will find ON-center/OFF-surround cells, and OFF-center/ON-surround

cells. The ON part responds to positive changes in intensity (increasing), while the OFF part does the opposite, i.e., responds to negative changes in intensity (diminishing). So, while considering that the center will allow for the maximum activation of the neuron, we can conclude that, e.g., an ON-center/OFF-surround cell will fire the most when only its center receives light. If both center and surround receive light, the neuron will not fire as much; while with no light at all, or light only on the OFF-surround part, the cell will not fire at all. Here, firing means eliciting a spike-train, or simply generating the electrical signal we have been discussing previously. Now, we are ready to enlarge our knowledge of ganglion cells.

1.2.2 Standard ganglion cells

Ganglion cells are the output of the retina. For many years, scientists only observed what now are called standard ganglion cells. This classification is given to midget and parasol ganglion cells, who respectively provide information for detailed perception, and action.

Midget ganglion cells represent around 70%-80% of the ganglion cells' population [38][115]. They analyze and provide to the rest of the system information of details and high-frequency high-contrast in central vision. They are also sensitive to color, and have slower conduction velocity compared to the parasol cells.

Parasol ganglion cells represent around 10% of the ganglion cells' population [38][115]. They analyze and provide to the rest of the system motion information, low-frequency low-contrast, and information from flashing objects. Differently to midget cells, parasol cells are insensitive to color, and are faster than midget cells to propagate their output.

1.2.3 Non-standard ganglion cells

Noticed later than their standard counterparts by the scientific community, non-standard ganglion cells are considered to be older in the phylogenesis [70], and to provide information for detection [70][107].

This detection, however, is rough but fast, and focuses on events or particular objects. Its goal is to induce survival-oriented actions on time [91], and to drive higher-level iterative processes with prior information [15][86].

Non-standard cells have been found to participate in blind-sight, i.e., where "clinically blind" patients report being unable to consciously perceive visual stimuli, yet they are able to accurately detect targets moving slowly, or to roughly localize stimuli [92][34].

When compared to standard cells, non-standard cells –such as small bistratified ganglion cells– account for about 10% of the ganglion cells' population [71][84]. Despite the notorious difference in proportion against the midget cells, parasol and bistratfied cells map the entire visual field thanks to larger receptive fields [189][58]. Here, Figure 1.6 shows us the dendritic morphology of ganglion cells in the macaque, and their receptive fields follow this fashion in terms of size.

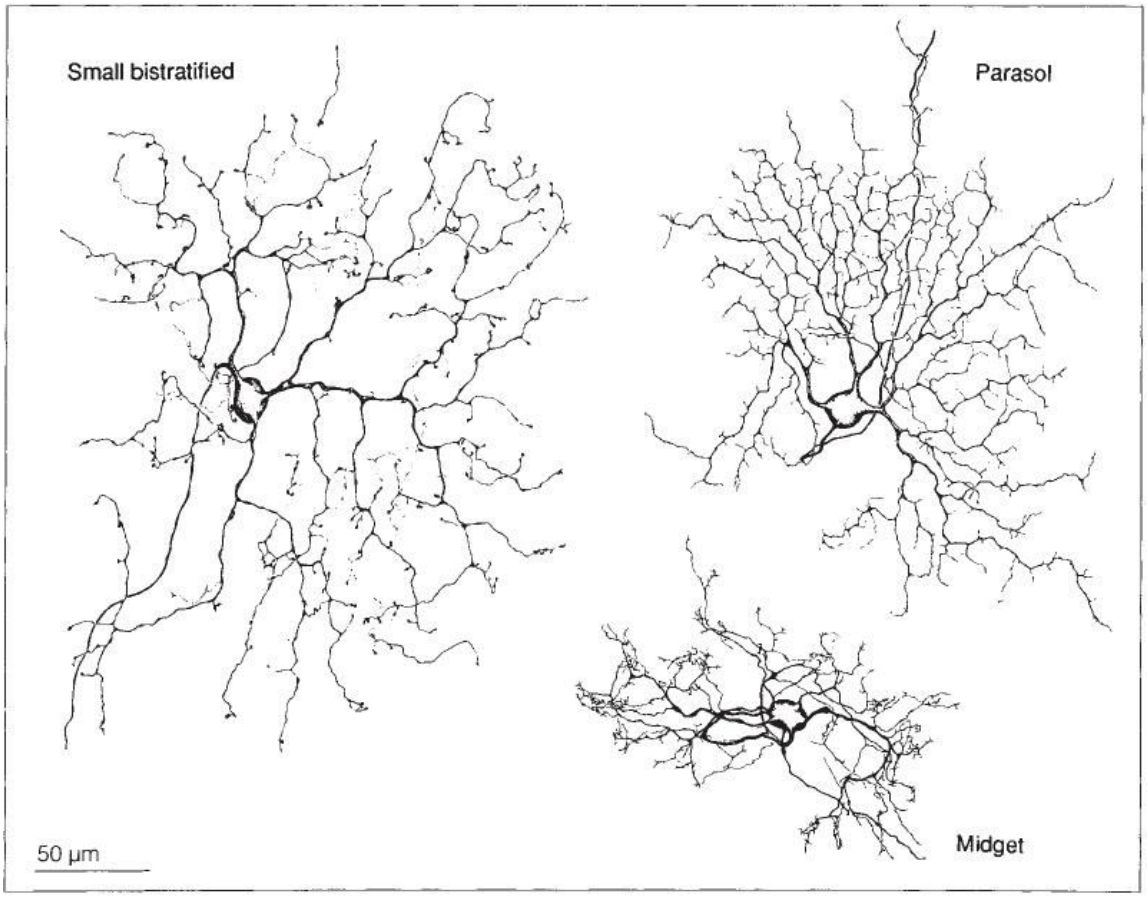

Figure 1.6: Dendritic morphology of macaque ganglion cells. Parasol and bistratified ganglion cells compensate for their reduced amount, compared to midget cells, with larger receptive fields. Image taken from [39].

We have argued that non-standard cells provide coarse detection capabilities. For in-

stance, some non-standard ganglion cells are able to produce sophisticated spatial and temporal pattern recognition on their own [62, 184]. This includes motion detection, directional selectivity, local edge detection, object motion and looming detection [107][62][184]. Nevertheless, the reliability of the detection is relatively low –it is difficult to identify complex patterns with a single and large RF– and it will have generally to be confirmed by a subsequent analysis with smaller and more numerous RFs of the standard pathway. These different functions could have developed over time, as researchers have found that during phylogenetical evolution, the eye was not a simple feedforward system: Feedback information from the remainder of the nervous system had been able to produce adaptive learning of sophisticated visual functions to "optimize the transfer of information" [160]. These capabilities could have evolved to the point of now being pre-wired, i.e. existent without any need for adaptation.

In a nutshell, non-standard cells provide fast, *a priori* event detection assumptions to the remainder of the visual system [91].

1.2.4 Projections of ganglion cells: The birth of visual pathways

Besides the standard and non-standard classification, we can group retinal outputs in streams, which is a notion we will use for the rest of this document. Under this scheme, we will have the Parvocellular [16], Magnocellular [16] and Koniocellular [70] pathways. These pathways start with, and keep the properties of, the information produced by midget, parasol and non-standard ganglion cells, respectively. They receive their names from different neurons in the thalamus, which we will discuss later.

An overview of the retinal projections and the pathways being born with them is shown in Figure 1.7.

Just as a reminder, midget cells and the Parvo pathway carry information for perception, while parasol cells and the Magno pathway carry information for action, and non-standard cells and the Konio pathway carry information for detection. This is the key difference between these three classes, and summarizes well their role throughout the whole visual system.

Before we review the thalamus, let us describe the stage right above, the cortex, so we can later easily discuss the thalamocortical aspects and interactions.

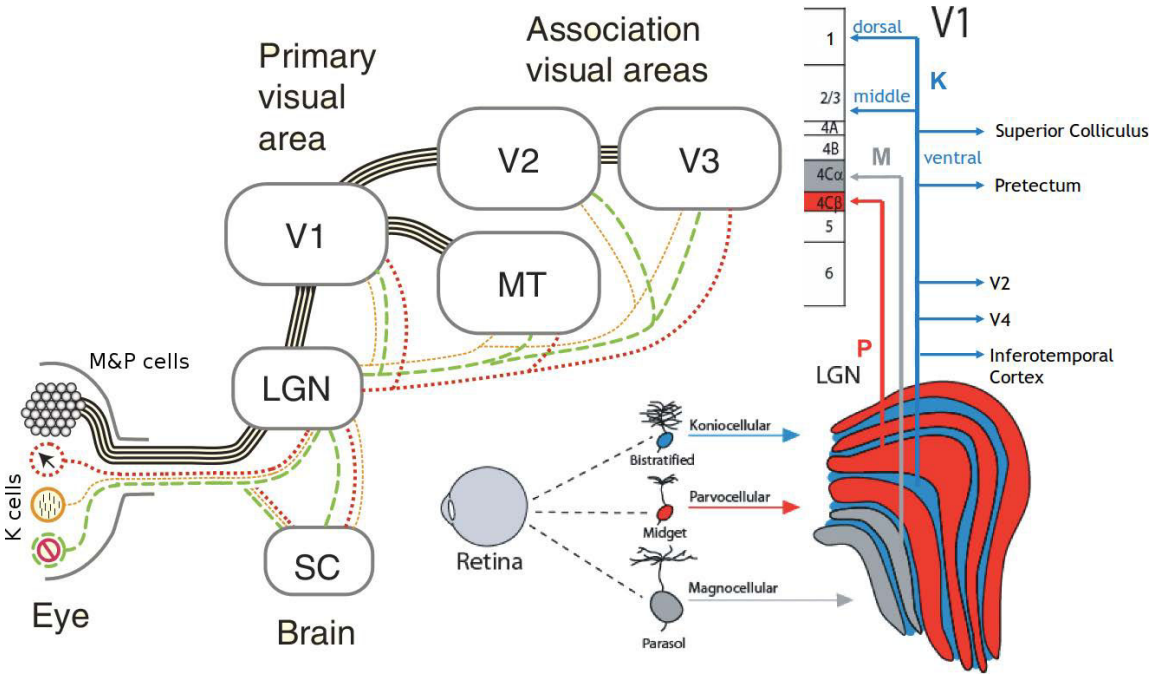

Figure 1.7: Different retinal projections. (Left) Midget and parasol projections are shown in black, while different non-standard channels are depicted in colors. Image taken from [107]. (Right) Projections to the lateral geniculate nucleus (LGN) and thereafter. Again we observe the widespread connectivity of Konio cells, that receive information from bistratified ganglion cells. Image modified from [115].

1.3 The cortex: The adaptable mainframe

The major processing power of our visual system is kept in the cortex. Like a large distributed mainframe, the visual cortex computes information to be used by several structures at the same time, building distributed interpretations/representations of the world, that are to be composed in higher cognitive levels. For the purposes of this document, we will focus on the earliest stage of the visual cortex: the primary visual cortex (V1) [18].

V1 is tiled with elementary and repeated neuronal circuits that authors call the cortical column [74]. It is basically a layered structure made by 6 levels, usually grouped as superficial (composed by layers 1, 2 and 3 upper), middle (3 lower and 4), and deep (5 and 6) layers. Figure 1.8 depicts it in a simplified manner. Here, it is shown that superficial layers receive information from other cortical areas and the matrix thalamus, in order to modulate information processing in the column, respectively, towards a stimulus expected from cortical inference or roughly detected from the non-standard pathway. Middle layers receive precise sensory information from the core thalamus, and with the information from cortical expectation and thalamic modulation, the output will be produced and communicated through the deep layers towards the thalamus as feedback, and to motor regions, like the superior colliculus.

As shown in Figure 1.7, V1 receives feedforward information coming from the thalamus –which will be described in the next section– from all three visual pathways. In addition, it receives information from other cortical areas.

A summary of the anatomical circuitry and their functions in the early thalamocortical loops of mammals –used to validate the thalamocortical connections used in our model– is represented in Table 1.1, adapted from [124] and [67].

In the introduction to this chapter, we mentioned the "what" (perception) and the "where/how" (preparation for action) pathways [63]. The "what" pathway, also called temporal –or ventral– stream, is involved with object identification. After layer 4Cβ in V1, information goes through areas V2, V3, V4 and on, towards IT. At the same time, the "where/how" pathway, also called parietal –or dorsal– stream, is involved with self-referenced localization (i.e. with oneself as point of reference). After layer 4Cα in V1, information goes through areas V2, V3, V5/MT and on, towards MST and FEF. All these links, pathways, and their interactions, serve to integrate information and achieve more and more developed processing at each higher stage.

Regarding the temporal propagation of waves [93][91], again we can take into account

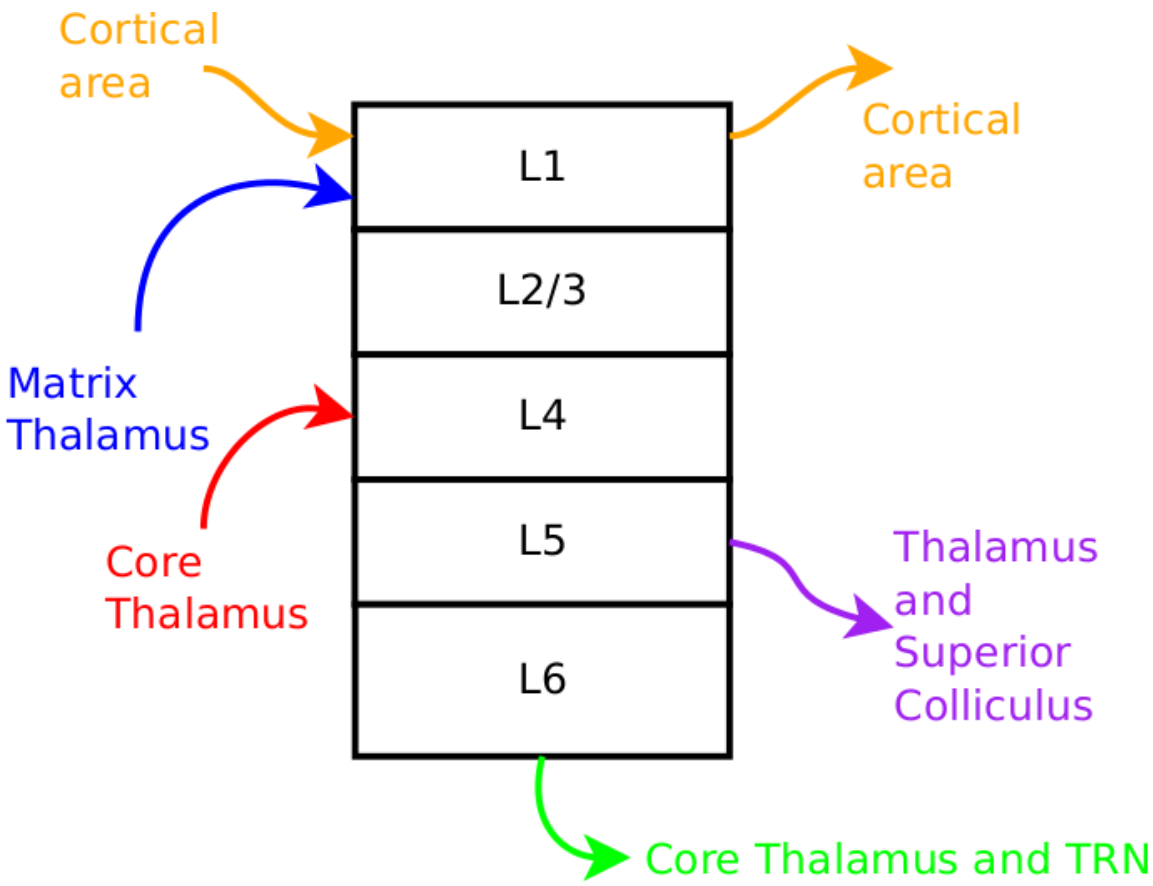

Figure 1.8: **Simplified cortical column.** Here, only a handful of information flows are represented, just to give an idea of the interactions of the cortical column with other structures. TRN stands for thalamic reticular nucleus, and core and matrix thalamic structures are explained in section 1.4.1. The superficial layers receive information from other cortical areas and the matrix thalamus, in order to modulate or bias processing in the column towards an expected, or unexpected, stimulus, respectively. Middle layers receive information from the core thalamus, and with the information from cortical expectation and thalamic modulation, the output will be produced and communicated through the deep layers towards the thalamus as feedback, and to motor regions, like the superior colliculus.

Table 1.1: Anatomical circuitry and functions of V1 connections.

Model connections	Type	Functional interpretation	References
First order core thalamic cells → layer 4 cells of V1	D	Primary thalamic relay cells drive layer 4	[10]
First order core thalamic cells → layer 6(1) cells of V1	D	Primary core thalamic cells prime layer 4 via the 6→4 modulatory circuit	[10] for LGN→6; LGN input to layer 6 is weak [15]; Layer 5 projects to 6 [Note1]
First order core thalamic cells → TRN	D	Recurrent inhibition to core thalamus	[152][82]
TRN → First order core thalamic cells	I	Inhibition of primary and secondary core thalamic cells, synchronization of core thalamic cells	[152]
TRN → TRN	I	Normalization of inhibition	[157][82]
TRN → TRN	GJ	Synchronize TRN and thalamic relay cells	[94]
TRN → Matrix thalamic cells	I	Inhibition of matrix thalamic cells	[87][173]
Matrix thalamic cells → Layer 5 cells of V1	M	To layer 5 through apical dendrites in layer 1	[173]
Layer 4 cells of V1 → Layer 4 inhibitory interneurons of V1	D	Lateral inhibition in layer 4	[103]
Layer 4 inhibitory interneurons of V1 → Layer 4 cells of V1	I	Lateral inhibition in layer 4	[103]
Layer 4 inhibitory cells of V1 → Layer 4 inhibitory interneurons of V1	I	Normalization of inhibition in layer 4	[2][103]

Model connections	Type	Functional interpretation	References
Layer 4 cells of V1 → Layer 2/3 cells of V1	D	Feedforward driving output from layer 4 to layer 2/3	[50][17]
Layer 2/3 cells of V1 → Layer 2/3 cells of V1	D	Recurrent connections in layer 2/3	[11][142][124]
Layer 2/3 cells of V1 → Layer 2/3 inhibitory interneurons of V1	D	Avoid outward spreading in layer 2/3	[112][124]
Layer 2/3 inhibitory cells of V1 → Layer 2/3 inhibitory interneurons of V1	I	Normalization of inhibition	[163][124]
Layer 2/3 cells of V1 → Layer 4 cells of V2	D	Feedforward information	[175]
Layer 2/3 cells of V1 → Layer 6(2) cells of V2	D	Feedforward information	[175]
Layer 2/3 cells of V1 → Layer 5 cells of V1	D	Conveys output from layer 2/3 to layer 5	[17]
Layer 2/3 cells of V1 → Layer 6(2) cells of V1	D	Conveys output from layer 2/3 to layer 6(2)	[15]
Layer 5 cells of V1 → Pulvinar	D	Feedforward information to V2 through the pulvinar	[152]
Layer 5 cells of V1 → Layer 6(1) cells of V1	D	Delivers corticocortical feedback to the 6(1) → 4 circuit from higher cortical areas, sensed at the apical dendrites of layer 5 cells branching in layer 1	[15][17][Note 2]
Layer 6(1) cells of V1 → Layer 4 cells of V1	M	Excitation fo layer 4	[161][15][124]
Layer 6(1) cells of V1 → Layer 4 inhibitory interneurons of V1	D	Inhibition to layer 4	[112][15]

Model connections	Type	Functional interpretation	References
Layer 6(2) cells of V1 → LGN	M	Direct feedback information to LGN	[156][15]
Layer 6(2) cells of V1 → TRN	D	Indirect feedback to LGN, to be used by TRN in order to regulate LGN	[68][152]
Layer 6(2) cells of V2 → Layer 5 cells of V1 → Layer 6(2) cells of V1 → Layer 4 cells of V1	M	Intercortical feedback from layer 6(2) of V2 to layer 1 of V1, where it synapses on layer 5 cells because their apical dendrites branch in layer 1, resulting in subliminar priming of layer 4 cells via the "layer 5 to layer 6(1) to layer 4" circuit	[131][140]

Table 1.2: **Summary of anatomical circuitry of early thalamocortical loops of mammals** Abbreviations: D = driving connections; M = modulatory connections; I = inhibitory connections; GJ = gap junctions. [Note 1] [15] subdivides neurons in layer 6 in 3 classes: Class I: project to 4C, also receive input from LGN, and project to LGN; Class IIa: dendrites in layer 6, receive projections from 2/3, project back to 2/3 with modulatory connections; Class IIb: dendrites in 5, project exclusively to deep layers (5 and 6) and claustrum. Here, these populations are clustered in 2 classes, layer 6(1) and 6(2), which provide feedback to thalamic relay cells and layer 4, respectively. [Note 2]: [15] ubdivides Layer 5 neurons in 3 classes: Class A: dendrites in 5, axons from 2/3, project back to 2/3 with modulatory connections; Class B: dendrites in 5, axons from 2/3, project laterally to 5 and the pulvinar; Class C: dendrites in 1, project to SC. Here, layer 5 neurons receive input from 2/3 (Classes A and B), as well modulatory input from nonspecific thalamic nucleus (Class C, apical dendrites in layer 1), and provides output to layer 6(1) and the pulvinar.

the "slower what" and the "faster how" streams, where the prior focuses in hierarchical processing (i.e. sequential), and the latter on preparing action processing (with a more parallel processing). These streams focus on the interpretation of the visual scene, where a hypothesis is developed by grouping information from the different receptive fields in order to "make sense of the environment" (see Figure 1.9). This process of binding information in the current hypothesis is another way to look at what a cortical expectation is. A cortical expectation is a certain information "predicted" by the cortex, and "expected" to be there, or to happen. An example would be for us to expect to see a ball that is thrown moving in a more or less straight line, rather than to see it moving like a serpent during its flight.

1.4 The thalamus: The collaborative harmonizer

The thalamus [146] is a structure in charge of regulating the information flow to cortical areas. It is located between the cortex and the midbrain, and communicates with several cortical and extra-cortical areas, including peripheral structures, such as the retina. It is thanks to all these connections, and what it does with them, that we call it a collaborative harmonizer.

The thalamus is composed by different clusters of neurons, each one called a thalamic nucleus. Figure 1.10 shows an overview of thalamic nuclei, while Figure 1.11 is a schematic of their different connections. From these nuclei –and in the scope of the present document– the most important are the lateral geniculate nucleus (LGN), the pulvinar, and the thalamic reticular nucleus (TRN).

To give a brief first idea: from a functional point of view [115], LGN works like a smart relay of retinal information, while the pulvinar does something similar with cortical information. TRN, however, will not relay any information and instead will regulate –by inhibiting the thalamus– the thalamocortical flows from, and to, LGN and the pulvinar.

Another important fact is that the thalamus will allow for a "current thalamocortical hypothesis" to exist. This is nothing else than the current information being processed, that is formed thanks to the feedforward flows. The feedforward hypothesis will be corrected through feedback information, particularly the one coming from expectations and goals (cf. Section 1.4.1).

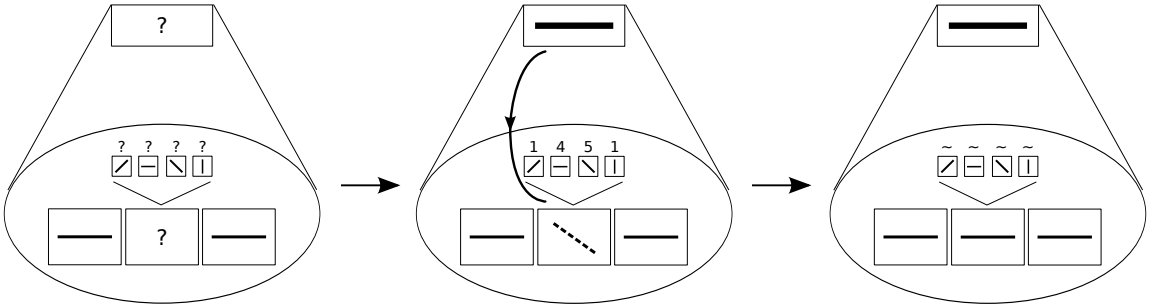

Figure 1.9: **Integration of information through thalamocortical and cortico-cortical interactions** This figure represents a simplification of the interaction between information flows, i.e. the interplay between feedforward and feedback information, together with local receptive field integration, and expectation corrections done through higher-level receptive fields. *Left*: The upper rectangle represents a higher-level unit (of V2, here), where the lines and the ellipse represent its receptive field, that consider 3 cells of a lower-level structure (of V1, here). Two of these cells identify a horizontal stimulus, while we delay the processing of the cell in between them to show how receptive fields, feedforward information, and expectation, work to define the output of a certain unit by integration. This delay could also be interpreted as uncertainty due to noisy or inconsistent signal. Here, this middle unit can identify 4 types of orientation, as represented by the lines in the smaller squares. *Middle*: The cell locally evaluates the preferred orientation, scoring the largest for a diagonal, being this the local feedforward hypothesis. However, it is depicted in the upper box that the higher-level unit, by grouping, has established a straight horizontal line as stimulus, and thus the expectation information (cf. Section 1.4.1), represented by the descending link, will force the unit to be "corrected" and ponder higher the horizontal line, despite the local score, and because of its global, higher-level, analysis. *Right*: The scores are no longer considered, and the units are in synchrony analyzing a horizontal line.

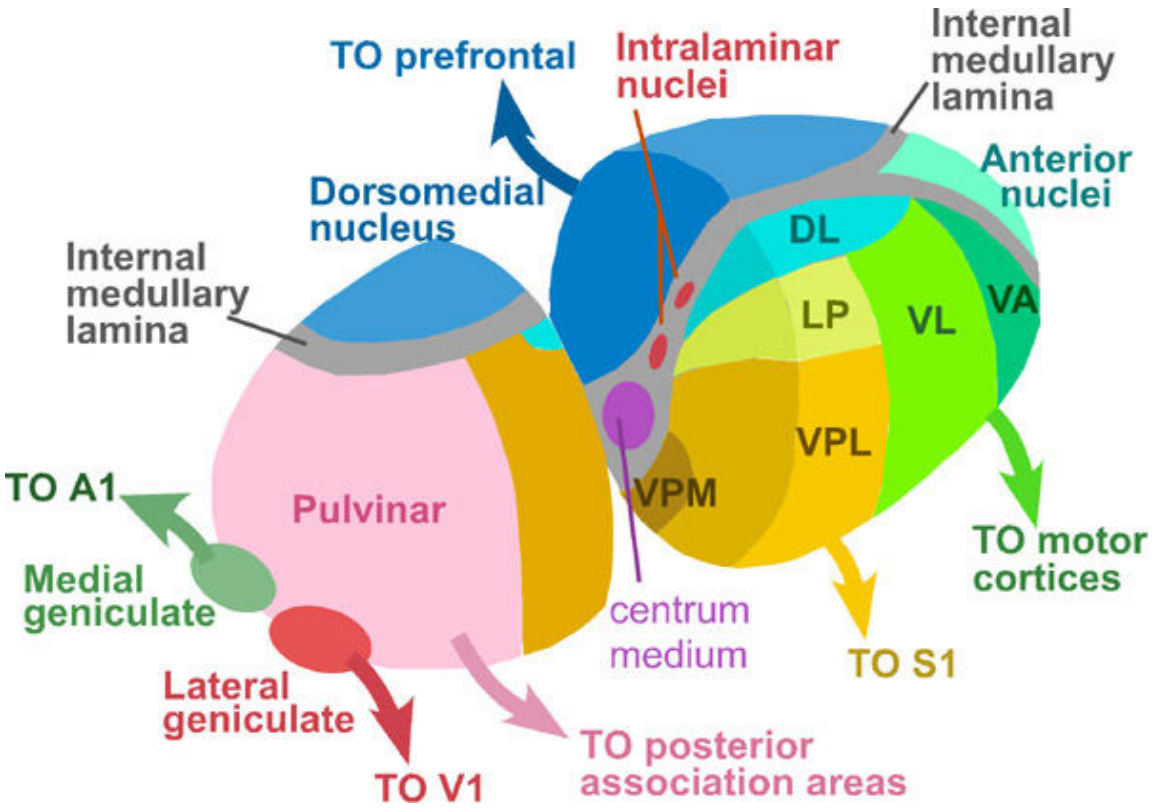

Figure 1.10: Overview of thalamic nuclei. Here, A1 is the primary auditory cortex, S1 is the primary somatosensory cortex, VA is the ventral anterior nucleus, VL is the ventral lateral nucleus, DL is the dorsal lateral nucleus, LP is the lateral posterior nucleus, VPL is the ventral posterolateral nucleus, and VPM is the ventral posteromedial nucleus. Image taken from [64].

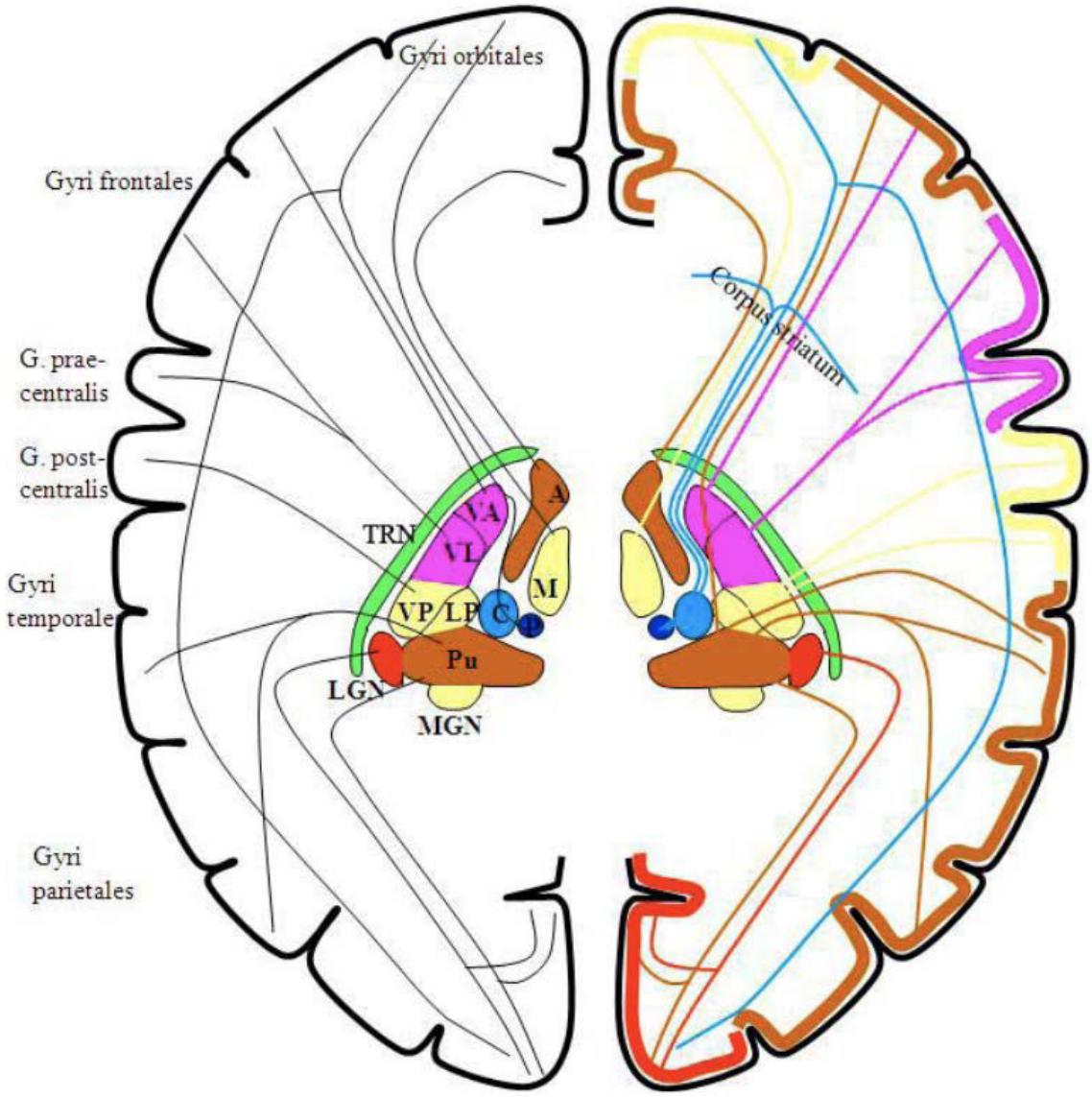

Figure 1.11: Thalamocortical connections and how TRN is involved. Here we see how TRN sort of wraps (like a plastic protection for a sandwich) the thalamic nuclei, receiving collaterals from both thalamus and cortex, and harmonizing these flows via inhibitory actions at the thalamic level. Image taken from [114].

1.4.1 Properties of thalamic structures

In order to better characterize thalamic nuclei, one must be first aware of the jargon used to describe them. Here, we will discuss their classification by order (first/higher order)[153], types of cells (core and matrix)[80][81], what their activation modes are (tonic/burst)[154], and how connectivity allows us to label their outputs (as driver or modulator)[154]. In addition, we will discuss the "no strong loops" hypothesis for thalamic (and cortical) projections.

First and higher-order nuclei

When we talk about order, we simply mean "what input". This makes first-order equal to peripheral, like we see with LGN receiving input from the retina, and higher-order equal cortical, like we see with the pulvinar receiving input from the primary visual cortex (V1) and other cortical regions.

Core and matrix cells

When we talk about core or matrix cells, we look at "where and how it outputs". The reason for having only two names rather than four is that cells project in only two ways. The first one, used by core cells, consists in projecting topographically to middle cortical layers (3 lower and 4), which is called the "precise" way. The second one, used by matrix cells, consists in projecting non-topographically to upper cortical layers (1, 2, 3 upper), and it is called the "diffuse" way. In addition, this diffuse way also considers other areas in the cortex.

Core cells produce driving flows, while matrix cells produce modulating flows (cf. Section 2.1.2).

Tonic and burst modes

The information transmission modes of thalamic neurons were first studied in slow-wave sleep [148]. Here, bursting was of major interest, where scientists observed these sustained rhythmic bursts across large cell populations, where the firing was synchronized. The first observations showed that bursting prevented the normal function of the cells, which at the time was considered only to be relaying information, through the tonic mode. However, in awake activities, a thalamic neuron will transmit information in tonic and burst mode (one of them being active at the time) [147].

The tonic mode is the linear transmission mode, where firing is somewhat regular, and thus it is considered that sensory information is transmitted via this mode. On the other hand, the burst mode is the non-linear transmission mode, where bursts improve the signal-to-noise ratio, and are thus thought of allowing the capture of new information.

These modes are supposed to be generated because of intrinsic properties of the thalamic neurons. Particularly, because of calcium (Ca2+) conductances in their T-type calcium channels. A T-type calcium channel is a low-voltage activated "tunnel" that allows for a calcium influx to enter a cell after a spike or a depolarizing signal. Here, depolarization is when the membrane potential of the cell becomes "more positive" or "less negative", while its conductance is a mathematical parameter representing the ease of electric current flow through this channel. So, these modes happen thanks to a threshold: when a cell is relatively depolarized for 100ms or more, T-type calcium channels are inactivated, thus allowing cells to fire in tonic mode. However, when a cell is relatively hyperpolarized (opposite of depolarized) for 100ms or more, T-type calcium channels are activated, and provoke the burst mode, where 2 to 10 spikes are generated per burst. Here, the excitatory cortical input (from layer 6) promotes tonic firing, while the inhibitory input from TRN promotes burst firing [104].

Our interpretation is that the burst mode comes in handy when looking for something new. This "something new" is linked to cortical expectations.

When cortical expectations are not met, we call it a mismatch. In order to say whether there is such mismatch, or not, feedforward information must be compared to the expectations, reflected by feedback information. This task is topographically carried out by TRN –receiving feedforward and feedback flows to compare reality against expectation–, who possesses inhibitory capabilities to regulate thalamic nuclei. In the case TRN resolves that there is no mismatch, sensory information can be transmitted through tonic mode. However, in the case of a mismatch, the burst mode is needed to improve the SNR, and to either validate cortical expectations by realizing that the mismatch is not as great as previously computed, or to allow for a topographically wider search in the information, as the SNR increase would provoke a larger inhibition in the mismatching regions, allowing for this search elsewhere in the topographic map.

Driver and modulator information flows

An information flow can be either a driver, or a modulator. Being a driver means that it will, by itself, be responsible for generating/modifying the current output of the receiving

structure. An example would be the output of core cells in the LGN towards layer 4 of V1. This information flow alone triggers cortical responses, altogether with being considered for first-order thalamocortical mismatch. A modulator, on the other hand, is unable to trigger a response by itself on the receiving structure, and instead will regulate (modulate) what is already being analyzed. An example would be the output of matrix cells in the LGN towards layer 1 of V1. This information flow will help to regulate, or empower (being excitatory), certain regions, but will not be directly responsible for the output, and will not be considered for the first-order thalamocortical mistmatch.

All this could be put in situation : driver information from the lateral geniculate nucleus, e.g. encoded in the Magno pathway, will be transmitted in tonic mode unless the thalamic reticular nucleus sends a modulating mismatch signal, which would require to block (maximal inhibition) the feedforward flow, switch to burst mode, and allow for a search elsewhere than the current focus point (or a new interpretation).

The "no strong loops" hypothesis

This hypothesis for thalamic and cortical projection establishes that there shall be no loops created only with driving information flows, as the consequence of having one would be uncontrolled cortical oscillations [35]. This hypothesis arises from graph theory, where the mathematical theory of directed graphs, or digraphs, is used. A digraph is a series of nodes (and in our case, thalamocortical structures) connected by lines, where each line shows the direction of the information transmission with an arrow. Here, if a digraph has a directed loop (i.e. loop with only driving information flows, in our case), then it is not possible to generate a hierarchy of levels. On the other hand, if there is no directed loop, the nodes (structures) can form a hierarchy, but it may not be a unique one.

In our case, this simply means that a stable system should not have such loops, and the early visual system does not contain any so far [35].

1.4.2 The complex relay: the lateral geniculate nucleus

LGN, or the lateral geniculate nucleus, is a first-order nuclei, composed by both core and matrix cells. In primates, it is composed by 6 main layers, where intralaminar structures are found between them. In layers 1 and 2 we localize Magno-cells, in layers 3-6 the Parvo-cells, and Konio cells are present in the intralaminar structures. The core part of LGN is composed by the 6 main layers, while the intralaminar structures are its matrix part.

In a previous section we discussed the midget, parasol and non-standard ganglion cells, and saw that these cells gave birth to the Parvo, Magno, and Konio pathways. Taking this into account, it is not surprising that the different cells in LGN share many properties of their retinal counterparts (cf. Figure 1.7):

- The Parvo cells carry slow and sustained neuronal activity for layer 4Cβ of V1 concerning color and shapes.
- The Magno cells carry rapid and transient information for layer 4Cα of V1 concerning motion, brightness and depth.
- The Konio cells process different kinds of non-standard information and project to upper layers in the cortex. The next section is dedicated to them.

In addition, core LGN receives strong cortical feedback from layer 6 of V1, together with a degree of inhibition from TRN. All these can be seen in Figure 1.12. This, we interpret, as a result of the mismatch between feedforward and feedback information (expectation).

1.4.3 Konio pathway and its projections

The Konio stream, or non-standard pathway, is here considered as "for detection". This raw, coarse, *a-priori* detection of visual events is done by integrating information from groups of non-standard retinal ganglion cells. The results of this detection can allow for survival actions to be done promptly [91], and also to drive higher-level processes with prior information [15].

Here, the Konio pathway is considered to be a quick pathway. This consideration does not arise from its processing speed, as we will see in the last section of this chapter, but instead from the reduced number of hops when compared with its Parvo and Magno counterparts.

There are 5-6 classes of Konio axons[2] afferent to V1. However, they seem to be organized in 3 Konio streams [24][70]:

- The dorsal Konio layer, that carries low acuity information and projects toward layer 1 of V1.
- The middle Konio layer, that carries information from central blue cones to layer 3B of V1.

[2] An axon is the nerve fiber of a neuron that allows it to transmit electrical impulses.

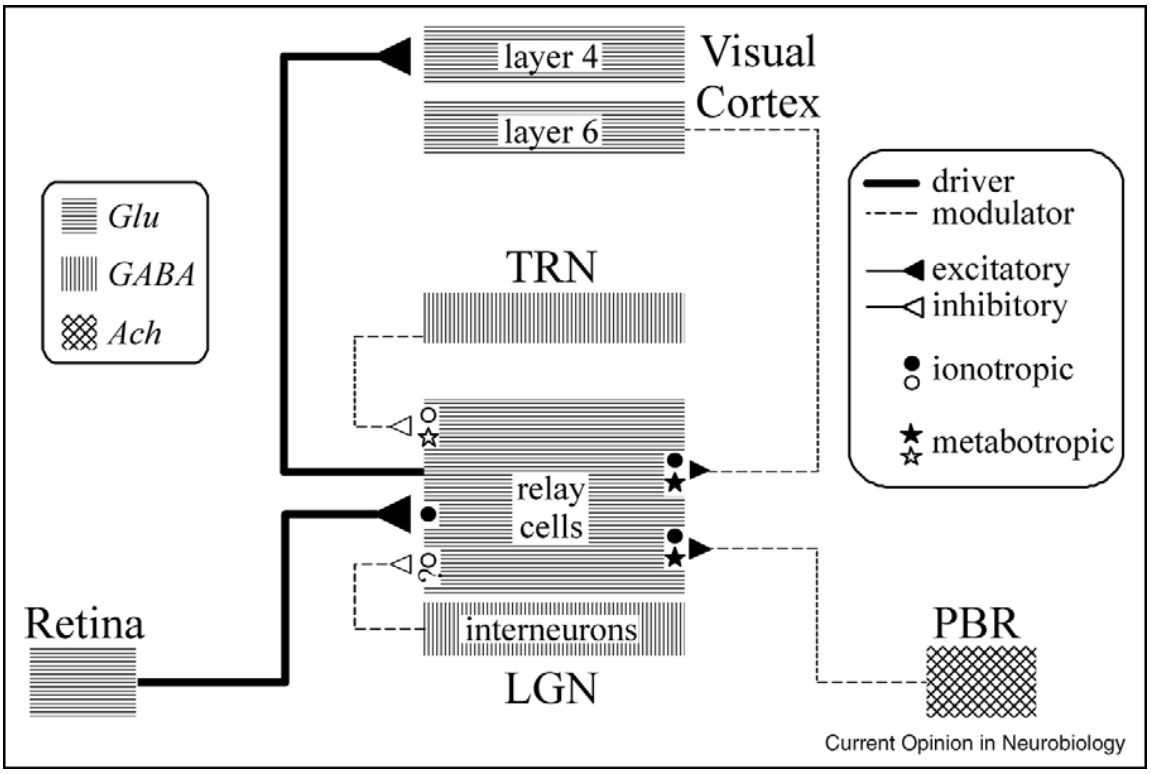

Figure 1.12: **Schematic diagram of circuitry for the lateral geniculate nucleus** The inputs to relay cells are shown along with the relevant neurotransmitters and postsynaptic receptors (ionotropic and metabotropic) Abbreviations: Ach, acetylcholine; GABA, γ-aminobutyric acid; Glu, glutamate; LGN, lateral geniculate nucleus; PBR, parabrachial region; TRN, thalamic reticular nucleus. Image and caption taken from [149].

- The ventral Konio layer, that is linked to superior colliculus and pretectum functions.

In addition, Konio cells connect, through LGN, to important multi-sensory structures like the amygdala. This region, in mice, is involved in the control of emotion [31], e.g. fear behavior, which is the behavior against fearful stimuli, which is detected globally.

Another behaviorally interesting characteristic of the Konio pathway is its participation in Blindsight [92][34], where the detection of moving targets and rough localization of stimuli are done subconsciously.

For the purpose of this document, Konio cells are particularly important for their modulation of the fine core information V1 receives from the Parvo and Magno pathways.

1.4.4 The inhibition center: the thalamic reticular nucleus

TRN, as mentioned previously, has a main role in regulating thalamocortical communications [90]. As shown in Figure 1.11, TRN somewhat wraps the rest of the thalamus, and most of the thalamocortical connections pass through it.

Receiving a duplicate of the thalamic feedforward driver information in what is called a "collateral" connection (or simply collateral), while at the same time receiving a collateral from cortical feedback information, TRN will inhibit both core and matrix thalamic nuclei if a mismatch is found. This inhibition will regulate thalamic processing in a topographic way, respecting the different resolutions from the different nuclei [154].

In addition, the synchronization carried out by TRN works at many levels at the same time. For example, it is cross-order, meaning it uses information from first and higher-order structures. It could also take into account other modalities, such as audition, which makes it multi-modal. This multi-level inhibitory mechanism is the result of three main components: GABAergic cells, cross-order local gap junctions[3] and inhibitory axons [150][82] (cf. Figure 1.12).

1.4.5 The higher-order thalamic nucleus: briefing of the pulvinar

The pulvinar is, in terms of vision, our higher-order thalamic nucleus. It is a collection of core and matrix cells that receives input from many cortical areas, and outputs to their immediately higher-order successor (e.g. V2 in case of V1). It also receives input from the Konio cells and the superior colliculus, and it is also regulated by TRN. Regarding

[3] That allow for direct electrical connections.

these facts, one could easily argue that it is pretty similar to LGN, which is true, however the pulvinar has quite a few other characteristics, e.g. learning, that make it earn its classification as a higher-order nucleus.

The pulvinar seems to be involved in visual spatial attention, where it would play a role in the initiation and compensation of saccades (eye movements) via its participation in the shift of attention [128]. It also participates in emotional processing, as part of the superior colliculus→pulvinar→amygdala pathway. These two structures, the superior colliculus and the amygdala, are discussed in the following sections.

1.5 The superior colliculus: The early sensory-motor hookup

The superior colliculus (SC) [109] is particularly devoted to eye movements [190][98], or oculomotricity. The SC, or optic tectum (or simply, tectum), is located on the roof of the brainstem, and it is a layered structure that respects visual topography. There are various eye movements, and for the scope of this document we will focus on saccades, which are rapid eye movements that bring a region of interest into the foveal (with highest resolution) region.

The visual inputs of the superior colliculus are the retina and the visual cortex, while it projects motor outputs to the brainstem, reticular formation and spinal cord to perform orientation movement.

Primitive visual processing, such as the one of the frog [99], is still present in mammals [41]. In such processing, non-standard ganglion cells consider only movement information and visual memory is restricted to objects staying in the visual field (cf. primitive detection functions by the Konio pathway). They are often called "event detectors". Two behaviors are particularly relevant for such system: gaze shifting, where saccades, head movements or other skeletal segments can be engaged [57]; and stereotyped defensive responses conserved across species [43].

Its superficial layers (e.g. 2a and 2b) are connected to sensory systems, mainly the visual one, and they shelter cells specially tuned for movement [88].

Its intermediate layers are linked to multi-sensory and motor systems, carry out multi-modal integration, and are mainly devoted to the control of eye movements.

The deep layers drive the motor system, generating a motor map. Here, saccade ampli-

tude (in primates) is represented logarithmically[4], from the rostral to the caudal extents, and saccade direction is represented linearly on the other axis [97]. Their main role in vision is to control fast displacement of gaze. At any one time, only one saccade can be performed (with an average of three saccades per second [7]), and this most convenient saccade is chosen taking into account criteria from reactive behavior to planning.

Several projections to the thalamus reach the striatum (in the basal ganglia), for the selection of motivated orientation (including saccadic) movements.

1.6 The amygdala: The mnesic and emotional muscle

Most of our behaviors are regulated by our desires, needs (including survival), etc. This is also true for visual behaviors, where subcortical structures play an important role, inducing neurophysiological changes and influencing behavior towards relevant stimuli –e.g. reflexes, or prioritizing the analysis of a target against others–. To comprehend how emotional information modulates processes in the early visual system, cortex included, it is thus necessary to assess the relevance of each component of the visual information, and to thus propose a behaviorally relevant model. To this end, we must mention the amygdala.

1.6.1 A few facts about the amygdala

The amygdala [96][164][40][83] participates in many behavioral functions, such as memory, decision making, and emotional reactions. Part of the limbic system, it is an almond-like shaped region in the medial temporal lobe, and achieves its goals thanks to numerous connections with other brain areas [139].

1.6.2 Amygdala and perception: attention and (un)awareness

As the sensory inputs gather massive amounts of information, filtering its irrelevant parts becomes crucial for perception. This is usually called selective attention, and has commonly been used for conscious perception, when top-down[5] influences from frontoparietal structures suppress cortical activity in these irrelevant regions. However, a healthy brain

[4] I.e., not in a Cartesian coordinate system, but a logarithmic transformation of such, that respects the collicular surface; basically a deformed polar coordinate system that also accounts for the differences of resolution between the fovea and the rest of the retina.

[5] From higher to lower areas.

intrinsically possesses mechanisms to perceive emotional stimuli non-consciously as well, and thus, bypasses the relevance constraints because emotionally relevant stimuli, such as fearful stimuli, are prioritized in a task [182]. In the adult brain of humans, several subcortical areas are involved in non-conscious perception of emotional stimuli (Figure 1.13). Visual encoding of emotional stimuli follows a path through the superior colliculus, the pulvinar, and then the amygdala, to continue to the substantia innominata and the nucleus accumbens.

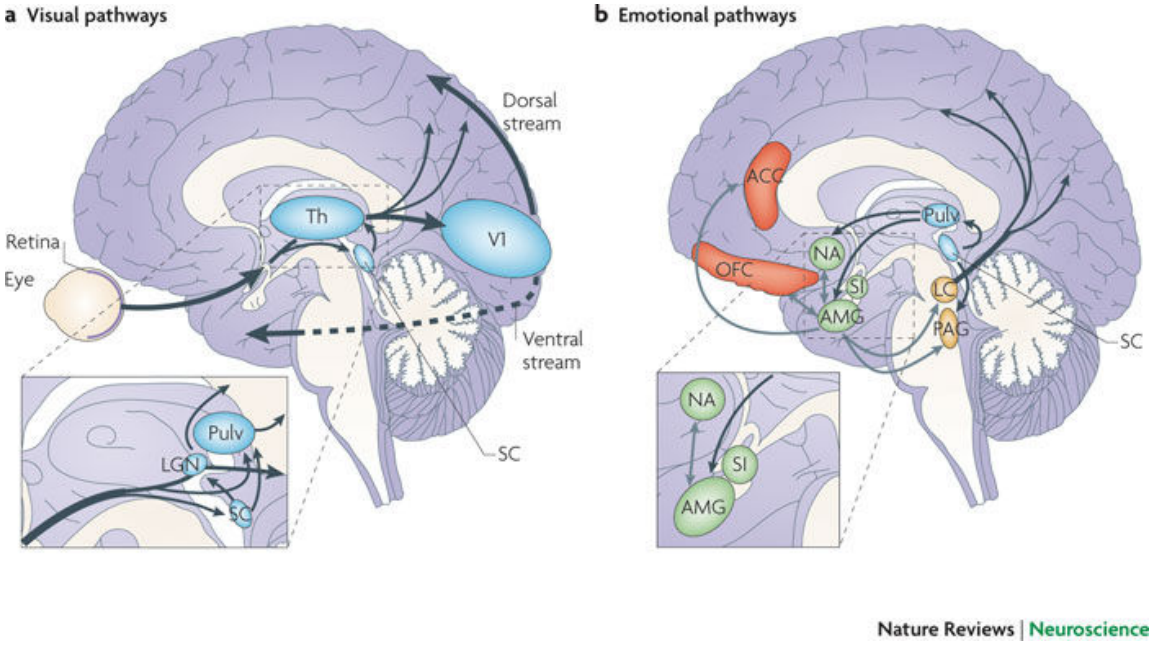

Figure 1.13: Cortical and subcortical visual and emotional pathways. Image taken from [164].

Under this scheme, the superior colliculus responds to coarse emotional stimuli, the pulvinar responds to salient visual targets, and the amygdala has been studied mostly regarding responses to danger, but also responds to stimuli such as happy or surprised expressions, though in a different manner when compared to fearful stimuli [158]. The difference between these structures resides in the fact that functional neuroimaging studies show that the amygdala is involved in both conscious and non-conscious perception of emotional stimuli, whereas neither the superior colliculus nor the pulvinar seem to participate

in non-conscious perception, with the exception of the non-standard pathways [145].

1.7 Temporal aspects of the early visual system

Naturally, when having a system with many actors, one of the interesting aspects is interactions. These structures manage their timing for precise operations by exchanging information, coordinating different processing, including behavioral responses adapted to emergencies, etc. Timing is the tracking of time when these operations are happening. Here, the (early) visual system processes information promptly: a complex natural image may be processed as fast as 75-150ms [170][177].

Normally, one measures these processing times in what is called latency, which is simply the amount of time between stimulation and response. Here, we use latency as the time since information was presented to the eye. This means that one can get estimates of local processing times by simply subtracting the previous stages.

The whole visual processing starts in the retina, where the midget cells, part of the Parvo pathway, have a center latency of 40-50ms, delayed 3-10ms because of its surround [84]. The parasol cells, part of the Magno pathway, are faster, with a latency of around 25ms [89][30]. The retinal Konio cells evoke latencies of about 40-60ms *in vivo* [36], but [49] shows *in vitro* latencies of about 50-70ms. These results correspond to those shown by [37].

In the thalamus, the Magno cells have a latency of about 33ms, while the Parvo cells show a latency of about 50ms [143][116]. [108] postulates that even if the Magno pathway is about 10ms faster to reach the cortex than the Parvo pathway, the convergence of the Parvo cells in the cortex could compensate for, or even reverse, the time advantage shown by the Magno cells. As for the Konio cells, in the Galago, they have a latency 10ms longer to that of the Parvo cells [77][116]. Cells in the Inferior Pulvinar (PI), Lateral Pulvinar (PL) and Dorsomedial Pulvinar (Pdm) show latencies of about 66, 64 and 84ms respectively [121]. TRN cells begin to act in the first 100ms after stimulus onset [138] and have a processing time of about 25ms [111].

Cortical areas show latencies (see [116] for a review, and [91] for a very nice meta-analysis over 48 different studies) of about 65ms for V1, 83ms for V2, 71ms for V3, 102ms for V4, 71ms for V5/MT, 74ms for the medial superior temporal area (MST), 72ms for the frontal eye field (FEF) [143], 100ms for the lateral intraparietal cortex (LIP) and 110ms for the inferior temporal cortex (IT) [116]. [136] shows latencies of 40-60ms for V1, 50-70ms

for V2, 60-80ms for V4, 70-90ms for TEO and 80-100ms for TE (TEO and TE are part of the inferior temporal cortex). These different results could be explained due to the different experiments performed -e.g. the results of [116] for IT were obtained with flashed stimuli, while on [136] moving stimuli were used-, with different stimuli and setups, but all were obtained from the primate system.

In the superior colliculus, superficial layers show latencies of 40-80ms, whilst deep layers (combining visual and motor modalities) show latencies of 50 to 150ms [188]. As regular saccades take 130-180ms in being produced [44], and by simple subtraction, this would mean that the latencies of deep layers are the about same values if we consider their activation from superficial layers. [101] shows that if a target moves "twice in brief succession" there is a delay in the response of about 150ms, but that the SC cells encode the delay of this second saccade, as the motor burst coincides with the saccade.

The dynamics just mentioned are summarized in Table 1.3.

Considering the previous numbers, we can understand the hypotheses of works such as those of Lamme ([93][91]). There, the temporal stream towards IT (linked to the Parvo pathway) could be regarded as with a more sequential processing, whereas the parietal stream, including MT, MST and FEF (and linked to the Magno pathway) could be considered more parallel in its processing.

To summarize, one can notice how fast the Magno pathway is, compared to the Parvo pathway in every stage, and that despite the differences in timing, the interactions between all the different participants is a challenge that should be taken into account without any central structure, as they all work locally in an "independent" fashion. These are:

- Hierarchical elaboration of object identification along the Parvocellular pathway.
- Preparation of action, in a parallel way, in the Magnocellular pathway, which also depends on object identification.
- The Koniocellular system can make interruptions if specific stimuli are detected (alert), or can modulate processing if a mismatch is detected.

It is using these temporal dynamics that the work presented in this thesis will be conceived and developed.

Table 1.3: Neural dynamics in the visual system

Structure	Latency (ms)	References
Parasol GC	∼25	[89][30][37]
Midget GC	40-50 + 3-10	[84][37]
Konio GC (in vivo)	40-60	[36][37]
Konio GC (in vitro)	50-70	[49]
Superficial SC	40-80	[188]
Deep SC	50-150	[44][188]
Magno cells	33 ± 3.8	[143][116]
Parvo cells	50 ± 8.7	[143][116]
Konio cells	∼60	[77][116]
Inferior Pulvinar	66.5 ± 16.1	[121]
Lateral Pulvinar	64.2 ± 19.9	[121]
Dorsomedial Pulvinar	84.3 ± 47.6	[121]
TRN cells	∼25	[111]
V1(4Cα)	∼44	[143]
V1(4Cβ)	66 ± 10.7	[143]
V2	83 ± 21.1	[143]
V3	71 ± 8.6	[143]
V4	102 ± 23.4	[143]
V5/MT	71 ± 10.3	[143]
MST	74 ± 13.1	[143]
FEF	72 ± 13	[143]
LIP	100 (65-180)	[116]
TEO	70-90	[136]
TE	80-100	[136]
IT	110 (90-190)	[116]

1.8 Summary: A circuit of loops and interacting flows

We have seen many facts about the early visual system in the previous sections. Perhaps an idea that should be emphasized is that of interacting information flows in a system composed of loops.

We here consider three main sensory information flows: the one linked to the Parvo pathway, the one linked to the Magno pathway, and the one linked to the Konio pathway. The first noticeable interactions take place at the primary visual cortex, V1, where standard information flows are modulated by the non-standard information sent from the matrix LGN. This modulation is also present in other cortical stages, where the pulvinar has a role similar to LGN, however adapted to higher order areas.

The stream linked to the Parvo pathway arrives at the temporal cortex to further communicate to the limbic system. It parses visual information into discrete objects related to memory, where a link between present input and stored information is established.

There are two Magno related streams. The first, after the parietal cortex, communicates to the somato-sensorimotor cortex, and specializes in extracting information to prepare and calibrate current action. The second, together with the Konio pathway, sends information to the superior colliculus and then to the reticular formation to regulate orientation and saccades.

There are several Konio related streams, and they are partially understood. One of them is the one starting at the retina, projecting to the superior colliculus, then to the pulvinar and subsequently to the amygdala. This stream is able to give emotional value to stimuli, to allow for learning, and also to send information to, e.g., the basal ganglia, for further processing.

In terms of loops, probably the most notorious in the early visual system are the thalamocortical ones. For the standard pathways, the thalamus sends direct information to the cortex, who sends feedback information directly to the thalamus. In addition, these connections generate mini-loops including synchronization from TRN, as the feedforward and feedback collaterals allow for the mistmatch computation to be carried out, closing the loop with the resulting inhibition. For the non-standard pathway, however, this loop is less obvious, as matrix cells project their output to superficial layers in V1, and the loop will be also closed with inhibition from TRN, but this inhibition will consider standard information (as it is the result of the mismatch mechanism).

A not-so-obvious loop is the peripheral one. Since eye muscles will be operated by

signals from the superior colliculus, retinal information –from parasol and non-standard cells– arriving at this structure could have an "immediate" (considering biological/reaction delays) impact on the collicular response. This means that what the retina will capture next, as the retina is a fixed tissue in the eye, will also be modified, and thus we have another loop.

The last loops we will discuss here are the ones created by cortical output arriving at the superficial layers of the superior colliculus. These information flows participate in the computation of the signals that will be sent to LGN and the pulvinar (cf. Section 1.5), who themselves will project to the cortex, thus closing the loops.

All these different properties are included in our modeling.

Chapter 2

Bio-inspired dynamical systems and algorithms

Contents

2.1 Implementing populations of neurons: the notion of minimal model 41

2.1.1 Spike vs rate models: why we have made the standard choice . . . 41

2.1.2 Driver/Modulator considerations 46

2.1.3 Specification and validation of parameter values 50

2.1.4 Filters and information processing 51

2.1.5 Dynamic Neural Fields 53

2.2 Functional view of the neural system: the systemic level 54

2.2.1 Functional interpretation of retinal mechanisms: non-local filtering 54

2.2.2 Functional interpretation of retinal mechanisms: visual event detection 56

2.2.3 Functional interpretation of thalamic mechanisms 59

2.2.4 Assembling populations into networks 60

2.2.5 Implementation details 62

2.3 Conclusion 64

Summary

The complexity of a model indeed depends on the related scientific objective. What does this system represent? Which task is performed? What is it composed of? At which level of detail should one represent its internal mechanisms? ... These are only four of the many questions that will arise when building a model. And the choices of implementation at the "how to" level are definitely in deep relation with the "what for" specification level.

More precisely, when modeling the early visual system, we must account for the different types of neurons, how they are grouped in populations, and at a higher scale, how the related networks process different kind of information, at different timing. This yields the functional view of the nervous system. For each point, simplification is mandatory for both pragmatical and methodological reasons, since our goal is to create a minimal, yet complete, systemic model. Despite these simplifications, interesting properties emerge. In order to study them it is crucial to specify how such model is evaluated and validated.

The goal of this chapter is to provide answers to these issues within the scope and context of this thesis.

Keywords: Neural Ensemble, Emergent Properties, Natural Images, Computational Modeling

Organization of this chapter:

Here, we discuss the "how to" of neuron population implementation. We make explicit the issues that must be taken into account. We focus on the early visual system. The different tools (formalism, software architecture, etc.) used to develop this implementation are described. Notations used in the rest of the paper are also given here.

The way we propose is to start from the smaller scale up to the global scale, i.e., from individual populations of neurons, to networks, and finally the system as a whole. Between each scale, the emergent properties are to be discussed. Furthermore, timing in information processing is a key issue, addressed here. Stability and computation convergence of this distributed computation are also included.

We, in addition, have to discuss topics in link with these computations: the fact we consider natural images, which is a major influence for the whole architecture and properties of the system, and the use of statistical learning implemented as a biologically plausible mechanism in order to explain the intriguing capability of the ganglion cells to perform

high-level visual event detection.

2.1 Implementing populations of neurons: the notion of minimal model

When implementing a neural ensemble, one faces many challenges. The primary question is basically the level of detail to be achieved. This decision directly impacts the complexity of the processing in most cases.

A reasonable decision is to develop a minimal model. But what does minimal mean? And what for? The generic answer is to choose the minimal level of details and complexity (i.e., minimal number of parameters, equations, etc.) that allows us to reproduce the studied phenomena, i.e. the available experimental data. This is the Occam's razor principle [169]. This choice has several virtues. On the one hand, estimation is more robust (e.g., the risk of numerical instability is reduced and the numerical significance of the estimation is higher). A step further, it avoids the risk of "over-fitting" the data [169]. A model with enough degrees of freedom to predict everything, simply predicts anything, and this explains nothing. On the contrary, a minimal model takes a risk in terms of prediction. Because it is highly constrained, it yields precise predictions about results not yet obtained. Also, it is falsifiable. These predictions can be tested during future experiments and the model is going to be *a-posteriori* confirmed or contradicted.

This major methodological aspect is going to be applied at different stages of our work. In the next section, it is going to drive the choice of neural model. When working with neurons, one of the first decisions is whether our neurons are to be represented by a spiking or a rate model. The scale of representation –either each neuron, or a group of neurons (e.g., a micro-column in the cortex) that have the same input/output behavior, or macroscopic variables representing the whole neural map activity– is the major issue.

2.1.1 Spike vs rate models: why we have made the standard choice

When considering a neural network, the designer can choose to build a model based on spiking neurons, or opt for a rate model, which by default consist of looking at the system under very different time scales. Let us discuss these options, and the reasons why we finally decide to use the rate model one.

In a spiking neural network, neurons have at least one state variable: the membrane potential V, which controls the firing of the neuron, in the sense that when a threshold membrane potential is reached, the neuron fires a spike. The simplest model that im-

plements this minimal representation of such a phenomenon is the integrate-and-fire (IF) model. It writes:

$$\dot{V}(t) = -\frac{1}{\tau} V(t) - e^{-\frac{1}{\tau}} \delta(V(t) - 1) + U(t), V(0) = 0$$

where $\tau > 0$ is the neuron leak time-constant, $U(t)$ the input normalized current and $\delta()$ is the Dirac distribution. A straightforward computation shows that when $V(t) < 1$ the system behaves as a 1st-order integrator of the input current, i.e., an exponential low-pass filter:

$$V(t) = \int_0^t ds\, e^{-\frac{t-s}{\tau}} U(s)$$

while, when $V(t) = 1$, integrating in the sense of the distribution leads to the fact that $V(t)$ is instantaneously reset to 0. This discrete event corresponds to the fact the neuron has fired a spike, i.e., an action potential. This minimal model of a spiking neuron has been proposed by Louis Lapicque [95], in 1907.

When considering discrete times, i.e., when sampling the time at a period $\Delta T < \tau$, the same model writes, using an elementary forward Euler discretization scheme $\dot{V}(t) \simeq \frac{V(t+1)-V(t)}{\Delta T}$:

$$V(t+1) = \gamma\,(1 - H(V(t) - 1))\, V(t) + U(t), V(0) = 0$$

where $\gamma = 1 - \frac{\Delta T}{\tau} \in]0, 1[$ is the discrete time constant, while the term $(1 - H(V(t) - 1))$ implements the potential reset mechanism (here $H()$ stands for the Heaviside function), as easily verified. This model is called the BMS model and has been extensively used by Cessac and collaborators to study dynamical properties of neural networks or reverse-engineering of neural networks parameters [25][29].

When used in a network, the state of each synapse is taken into account in the input $U(s)$ and the minimal representation writes for a neuron of index n:

$$U_n(t) = \sum_m W_{nm}\, H(V_m(t) - 1)$$

where W_{nm} is the synaptic strength for the afferent neuron of index m to the efferent neuron of index n, while the use of the Heaviside function allows to take into account the fact the information is transmitted only when the neuron spikes.

It is interesting to provide the reader with this level of detail for a couple of reasons.

- This is really a good example of a minimal model, and the references show that a lot can be learned even with such a simple choice. For instance, choosing a simple model does

not mean it is a "trivial" model. In this case, complex neural network dynamics emerge at a higher scale [25], while it has been shown that the programming of such network in the deterministic case is equivalent to a precise algorithmic problem (namely a LP-problem) [28].

- In the sequel, at the macroscopic scale of cortical and sub-cortical maps, we are going (with the reset mechanism) to reuse the same basic derivation to propose a minimal 1st order implementation of time-delays as observed in biological experimentation.

A step further, in 1952, Hodgkin and Huxley proposed a conductance-based model –commonly known as the HH model–, which describes how spikes are generated and transmitted directly between neurons. It can be thought of as a differential equation with four degrees of freedom that vary with respect to time t. The system is non-linear and cannot be solved analytically. However, several numerical methods are available to analyze it. The four state variables of the system are $v(t)$, $n(t)$, $m(t)$, and $h(t)$. Respectively, they represent membrane voltage, potassium channel activation, sodium channel activation, and sodium channel inactivation. In this case, since there are four state variables, visualizing the path in the phase space is not trivial. Usually, one can plot 2 variables at a time, where a limit cycle can be visualized. However, this method is ad-hoc to visualize a 4-dimensional system, and thus does not prove the existence of the limit cycle. A better way to study it is to analyze the Jacobian of the system, evaluated at the equilibrium point. In this case, the eigenvalues of the Jacobian indicate the existence of the center manifold, while the complex eigenvectors reveal the orientation of this manifold. This is because, despite having 4 dimensions, the system collapses onto a two-dimensional plane, since there are two negative eigenvalues, and their associated eigenvectors reduce to zero as time increases, while the other two eigenvalues are complex and have slightly positive real parts. In this case, any solution starting off the center manifold will decay towards the center manifold, and the limit cycle will be contained on the center manifold.

If one considers the injected current I to the membrane as the bifurcation parameter, the HH model undergoes a Hopf bifurcation. Here, increasing I leads to increasing the firing rate of the neuron. However, because of the Hopf bifurcation, there is a minimum firing rate. Also, as the cells will fire when stimulation surpasses a certain threshold (the all-or-none law), there occurs a canard transition [183], which is a sudden jump in amplitude, giving the characteristic wave form of the HH model.

Since this model is not a minimal model, many simpler different models, such as the FitzHugh-Nagumo model and the Hindmarsh–Rose model have been developed.

The FitzHugh-Nagumo model [79] is a two-dimensional simplification of the HH model. Its motivation is to extract the essential mathematical properties of excitability and propagation described by the HH model. Its advantage is that while in the HH model one can visualize projections of its four-dimensional phase trajectories, the FitzHugh-Nagumo visualization allows to observe the full solution. This allows to geometrically analyze the behavior of the neuron. The main drawback of the FitzHugh-Nagumo model is that it is not as realistic as the HH model, which is biophysically plausible, or, in other words, that it is too mathematical. This is not really a great drawback, considering it is a great tool for studying neural behavior, as discussed previously. In addition, there are several variants of this model too. One example is the one shown in [51], where the focus is on cooperative variables, and adding the calcium dynamics to account for more types of excitability than previously shown. Also, the passage from a HH model to this variation of the FitzHugh-Nagumo model is straightforward, and presented in detail in [52], while the importance of the inclusion of calcium dynamics is presented in [46].

The Hindmarsh–Rose model [72] aims to study the bursting behavior of a single neuron. To this end, it uses a system of three dimensionless ordinary differential equations. The three variables $x(t)$, $y(t)$ and $z(t)$ represent the membrane voltage, the fast sodium and potassium behavior, and the behavior of slow (e.g. calcium) channels. Its advantage is that it is relatively simple, while providing a good qualitative description of the neural dynamics. Its drawbacks are that, as with the FitzHugh-Nagumo model, it is not biologically plausible, and that it presents unpredictable behaviors, such as chaotic dynamics, if its eight parameters are not tuned properly.

Let us now focus, not on the model, but on the information coded in such a network. All neurons fire action potentials. The main simplification is to assume that neither the shape, nor the magnitude of the action potential, but only the *time* when such event occurs matters. This appears to be a fairly good approximation on the whole nervous system. This is mainly due to the fact that shape and amplitude are approximately fixed and stereotyped for a given neuron. In the case of chemical synapses, the relevance of the assumption is also related to the fact that the emission of the synaptic neurotransmitter is somehow a "all-or-nothing" mechanism: The neurotransmitter emission does not depends on the action-potential shape. In the case of gap junction (i.e., an electrical synapse) models that maintain this assumption appears to be still relevant [32].

As a consequence, *spike is the code* [127]. However, do all spike times matter? The main aspect is that spike time precision is bounded [27]. As a consequence, this code is of rather

limited precision and in coherence with Bialek pioneer works, the authors have shown than the information rate of such code is below 1 Kbyte per second per neuron, even when taking all spike times into account. This weakens somehow enthusiastic positions about rank order coding [120][42] or "liquid state machines".

A step further, the answer really depends on the neural sub-system, and on non-trivial timing characteristics. An extreme situation is the early vision system in fast brain paradigm. In this situation, one spike is enough to trigger high-level categorization of an object [170] (which does not mean that other spikes do not matter). In the retina, using natural images, it has been experimentally established [113] that the spike code is sparse and reproducible: Spike times matter, in this situation. Furthermore, in the retina, spike synchronization is directly related to local image segmentation since homogeneous zones correspond to ganglion cells that fire in phase [62]. The fact that spike times and synchronization is an important cues in the nervous system front end is coherent with the fact that such spikes are generated by coupled mechanism. On the other hand, in the basal ganglia for instance, up to our best knowledge [126], the neural structure afferents are so different that spike synchronization is entirely blurred. This happens because they come from totally asynchronous parts of the brain, and various different stages of the processing of sensory input. This fact has an important consequence for us: though we are going to consider spike synchronization from retinal input at a mesoscopic level, when considering feed-backs from brain areas non-directly connected, it seems that we can forget about such synchronization.

In such cases, only the spiking rate matters. A rate code focuses on the mean firing rate, which is a temporal average, i.e. the number of spikes that fall in a time window, divided by the duration of this window. In other words, rate corresponds to the 1st order momentum of the time distribution. At a probabilistic level, the rate is simply the marginal probability that the neuron fires at a given time, irrespective of all other cues. The rate code has been broadly used for over 80 years. One point is the simplicity to measure rates experimentally, whereas multi-electrodes devices break this barrier. A more important point is that rate captures well-identified information in several parts of the brain: from sensory-input (the filtered image intensity in the retina or the sound frequency band magnitude in the cochlea) to the motor output (e.g., the muscle contraction driven by motor neurons). Another important fact is related to modeling: while the mathematics of spike times is unusual, based on discrete event system formalism for instance in the deterministic case [129], or on sophisticated stochastic derivations in the probabilistic case

[122], using rates allows to reduce the information provided by a neuron to a simple real number. It must be pointed out that this is not only "the simplest simplification". Rate models are formally derived, using the rigorous mean-field formalism [26] and the model reviewed in the sequel of this chapter is directly coming from such works.

At this stage, how can we reconcile rate models with the fact that input synchronization matters? The answer is given by the fact that, as far we are concerned, beyond rate, the main temporal information is spike correlations, i.e., 2nd order momenta of the time distribution [127]. Up to 80% of the information is represented by 1st order (rates) and 2nd order momenta. This means that we not only consider a scalar representation (i.e. a unique number) of the neuron activity, but a vectorial representation at the network level. Considering the retinal output, as already mentioned, the situation is even more precise: we need the rate and phase [62], the latter allowing to code for the grouping of regions. This has been extensively studied in a collaboration realized at the beginning of this thesis [168].

In this work we consider mainly rate models, plus additional scalar quantities to take into account specific phenomena. Interactions of interlaced information pathways in the system of brain loops only consider rates, because as other authors we can assume with no risk that spike synchronization is blurred, at least at our level of description.

2.1.2 Driver/Modulator considerations

In 1998, Sherman and Guillery proposed that we can distinguish two types of inputs to cortical neurons; drivers and modulators. Driver signals are carried by fast ionotropic receptors, whereas modulators correspond to slower metabotropic receptors [151]. These two forms of input help to explain how, for example, sensory driven responses are controlled and modified by attention and other internally generated feedback signals. However, the distinction between driver and modulator inputs is mainly functional and changeable rather than anatomical and fixed. Driver inputs are carried by excitation and inhibition acting in a push-pull manner (increases in excitation are accompanied by decreases in inhibition and vice versa) [1].

Modulators correspond to excitation and inhibition that they increase or decrease together. A step further, [54] proposes a link between feedforward/feedback connections and the driver/modulator property.

In [54] the visual cortex is considered as a hierarchy of cortical levels with reciprocal extrinsic cortico-cortical connections among the constituent cortical areas [48]. The no-

tion of a hierarchy depends upon a distinction between forward and backward extrinsic connections. This distinction rests upon different laminar specificity [130][140].

In this context, *forward connections are driving and backward connections are modulatory*, as suggested by reversible inactivation [141][60] and functional neuro-imaging [13]. In some paradigms, backward connections may also be functionally driving the signal if their latencies are shorter than forward connections between distant cortical maps [171]. This fact is compatible with the present formalism.

More precisely, *forward* connections are concerned with the promulgation and segregation of sensory information, consistent with: (i) their sparse axonal bifurcation; (ii) patchy axonal terminations; and (iii) topographic projections. On the other hand, *backward* connections are considered to have a role in mediating contextual effects and in the co-ordination of processing channels, consistent with: (i) their frequent bifurcation; (ii) diffuse axonal terminations; and (iii) non-topographic projections [140] (iv) slow time-constants.

Backward connections are more numerous and transcend more levels, e.g. the ratio of forward efferent connections to backward afferents in the lateral geniculate is about 1:10/20. Another example: there are backward connections from TE and TEO to V1 but no monosynaptic connections from V1 to TE or TEO [140]. Backward connections are more divergent than forward connections [191], one point in a given cortical area will connect to a region 5-8mm in diameter in another. For instance: the divergence region of a point in V5 (i.e. the region receiving backward afferents from V5) may include thick and inter-stripes in V2, whereas its convergence region (i.e. the region providing forward afferents to V5) is limited to the thick stripes [191]. They are faster than direct lateral connections [116]. As a consequence, forward connections preserve retinotopy in visual areas, whereas backward connections do not [14].

This is summarized by [54] as reported in Table 2.1.

Following [14], we must emphasize the fact that cortical visual processing requires information to be exchanged between neurons coding for distant regions in the visual field. Feedback connections from upper-layers are best candidates for such interactions because Magnocellular layers of the LGN very rapidly project a "first-pass" information used to guide further processing in IT. One step further, [5] demonstrate that the so called "horizontal connections" (i.e. within a cortical, e.g. retinotopic, map) are not fast enough to account for such a transfer, considering the known timings of information transfer [116].

More generally [54], feedback connections are essential when the relationship between

Forward connections	*Backward connections*
Sparse axonal bifurcations	Abundant axonal bifurcation
Topographically organized	Diffuse topography
Originate in supragranular layers	Originate in bilaminar/infragranular layers
Terminate largely in layer 4	Terminate predominantly in supragranular layers
Postsynaptic effects through fast	Modulatory afferents activate slow
AMPA (1.3-2.4 ms decay) and	(50 ms decay) voltage-sensitive NMDA receptors
GABAA (6 ms decay) receptors	
Forward connections are concerned with the promulgation and segregation of sensory information, consistent with: (i) their sparse axonal bifurcation; (ii) patchy axonal terminations; and (iii) topographic projections.	*Backward connections are considered to have a role in mediating contextual effects and in the co-ordination of processing channels*, consistent with: (i) their frequent bifurcation; (ii) diffuse axonal terminations; and (iii) non-topographic projections [140] (iv) slow time-constants.

Table 2.1: Forward/Backward connections connections main properties, from [54]. Postsynaptic/modulatory effect is a conjecture, so is assumptions on synapses mechanisms.

retinal inputs and the stimuli that generate them is not invertible. This is the case for practically all situations of vision outside the laboratory because of the interactions between the stimuli and the importance of the context for a given stimulus [54]. In the work of Rao and Ballard[125], the way internal representations and incoming signals are combined is mainly subtractive : only differences are transmitted to higher levels. However, all studies of feedback connections so far [14] converge to conclude that feedback influences act to potentiate the responses of neurons at lower levels. In our framework, this occurs by tuning the cortical map parameters, formalized now.

The question here is to analyze such interactions when considering regularization mechanisms, i.e. study how our model may be used considering several interacting cortical maps.

If we focus on the thalamus, not all afferents to thalamic relay cells are equal, and it is important to identify which input carries the information to be relayed. The retinal input to the lateral geniculate nucleus and medial lemniscal input to the ventral posterior lateral nucleus are drivers because of their ionotropic characteristics (cf. beginning of this Section). All other inputs, as being feedbacks, such as those from layer 6 of cortex and the midbrain, are modulator inputs and determine how driver inputs are relayed.

A step further, one aspect of this modulatory role is the control of the firing mode and its switching between tonic and burst [148]. The firing mode concerns all cells in LGN (Parvo and Magno [148], but also Konio [181]) and is controlled by cortical feedback connections [148] and TRN [90]. The functional role of this switch might be related to proper information transmission and processing, as pointed out in [148]. One goal of the present work is to analyze this assumption, considering the early visual system as a whole.

Regarding LGN and pulvinar, as the pulvinar has many similar points with LGN, but receives cortical information (from several areas) instead of peripheral (retinal) information, these firing modes are also controlled by the cortex and TRN. The functional role of these modes could be the same as in LGN, but for cortical information.

In the retina, the standard cells project to the core cells in LGN, while non-standard cells project to the matrix cells in LGN. In addition, parasol cells project to the superior colliculus. Standard retinal cells code characteristics such as color, contrast, motion and texture, while non-standard retinal cells code coarse prediction, segmentation and looming motion, among others.

A step further, this duality of input types might be applied to other brain pathways. One instance is the glutamatergic pathways in cortex [115] where this driver/modulator distinction holds. For example, information arriving at the cortex from the Magno cells of LGN is first sent and processed in the parietal cortex. Only then, lower visual areas (V1 and V2) carry on with their processing, i.e. information is retro-injected from the parietal cortex to guide, modulate, further processing of Magno, Parvo, and Konio-related information [14]. These feedback flows are modulatory, since they do not directly generate an output, but instead allow for the modulation of the selectivity or specialization of these lower-order areas [55]. These considerations are useful for our work as we implement local topographic modules, where the different information flows will interact following the driver/modulator classification.

In our work, we propose a minimal implementation of the fact that driving information is regarded as a base term, while modulators are considered as multiplicative/additive. The basic equation we consider writes

$$y = d * (1 + m)$$

The output y depends directly on d, the driving signal, while the modulatory part acts as a gain adjustment. The multiplicative sign $*$ may stand for either a simple local multiplication (i.e. a gain) or a local convolution. The latter choice allows us to implement the

fact that modulatory feedbacks are divergent and also correspond to a spatial filtering of the upper layer information.

2.1.3 Specification and validation of parameter values

Minimal model also implies to keep a reduced set of parameters. Here, we reduce adaptation gains and limiters (lower or upper bounds, i.e. threshold and saturation) to a minimal set. This is obtained by the following generic specification choices:

- all quantities are normalized to avoid any offset/gain scale change,
- linear models (i.e., without additional parameterized non-linear bounds) are used, except if non-linearity is mandatory[1],
- spatial and temporal convolution kernels are avoided when the related temporal or spatial scale is negligible,
- each parameter is specified with a default value (e.g., offset to zero, gain to unity, etc) and modified only if required.

This is the reason why our "$y = d * (1 + m)$" is proposed keeping the amount of parameters to a minimum.

Despite these factors, these simplified conditions precisely correspond to efficient results regarding our numerical experiments on real images. This will be a major result of this work.

A step further, numbers have to be chosen. They are, indeed, taken from biological data. However, not the value but the value range or order of magnitude is meaningful. In our case, we have use the simple, deterministic (avoiding probabilistic formalism) but systematic design choice.

- A prototypical value is chosen from the literature
- Model performances are systematically tested for each parameter value variation, with the following rules:
    1. If a small (say, $\pm 10\%$) variation impairs the performances or qualitatively change the system behavior, this means that the model is *inappropriate*

[1] Provided by the literature, or part of the hypothesis with corresponding justification.

2. If a large (say, ±100%) variation does not affect significantly the performances, this means that the parameter is
   - either *useless*, thus set to a default value,
   - or a scale constant, used to map one numerical range to another, also set to a fixed value
3. Otherwise, this means that the parameter is meaningful for the given model

A model is thus numerically *inappropriate* if a tiny value change impairs the obtained behavior. This does not correspond to the biological reality, where parameter value variability is widely observed. This also means that the model is *not robust*, i.e. it behaves "by chance" as expected. Equivalently, it means that the model predicts unexpected spurious behaviors, thus is not a pertinent representation of the observed phenomenon.

A systematic test of parameter values has been conducted, as ensuring stability is an important component for the performance of the simulation. To test this aspect, we simply vary each parameter in the simulation and run it again, once for every change, so as to check how results differ due to this variation. This could be a healthy measure as well to recognize if a parameter is not adding anything to the result, so as to remove it and/or modify the computation accordingly.

Here, variations of -100% to +100% are used for the parameters, where in most cases they cause only violations of bio-plausibility –meaning a unit has more than 100% activation– however some instabilities have been encountered, and are reported in Section 4.2.2.

2.1.4 Filters and information processing

Any device transmitting part of its input to its output can be called "a filter". This includes transforming the signal, removing part of it, and the broad idea here is that the essential features of the analyzed stimuli are kept, while some parts are enhanced, diminished or simply modified.

Specially relevant for this work are spatio-temporal filters. Considering image processing, spatio-temporal filters will be mainly used for smoothing, via convolution with a certain kernel (matrix). This "smoothing" is also a way to interpret the processing in a receptive field (cf. section 1.2.1) computation, where information from neighbor cells in the structure is taken into account for the computation of the output of the analyzed neuron.

Motion filters follow a similar idea, where information from a region yields the output of a unit, computing temporal differences (i.e., velocity related information). The emphasis

in analyzing motion is obvious, it is a different functional treatment, but the principle is the same: removing the useless information (contrast, etc..) and only considering motion.

We, obviously do not claim that this is sufficient to encounter for early-vision and cortical-vision processing (see [47], for a complete modeling of visual motion processing). We claim that this is the minimal fallback specification, and we will observe that it is numerically sufficient for the thalamus modeling (while more sophisticated mechanisms are required at the visual front-end level).

The spatial filters we employ are generic Gaussian filters, while the temporal filters are exponential filters. These choices are to keep the model minimal. A generic isotropic Gaussian filter can be expressed by a spatial convolution kernel of the form:

$$f(\mathbf{x}) = a\, e^{\left(-\frac{|\mathbf{x}|^2}{2\,c^2}\right)} + b,$$

where a, b, c are real variables, i.e., the filter gain a, offset b, and width c (i.e. radius). It is a minimal representation of smoothing.

A generic exponential temporal filter is represented by a temporal spatial convolution kernel of the form:

$$f(t) = e^{-\frac{t}{\tau}},$$

where τ is the time constant for the exponential decay. It is a minimal, first-order, differentiable representation of a delay, comprising both the processing time, and the transmission time in one value.

Here we use three information incoming flows, and their retinal implementation [186] (cf. section 2.2.1) is particularly interesting. Differential motion filters are used to compute the Magno-like information, where not the optical flow but image intensity temporal difference is computed. It thus accounts for positive or negative variations only (i.e. without the direction of the movement vector). Spatial filters are used for the Parvo-like information, where the idea is to estimate the image contrast. This is easily generalized to color (i.e., multi-channel images), though for this version of our work we only use the image monochrome contrast, but color intensity information. With such a linear model, three important features of these two retinal standard pathways are neglected: Contrast gain control [187], saturation and threshold. This is however acceptable in our context.

On the contrary, a combination of different filters is not sufficient when considering the Konio related information processing [62]. In this case, non-standard retinal ganglion cells processing includes a combination of motion, contrast, and color information, to account for

the pre-wired stimuli they are tuned to (cf section 2.2.1) and more sophisticated algorithmic modules are to be considered.

2.1.5 Dynamic Neural Fields

Neural fields are tissue level models that describe the spatio-temporal evolution of coarse grained variables such as synaptic or firing rate activity in populations of neurons [33].

The underlying Dynamic Neural Field (DNF) theory is mainly concerned with the functional modeling of neural structures where information is considered to be encoded at the level of the population rather than at the level of single neurons. Such models first appeared in the 50s, but the theory really took off in the 70s with the works of Wilson and Cowan [185] and Amari [4]. At the level of a single neuron, the model that is used is a mean frequency model, while the electrical activity of a neuron is approximated by a single potential. However, there also exists several spiking neuron models that represent both a finer and more accurate model of a real biological neuron. In the framework of the DNF, such models allow to bypass the inherent limitations brought by mean frequency models [137], this being taken into account via vectorial neural state [12]. Furthermore, neural-fields also allow to consider high-level representation of cortical computations [180].

These models most generally use excitatory recurrent collateral connections between the neurons as a function of the distance between them and global inhibition is used to ensure the uniqueness of the bubble of activity within the field [133]. They exhibit so-called bump patterns, which have been observed in the prefrontal cortex and are involved in working memory tasks [53] or high-level cognition [166].

The dynamics of pattern formation in lateral-inhibition type neural fields with global or local inhibition has been extensively studied in a number of works where it has been demonstrated that these kinds of fields are able to maintain a localized packet of neuronal activity that can, for example, represent the current state of an agent in a continuous space or reflect some sensory input feeding the field [133]. A step further, the linear response of neural fields to localized inputs subject to finite propagation speeds has been studied in [75]. The characteristic behavior of such fields is the formation of very localized packets of neural activity that tend to represent some consistent information which is present at the level of the input [66].

The main computational properties (see e.g., [133] for a review) of such neural field are:

1. filtering of the output bump shape: increase versus decrease of size, volume, etc.

2. selection of the output bump among several input bumps,

3. tracking of a moving input bump at the output level,

4. remanence of the output bump after the partial or total suppression (inhibition) of the input bump.

We are going to consider filtering and selection behaviors in this contribution and discuss the tracking and remanence mechanisms also.

Here, we use them as a "summarizer" of how the cortical column works, as well as the mechanism how the deep superior colliculus chooses the most salient stimulus.

Let $u(x,t)$ be the membrane potential of neuron x at time t, f a transfer function, y the distance between neurons x and x', v the velocity of an action potential along axonal fibers, and w a lateral kernel function. Then, the evolution of $u(x,t)$ is given by:

$$\underbrace{\tau}_{Time\,constant}\frac{\partial u(x,t)}{\partial t} = \underbrace{-u(x,t)}_{Decay} + \int_{-\infty}^{+\infty} \underbrace{w(y)\, f\left(u\left(x', t-\frac{|y|}{v}\right)\right)}_{Lateral\,interaction} dy + \underbrace{I(x)}_{Input} + \underbrace{h}_{Threshold} \tag{2.1}$$

Normally, equations for $w(y)$ are differences of Gaussian (DoG), where one can find local, global or asymmetric inhibitions.

Dynamic neural fields (DNFs) evolve dynamically under the influence of sensory inputs as well as strong neural interaction, generating elementary forms of cognition through dynamical instabilities. Through DNFs one can establish links between brain and behavior –such as decisions regarding saliency–, and thus the modeler can derive testable predictions and provide quantitative accounts of behavior. This is our aim when using them in the cortex and the deep superior colliculus.

2.2 Functional view of the neural system: the systemic level

2.2.1 Functional interpretation of retinal mechanisms: non-local filtering

Understanding the retinal output, i.e., the output of the different networks that end in the retinal ganglion cells, keeps challenging scientists, nowadays more than ever. One approach could be to observe the retina at a mesoscopic level, where the properties of the different

cells are comprised within the network, with an emphasis in the function of the biological tissues, like explored in [168].

Since the main biological constraint of the retina in terms of information transmission is the 10^2 compression factor for Parvo cells up to 10^3 for other GCs in the optical nerve, reducing the noise with respect to the signal is a major issue. The noise added by the photo-transduction mechanism is obviously to be filtered, but what is to be considered as signal versus noise in the incoming visual flow is task dependent. For instance, the background motion induced by ego-motion is a "noise" with respect to object motion recognition but a relevant signal with respect to gaze stabilization (the optokinetic reflex for instance has the background motion as main input cue). Furthermore, there is a "local" notion of noise (i.e., a random spurious additive signal, locally correlated in space and time, or not), but regarding the visual perception, there are other notions: A notion of "outliers" (i.e., spurious piece of signal not to be taken into account to avoid bias, e.g., a spurious light reflection) and a notion of "inliers" (i.e., piece of signal coherent with the ground base data but inducing a misperception, e.g., a shadow.

The concept of noise reduction is no more related to a local filter, but to non-local operators, since the context matters. In other words, filtering means estimating a given zone in the image, thus to perform image segmentation. This non-local idea of filtering corresponds to the grouping of homogeneous information, reducing small or spurious non-significant variations, and then produce a reduced representation in which outliers are eliminated because they are not homogeneous with respect to the information neighborhood, while inliers are grouped in another region to be further treated as signal or noise depending on the perceptual task. Such mechanism of synchronization is well-known in the retina [61][155]. In a nutshell, spiking rate of GC for the signal intensity and inter-GC synchronization codes from the fact they correspond to the same signal region. In other words, the relative phase between the periodic GC spiking generators code for the region indexing. This is in relation with the fact that shared noise from photo-receptors is a major cause of correlated firing [65], so that synchronized GC outputs correspond to activity with the same stochastic signal characteristics.

Furthermore, it is important to point out that we do not group regions of homogeneous "intensity" but regions of homogeneous response to the 2D+T filtering discussed above, e.g., of the intensity, intensity variation, contrast, local edge or motion pattern, etc. It is important to remark that time, here, is considered only as a local feature. As a consequence, such mechanism should be able to segment on complex local spatio-temporal

patterns. In particular, as very nicely explained in [62] after [73], texture motion, even if the average local intensity remains constant, is locally detected: During texture motion, different intensity-variation cells respond at different time to different spatial patterns at their receptive field locations, showing the same activity profile, inducing a cumulative effect related to strong rectification (summing only positive responses in the neighborhood with both excitatory and inhibitory responses). It is a perspective of this work to numerically verify that texture motion is also compatible with such variational approach, as discussed by [117]. This is, however, a rather easy task since such cue is easily computable by such variational approaches [6].

In [168], a variational framework is implemented as a simple mechanism of diffusion in a two-layered non-linear filtering mechanism with feedback. The goal is to capture specific functionality, such as a response adapted to the stimulus, the reduction of non-local noise (i.e. segmentation), and the detection of visual events. For this last point, several visual cues are taken into account: contrast and local texture, colors or edges, and motion. The work presented in [168] was developed with a special interest in natural images.

To achieve such goal, computer vision methods are used, using the two-layered network mentioned previously as the input transducer, where the visual event detection is carried out by a prototype-based non-linear diffusion algorithm.

As discussed in section 2.1.4, these motion cues are grouped and used depending on what information flow is treated. In the case of the midget cells (part of the Parvo pathway), the cues are image contrast and color bands –though we only use the contrast one so far for this pathway–. In the case of parasol cells (part of the Magno pathway), the cue is differential motion. And in the case of non-standard cells (part of the Konio pathway), cues of contrast, color and motion are used to provide the coarse detection capabilities of these cells (cf section 1.2.3).

2.2.2 Functional interpretation of retinal mechanisms: visual event detection

The retina is able to detect sophisticated visual events such as:

(i) Fine spatial information, as observed qualitatively with natural image sequences, a GC being often either silent or sparse by deterministic firing for a given image category [159];

(ii) local approaching motion, which is known as being computable by a local divergence

filter [162], i.e., the weighted sum of dedicated local masks.

Such a functionality includes anticipation, either motion extrapolation or omitted stimulus response [144], these complex computations coming about through the interplay of rather generic features of retinal circuitry [62]. In both cases, as expected, spatio-temporal pattern yields adaptation (delay reduction in the former case, response habituation in the later) and an unexpected event induces a strong reaction. The time window order of magnitude is the second. This is thus not directly derived from a 2D+T filtering mechanism (its temporal window being too short) but by a local fading memory of previous input, thus using regressive feed-backs, and the simpler model we propose here is a simple auto-regressive mechanism. The key point is that this induces a switching mechanism, the detection of a visual event modifying the local parameters on the retina. With [62] we assume that the switching "may be initiated by much more subtle image features", precisely by the detection of a given visual event.

Regarding the detection of such fast visual event, it has already been investigated in detail how GC and subsequent layers can produce early responses to a visual event [177][171]. We assume here that, if such a mechanism is able to produce a detection at early stages in the visual system, it is likely produced by a large contribution of the retinal processing. This is plausible because the corresponding bio-plausible most efficient computational method is a one layer method implementable a simple non-linear filter with threshold effect [179]. This is related to the so-called Support Vector Machine (SVM) algorithm, and the bio-plausible implementation is a simple competition between units coding similarities with respect to prototypes. This may be implemented as a two steps process: correlation with prototyping responses and competition between the outputs, as implemented in a standard one-layer architecture with lateral inhibitory connections, which is the case of the OPL.

We do not study here how the retina has learned throughout evolution to recognize such events (remembering that the retina of animals, before that of mammals, was provided with feedback of descending pathways from the brain, which has probably played a role in this learning process). But referring to the statistical learning theory and the related SVM algorithm [179] allows us to assume that only a *little* set of prototypes has to be recruited for the detection of an event. Moreover, "approximate" prototypes are sufficient, since the prototype of a category can be wrong as far as it is less wrong than a prototype of another category. It is thus reasonable to assume that this is a biologically plausible functional model of the retina, since it is able to detect rather complex spatio-temporal visual events.

As already pointed-out, the major argument is that it is pertinent to use the full retinal resolution to perform the recognition before the optical nerve spatial compression.

This view is also coherent with the observation that in the presence of natural stimuli, GCs have a sparse and deterministic behavior. Sparse because they react in terms of detection of not a given visual event. Deterministic in the sense that they fire a spike response at reproducible times. This is also coherent with observations already reviewed that the response is not limited to a "local visual field", since there is no significant visual events at such small case, but at higher sizes of the visual field. The fact that the response of Konio cells corresponds to events in a $10deg$ of the visual field seems properly tuned to natural visual events [70].

In machine learning, a support vector machine (SVM) is a supervised learning model with algorithms that analyze data and recognize patterns. In our work, it will be used as a classification tool.

Given a few training sets (groups of stimuli, manually classified into categories), an SVM algorithm builds a model that assigns new examples into the categories, making it a non-probabilistic linear classifier. The idea is that these categories will be represented in an N-dimensional space with clear separations, where new examples can be mapped, and thus their category predicted.

Basically, in this work an SVM is used for stimuli discrimination in non-standard ganglion cells, part of the Konio pathway. Considering that the training mechanism used for them can be considered transparent[2], an SVM is well suited to allow for a multi-dimensional categorization, where an N-dimensional space with sub-spaces for the different categories will be generated. This tool is then applied topographically, thus having a non-standard topographic categorization mechanism to analyze the different regions of the incoming visual scene. The resulting information will be used as the non-standard retinal output.

In [179], the authors present a Hebbian Learning Rule for an SVM classifier. This means that neurons can strengthen their synapses through adaptation to stimuli, and thus "learn". In our case, however, as we stipulate non-standard ganglion cells have pre-wired mechanisms, we want this learning to be done beforehand, and not to be modified afterwards. The principles used in [179] are reused in [168] (cf. section 2.2.1), giving us the first step to generate our mold to shape the pre-wired mechanisms here considered.

[2]Since they are considered having pre-wired mechanisms, and thus the training is done before the actual simulation.

In order to train such a classification tool, different "training sets" are given to it, where a multidimensional space is evaluated, so as to have a clear separation between the mappings of the different training sets. For the sake of simplicity, though not really a proper practice, one can use a few samples of the real stimuli to generate the categories for the training set as in [179] and [168]. The situation is robust enough for this to be efficient, as visible also in our result. This is a good argument in favor of the fact we propose here a robust mechanism of categorization.

2.2.3 Functional interpretation of thalamic mechanisms

The thalamus is here considered only as composed by LGN and TRN. Considering that it is the synchronization center between retinal, collicular, and cortical information, the relevance of the computations here carried out deserves a deeper explanation.

Intuition, inspired by [67] and others, leads us to develop a mismatch algorithm for TRN. Since TRN receives both retinal feedforward, and cortical feedback information, one can think that the following inhibition to LGN will target the elements that are not really being considered in the cortical analysis, so as to help with the processing of the "important information". However, an alert mechanism first developed in the retina, and verified by the superior colliculus, can override this "importance", and allow for other information to be prioritized. For example, when an organism is feeding itself, and a predator is suddenly detected attacking this organism. Here, an action must be carried out as soon as possible, or else the organism could have an unhappy ending on site.

The core part of LGN is by default a relaying one. However, when including cortical feedback, inhibition from TRN, and the collicular alert signal, the computation paradigm shifts accordingly. Out of these three, the one not precisely considered here is the first, the cortical feedback. This flow serves as a reinforcer for "important information", enhancing its treatment with excitatory modulation [181].

The matrix part of LGN is by default a modulatory one. With non-standard flows of information as input and output, this structure will transmit a modulatory signal to the cortex, that may include an alert, result of the detection of threatening stimuli without perceptual awareness [100]. Intuitively speaking, out of all the possible "important" targets (retinal prewired stimuli, cf. section 1.2.3), it should topographically detect one, and transmit it, so these targets can be prioritized.

2.2.4 Assembling populations into networks

Once having local models for cell populations formalized as neural maps, connectivity betwen such maps is the way distributed larger-scale functions are implemented.

Here, a prime complexity is the concurrence of structures with different timings. Fast raw processing allowing to raise the alert and interact with slower more detailed computations, allowing the system to perform pertinent behaviors. This timing aspect includes both processing bandwidths and delays of the different structures to communicate the present data, the latter as a function of the processing time and transmission delays.

Another complexity is related to the different resolutions that interact (e.g. Parvo, Magno and Konio pathways have small, middle and large resolutions), with divergent and convergent links. As detailed in this chapter, each functionality is implemented at a suitable resolution. As a simple example, there is a need to detect a predator urgently, but no need to detect precisely its location since the induced behavior (run for your life!) only needs the rough escape direction.

These two computational aspects are included inside an architecture with loops, including feedbacks, as made explicit previously. So the task is a beautiful one: to have everything working properly considering phenomenological models, taking the real neural architecture and biological constraints into account.

The issue is not only putting all modules together in order to make them work, but to construct a global view of the functionality of the system. Unfortunately, at this level of complexity there is no closed-form result that guaranties stability and convergence, and we must proceed using heuristics. Let us detail our method:

- **Ensuring stability: Fighting against loops** Basically, two potential issues that can arise from loops: accumulation and persistence.
  - *Accumulation*, i.e. unbounded drift, corresponds to the fact that, within a loop in continuous work, certain variables potentially keep increasing (or decreasing), without regulation. Implementing saturation mechanisms, *de facto* avoids –but does not solve– the problem (yielding system blocking or oscillations, etc.). Here, we use another design choice: consider as much as possible linear operators in loops. In such a case, ensuring stability is a well-defined and known task, with straightforward solutions. When non-linearity is introduced we easily maintain the stability since they add more bounds. This simplification is equivalent to upper-bound our non-linear system by a stable linear system. This

design choice includes the thalamocortical loop, which could have potentially non-stop increments of signal value as the internal connections could have kept feeding the cortical feedback, but that remains stable in our model (as in the biological reality).

- *Persistence* means that a certain variable value stays circulating in the loop without vanishing, despite not existing in the input anymore. This property is indeed precious for short-term memory, e.g., taking previous contextual data into account. The problem here is to control this persistence. For example, when a mismatch is detected, the feedforward information transmitted again via a feedback is important to detect the mismatch, but has then to be canceled (see section 1.4.1). The key-point, in such a case, is to change the system regime: A thresholding mechanism takes care of introducing fast temporal decays. This is implemented very naturally via a driver/modulator mechanism: The driving influence of the input, as the feedback is modulating, can be canceled/maintained depending on the task.

Indeed, in both cases, there is no external mechanism (supervisor) checking these values: it is an emergent property of the system. Furthermore, we have experimented a very simple but powerful method to numerically "fight against loop". The idea is to start with a system in open-loop (choosing a minimal set of connections cut in the network graph). The knowledge of the phenomenological role of each sub-system helps finding the pertinent cut. Then we incrementally close the loops (no more than five in our model) and can numerically verify both accumulation and persistence.

- **Ensuring convergence: How to stack modules** All modules need to be thoroughly stacked to ensure everything will work as a solid structure. Let us consider the two main points: resolution mapping and information fusion.

  - *Resolution mapping* corresponds to the fact that due to convergence and divergence connectivity, there is an ability to "zoom" in or out the processed data. Making the different maps congruent with each other is straightforward. Less obvious is the effect on the dynamic. As carefully studied by [180] on a generic example, spatial diverging feedback acts as a temporal stabilizer, avoiding introducing temporal delays. Let us detail this key point: When a closed-loop oscillates, one trick is to increase the feedback delay which decreases the oscillation frequency up to a non-oscillating bifurcation. However, this is not a very

efficient choice, in terms of system reactivity. Here we do not consider a punctual system but a data field. If spatial filtering is introduced, local oscillations are averaged by other random values and, providing the system is not feed-up with a constant homogeneous value, stability is obtained. Each unit benefits from neighbors thanks to such linear kernels.

– *Information fusion*, in this context, affects processing in two ways, the driver/modulator computation paradigm (cf. Section 2.1.2) and, beyond, the fact that different cues are bound together, for instance the Magno-related and Parvo-related motion and contrast data ("related" because they correspond to the same area in the visual field). Here, a simple linear mixing of the two data maps does the trick. This is a strong limitation, since we do not take into account the physics of the information. For instance, when combining contrast magnitude with intensity variation (i.e., Parvo and Magno) we obtain optical flow information. This combination is however not linear, and it has to be computed as the ratio of the latter by the former [47]. Luckily enough, this is going to be sufficient in our numerical experimentation as we focus on visual gaze (saliency).

Dealing with loops is thus a specific topic. Knowledge comes from the literature, where the different anatomical connections are described, and the only major consideration here is the "no-strong-loops hypothesis" (cf. section 1.4.1). Since we cannot provide *a priori* information about what happens in such a complex system, this work aims to recreate such an auto-organizing system, in order to experiment (using numerical experiments) what is observed in terms of stability of loops.

2.2.5 Implementation details

Though, it is admitted that thanks to evolution, more complex capabilities have emerged for the whole network by natural *essay and error*, i.e. mutations in interaction with self-system organization [119], the PhD duration was a bit short to wait for our system to auto-program the required modules by itself. Computational models do not have the time to evolve and the modeler has to compensate with good approximations and faster learning algorithms.

In the case of the work presented in this thesis, and through the systemic approach, each component is modeled in a simple but bio-plausible way and integrated, to this end, as a dynamic asynchronous ensemble of modules. This is built on top of DANA [132],

a framework specialized in such distributed processing mechanisms, where each unit is considered as a set of arbitrary values that can vary along time under the influence of other units (including itself), while also being able to implement local learning capabilities.

In such a framework, a network is: distributed, i.e. there is no central supervisor; asynchronous, meaning there is no central clock; numerical, which means computations are explicit and no symbols are used (as in algebra); and adaptive, so something may be learned. In the version used in this work, however, synchronous approximation is used as results are similar when properly considering the time-related variables of the differential equations [165][134].

As shown in the previous chapter (cf. section 1.7), several different time variables are part of the system here studied. Not only the different timings in transmission, but also in processing must be considered. Fortunately, as one uses differential equations in DANA, here the main task is creating proper equations that will represent asynchronous results, when the actual computations are synchronous. To do this, two parameters are to be carefully tuned in the differential equations [165][134]: the time constant τ, linked directly to the neural timing (e.g. 100ms for changing in burst/tonic modes, cf. section 1.4.1), and the integration time step Δt (e.g. 10ms to be small enough to consider real spiking times, even when working with rates; cf. section 2.1.1). These time variables are considered as constants. Other constant time variables are the different latencies, which are included either as delays outside, or time constants inside the equations. The choice of having both options is only made for readability of the equations, as they can be included directly inside the processing mechanism of each structure.

Our system targets natural image scenarios, where it will explore the scene and, depending on the results from the different evaluations, will change its attentional focus. A natural image, or an image from a natural scene, has a statistical structure the visual system is adapted to [76]. For example, if some dangerous stimulus is present, while other "normal" stimuli are there as well, it will focus its attention on the dangerous one. The input to the system is the visual stimuli presented to the retina, and transformed into an activation map. In this work, sequences (of natural images) are used. Sometimes these "natural" images contain "not-so-natural" stimuli, like man-made objects, that have not had the time to be included in our pre-wired streams, considering evolution. Despite this fact, and just for illustrative purposes, one can train a non-standard stream to be attentive to man-made objects. When working with natural images in a computational model, one core decision is whether we want our model to be biologically plausible, this meaning

that the algorithms should respect and predict results measured from biological systems of the studied type or structure. In order to work with these images, we will use the CImg library[3]. Re-using the work of [168], we have written a Python wrapper to extend not only the additions to the CImg library, but the library itself.

Once finished, one would like to measure the performances of the simulation. To this end, the easiest test is to check whether the focus corresponds to a relevant target, which corresponds to a qualitative analysis, and could be easily done by an external observer. This can be done either qualitatively, where an external observer could say that the results seem good, for instance; or quantitatively, where a numerical value will determine the "goodness" of the model. Moreover, a sometimes hidden aspect is how well a simulation responds to variations of its parameters, where the quantitative analysis is essential.

In order to quantify the performances, one can instead consider –for simplicity– a fake focus point, where a subject would (more or less) focus, and compute the (euclidean) distance between the subject focus and the simulation given point. Of course this analysis would be more realistic if an actual device would measure the focus of a subject, or the average focus of many subjects, but for the sake of simplicity the previous approach has been used in this work.

Notations used in the next chapter

In the next chapter, all equations use the notations of Table 2.2.

2.3 Conclusion

When developing a minimal model, the main idea is not only to reduce complexity to a level easy to handle, implement, and explain, but also to guaranty both minimal complexity and falsifiability of the model. By minimal complexity, we mean that to reproduce a given behavior, we have chosen non superfluous mechanisms, so that the model is not going to predict spurious results. By falsifiability, we mean that the model does not predict everything, thus anything, but take the risk to bet some new unpredictable phenomenon.

In our case, the complexity of the early visual system is first distributed among the different structures, generating *modules* where *local computations* are carried out. The idea of distributed complexity arises from complex, emergent, behaviors: we implement local

[3] http://cimg.sourceforge.net

Table 2.2: **Notations used in the different equations**

Symbol	Meaning
$\times$	Convolution in time
$*$	Convolution in space
$a_x, b_x, c_x, ...$	Gain or Kernel for connection x
$H(x)$	Heavyside function of x
$\overline{H}(x)$	$1 - H(x)$
$\mathcal{L}$	$\begin{bmatrix} 0 & 1 & 0 \\ 1 & -4 & 1 \\ 0 & 1 & 0 \end{bmatrix}$
$\mathcal{Z}$	$\frac{1}{16}\begin{bmatrix} 1 & 2 & 1 \\ 2 & 4 & 2 \\ 1 & 2 & 1 \end{bmatrix}$

computations, and through the different interactions, structures and loops, the complex computations are possible. For each structure, we consider its known anatomical inputs (cf. Chapter 1), where if their role is not fully known, we hypothesize on how they could work inside the local computation.

Each local computation is itself a simplification from the "full mechanism". Our local computations are either taken from the literature, or based on it and reduced. For instance, we reuse algorithms for standard retinal cells, while the mismatch mechanism for TRN is based in work such as that of [67]. In short, the idea is to keep the model as linear as possible, minimizing the amount of non-linearities, where computations can be expressed as spatio-temporal convolutions, where the temporal ones are first-order as they can be represented by delays.

Apart the straightforward combination of drivers and modulators (cf. section 2.1.2), the cortical column (cf. section 1.3) is reduced to a dynamical neural field (cf. section 2.1.5), which represents the behavior of the column in a simplified way.

Among the restrictions, one should also take into account the fact that the resolution of our system is homogeneous, i.e., not making a serious distinction of density of certain neurons in central and peripheral regions. Also, binocularity is not directly considered, as we work with one information flow.

As for the different parameters of this model, we have chosen them by hand, and test

the ensemble while testing the individual modules. We could have also done a systematic research (e.g. [8]) to tune the parameters, but we have opted for an *a posteriori* validation.

Chapter 3

Implementing a non-standard early visual system

Contents

3.1 Summary of previous sections 69

3.1.1 Architecture of the system 69

3.1.2 Dynamics of the system 70

3.2 Our model of the early visual system: modular view 71

3.2.1 Retina: Standard and non-standard cells 73

3.2.2 Thalamus 75

3.2.3 Primary visual cortex 79

3.2.4 Superior colliculus 79

3.2.5 Summary 82

Summary

The previous chapters have given the bases to understand this work. In this chapter, we present the different modules of our model, while in the next chapter, numerical results will be presented.

Each module carries out a local computation, and corresponds to a well-identified brain structure. Here, indeed, global emergent properties are not hard-built, but eventually appear as a result of the interactions between the different modules.

The main goal with these modules is to capture the essentials properties stated in the literature, regarding input/output processing. As simple as we can without losing performance and generality, as discussed in the previous chapter.

Keywords: Implementation, Early visual system, Dynamics, Architecture

Organization of this chapter:

We start with a brief summary of the key points previously discussed in terms of architecture and dynamics, to then discuss each module in detail.

For each module, we give its functional description and the expected algorithmic logic of its processing, where more developed functions emerge from its interactions with other modules.

3.1 Summary of previous sections

In order to point out the essential points of the previous two chapters, we here provide a short summary, before proceeding with the description of the implementation of the work proposed in this thesis.

Each section contains also specific reminders for each structure.

3.1.1 Architecture of the system

It must firstly be reminded that three visual pathways are elaborated from the mammalian retinal circuitry [107]. In addition to the Parvocellular visual pathway (mainly involved in contrast perception) and the Magnocellular pathway (mainly involved in motion perception) –respectively feeding the ventral *for perception* and the dorsal *for action* cortical axes [115]–, the Koniocellular pathway performs non-standard visual processing [107] (mainly involved in detection), with a variety of responses corresponding to a global analysis of color or motion distribution in the visual field for the detection of biologically significant patterns (e.g. looming or approach-like pattern of a predator, highly periodic patterns corresponding to snake movements [78]). This is in fact an ancient visual pathway, inherited from amphibians where the visual system is mainly limited to the retina extracting this kind of basic information (preys and predators detection) and directly activating the tectum, a visuo-motor structure responsible for orientation and action (fleeing or catching). Such a primitive analysis has probably some advantages, since it was kept along phylogeny and even described as complexified in primates [70][78]. As in amphibians, the Koniocellular pathway is still directly connected to a sensorimotor structure, responsible of orientation (and saccades), called the Superior Colliculus (SC) in mammals [102]. A part of the Magnocellular pathway also reaches the SC (in a distinct visual layer, [102]) and both Konio and Magno flows are then sent back to the thalamus (resp LGN and Pulvinar [102]). The visual layers of the SC also receive more elaborated visual information from a variety of cortical areas, that might also ultimately activate deep motor layers of the SC for orientation (mostly by saccades) and consequently attention to the stimulus, whereas rapid defensive reactions in case of emergency are also reported [41][43]. In that sense, the SC can be seen both as a primitive sensorimotor structure receiving basic information about the location (and not the identity) of loci of interest (threat, salient motion), triggering automatic movement of orientation when the intensity of stimulation is strong enough;

and as a more elaborated structure, like a saliency map, where various cerebral structures accumulate their own preference on the next place to focus on, and compete for the actual choice of the next saccade [41]. Additionally, [85] reports that, in the human, ultra-fast saccades (120ms) towards images of animals exist, reinforcing this idea.

Of course, consistent with the development of cortical influence in higher mammals, the different information flows also project directly in LGN toward the cortex, the three kinds of cells being kept separate in specific geniculate layers [153] and forming the higher road, as evoked above. Whereas the Parvo and Magno LGN layers project through (distinct sublayers of) layer IV of V1 towards the ventral and dorsal cortical axes to recognize objects and prepare actions for the visual stimuli, the Konio LGN layer has a modulatory role on them, with a projection to layer I of V1 [82].

3.1.2 Dynamics of the system

The above mentioned projection of the Konio, Parvo and Magno pathways, respectively to the upper (Konio) and middle cortical layers, is more generally described as a key feature of thalamocortical connectivity, having a strong impact on the dynamics of this network. Core regions of the thalamus send, locally, highly-ordered information to layer IV of the cortex (as it is the case for the Magno and the Parvo thalamic layers), whereas matrix regions (like the Konio thalamic layers) send a diffuse information to layer I of widespread cortical regions [82]. The former thalamocortical input has been described as a driver input, bringing the perceptive information to the cortex and the later as a modulator input with a longer and more global influence [149]. Loops between thalamus and cortex are closed with layer VI of the cortex sending back a modulation to the same core region of the thalamus and layer V sending a driver output toward higher order thalamic regions and toward the SC [82].

This reciprocal connectivity is an important ingredient to the thalamocortical dynamics, with the involvement of the Thalamic Reticular Nucleus (TRN) that sets the main synchronization modes by its inhibitory influence on the thalamus, triggered on the basis of the feedforward and feedback information exchanged between the thalamus and the cortex and crossing TRN in a topographic way [110]. In coherent mode, the tonic activity of thalamic relay cells lets the core region send its driving perceptive information to the cortex, resulting in gamma oscillations. In case of attentional demand (due to the occurrence of an unexpected event or to a cortical demand), the TRN inhibits thalamic relay cells (burst mode). As a result, the diffuse modulatory connectivity of the matrix cells will

possibly propose a new pattern of activation in the cortex, setting the attention in another region that will be subsequently more deeply analyzed in tonic mode [81].

3.2 Our model of the early visual system: modular view

The aforementioned architecture and dynamics set the bases for our computational model, which is shown in Figure 3.1. Here we can observe the different activation maps of the included areas, how they connect with each other (architecture), and their temporal dynamics from stimulus onset (dynamics). Computations are done locally, and systemic properties emerge naturally, such as stability and synchronization, while no "conductor" has been developed, showing once again that it is the system itself who provokes and allows for these properties to appear.

In the figure, red arrows are part of the standard pathway, whereas blue lines are part of the non-standard stream. Green arrows represent regulatory flows from TRN (inhibitory), and cortical feedback (excitatory), which are considered as modulatory, but do not make part of the non-standard pathway. Here, driver flows are drawn in solid lines, while modulating flows use dashed lines.

As a reminder (cf. Section 2.1.2), a driver flow is a main information stream, allowing the recipient structure to produce its output based on it (i.e. independently of the existence, or not, of a modulator). It is the case of, e.g., the input from the core thalamus to the cortex. On the other hand, a modulator information flow is unable to trigger a response, solely, on its recipient structure, but instead participates in the process by adjusting the response to the driver stream, particularly to make it more effective. In this case we can consider the input from the matrix thalamus to the cortex, providing contextual information to bias cortical treatment towards a more relevant, maybe unattended, stimulus.

Another reminder is recommended to understand the key regulating role of TRN, and it is about the tonic and burst activation modes (cf. Section 1.4.1). In tonic mode, the core and matrix thalamus send their information "as expected by the cortex", which means that there is no great difference between cortical and thalamic information, where this difference is measured by TRN. However, if this difference is great enough, TRN will communicate this situation to both core and matrix thalamus, making them switch from the tonic mode to the burst mode, where feedforward information is partially blocked, either to allow for exploration on the scene, or to force feedback information at the thalamic level to finish the analysis of the current visual hypothesis, which we originally call "forced feedback", and it

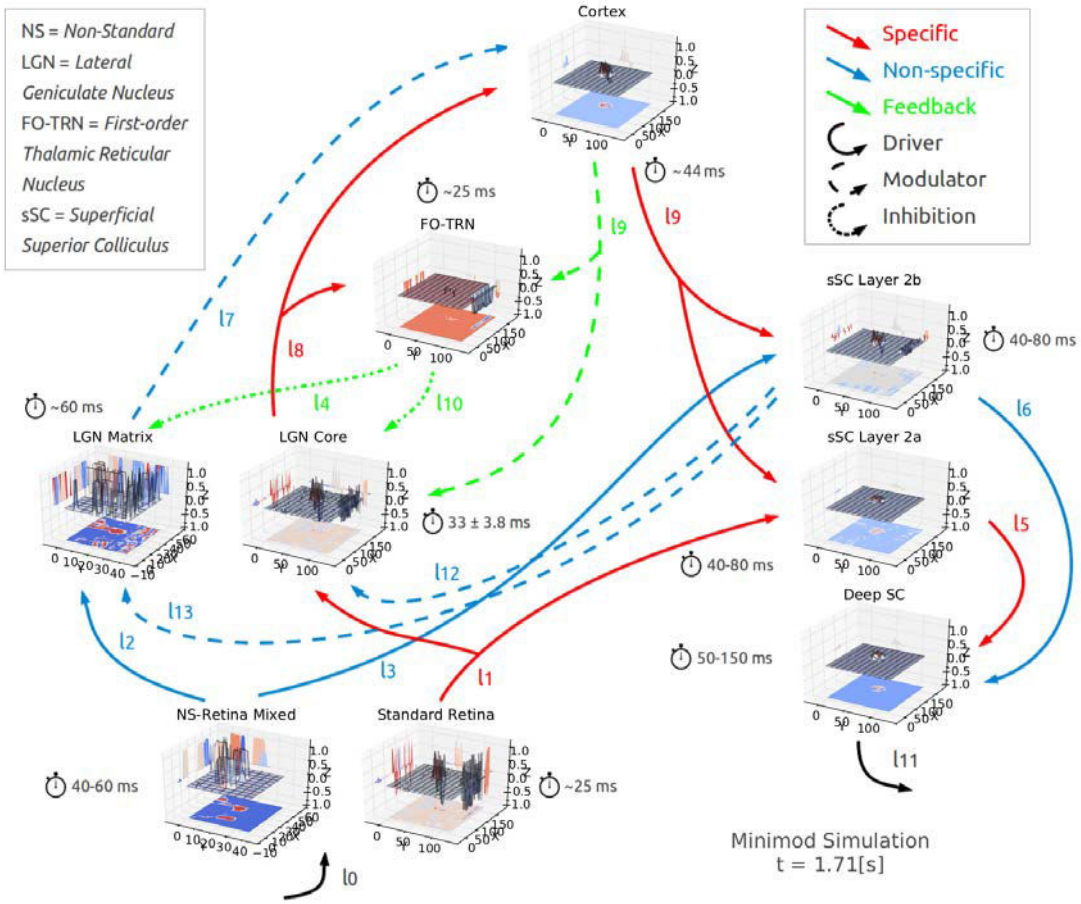

Figure 3.1: **Model diagram.** This retino-thalamo-cortico-collicular architecture contains anatomically validated connections. Here, only the Magno and Konio parts of the system are shown for visibility. It includes driver/modulator processing of information flows [149] and burst/tonic activation modes [147]. It also proposes and implements a regulation mechanism of the thalamic reticular nucleus [90] for the feedforward information to the cortex. The input used is a sequence of images, and the output is the representation of the deep collicular visual orientation response to such input. Here, each structure implements a spatio-temporal non-linear filter, except the primitive cortical structure that serves as an integrator, and the deep superior colliculus, where target selection is performed by dynamic neural fields. Latencies at each level are displayed for reference, and are included in our computations.

follows the same idea as the cortical process shown in Figure 1.9, but at the thalamic level and with this different computation (cf. Section 3.2.2). Whether to explore or to force feedback information will depend on the situation, and it will also be an emergent decision from the system (cf. Section 3.2.2).

To understand this figure, and the model, we also need to explain the different mixing mechanisms. At the retinal level, mixing in the non-standard area represents an accumulation of activation, which could be considered as looking at the ensemble of pre-wired stimuli, and topographically adding them. This is an oversimplification, as it could happen that two different pre-wired stimuli share a region (cf. Section 3.2.1). At the thalamic level (matrix thalamus), mixing comes from the activation modes being topographic, and since in burst mode we seek for another hypothesis (or, better said, inhibit the previous one) there could be an extreme transition case where topographic information generated from two (or more) pre-wired stimuli is communicated to the cortex, and thus we use the term "mixed" for simplicity (cf. Section 3.2.2). This inhibition follows the idea of "attenuation before semantic analysis" of the model of selective attention by [172], however this experiments were carried out with auditory stimuli.

A final explanation needed is for the alert mechanism. This mechanism communicates a region where an important, critical, stimulus has been found, and thus should be prioritized, either for immediate action (even subconscious, as a reflex) at the collicular level, or for biased processing in the thalamocortical loops. The alert signal is generated at the non-standard retina level, where certain stimuli are pre-wired in the Konio detectors, that will generate a coarse estimation of the visual scene, which is nevertheless essential to properly bias treatment in the early system (cf. Section 3.2.1).

We implement our model using the DANA framework [132] (cf. section 2.1.5).

In the next sections, all equations use the notations of Table 2.2.

Now, let us look in detail at each structure.

3.2.1 Retina: Standard and non-standard cells

The first stage in the feedforward information flow is the retina. Here, for the sake of simplicity, we use well established and biologically funded retinal models present in the literature.

The standard retina is represented by parasol and midget cells. Parasol cells transform the image sequence into a sequence of local movement information with high resolution (about 2°), while midget cells transform the image sequence into a sequence of contrast

information with about three times higher resolution.

The non-standard retina detects visual events in the image sequence. Its cells have large fields, and thus provide low resolution responses (about 10°). Additionally, we set a threshold for pre-wired (cf. Section 2.2.2) stimuli, and generate a third retinal flow. If the pre-wired activation surpasses this threshold, the response will be considered as critical, generating an alert for the system, meaning that the information triggering the alert should be studied as soon as possible, as it represents a possible immediate danger. If the information does not surpass this threshold, it means that the system is not really sure of the existence of this stimulus, and thus does not trigger the alarm mechanism. This mechanism follows the "event/emergency" viewpoint of works such as [41] and [43], where this flow is sent to the superior colliculus.

Thus, we have three retinal outputs: the standard output (midget and parasol, i.e. Parvo and Magno); the non-standard, target specific output (each detector for a specific target, e.g. predator, sexual partner, food); and the non-standard mixed target output. They are respectively called l_1, l_2 and l_3, where the index "alert" or "mix" is used for l_3 to denote whether the flat mixed information is used, or the alert signal. Here, the flat information is the accumulation of information, while the alert signal will trigger biased processing in the rest of the system. This flat information follows the idea that the information is not precise in the superior colliculus, and thus the SC lacks details about the identity of the target; while the alert topographically shows where the attention should be prioritized.

We need to adapt our retinal inputs to the format of the rest of the model. To this end, we apply a sigmoidal normalization of the form:

$$\mathbf{u_x} = 2 * \frac{1}{1 + e^{-4\,\psi\,\mathbf{u_x}}} - 1 \tag{3.1}$$

where $\psi = 0.06$. Also, we need to generate the alert signal for the non-standard retina. For simplicity, we threshold the mixture of the non-standard information such that:

$$_{alert}l_3 = \max(_{mix}l_3, \psi) \tag{3.2}$$

where $_{mix}l_3$ is defined by Equation (3.21).

To account for the latencies in the retina, we include temporal convolutions of the form:

$$\mathbf{l_x} = \gamma_x \times \mathbf{u_x} \tag{3.3}$$

where

$$\gamma_x(t) \stackrel{\text{def}}{=} \frac{1}{\tau_x} e^{-\frac{t}{\tau_x}} \tag{3.4}$$

and t is the time, and τ_x the time constant for γ_x –based on the latencies, with $\tau_1 p = 25$ms (parasol), $\tau_1 m = 45$ms (midget), $\tau_2 = \tau_3 = 45$ms (bistratified)–, while $\mathbf{u_x}$ represents the computation without delay. This nomenclature for γ_x will be used for the rest of the structures, in order to include their respective latencies.

The implementation here mentioned corresponds to that of [168], where a Python wrapper was written to reuse it.

3.2.2 Thalamus

The thalamus regulates feedforward information, depending on internal (e.g. needs or cortical feedback) or external (stimulus novelty) criteria [146]. Here, each local computation is important, but most important is the synergistic effect between the structures, which generates such regulation mechanisms. This regulation considers both rough and precise influxes arriving from the retina, where they are kept separate through the Konio, Parvo and Magno pathways, respectively, and consists on switching or mixing. Switching refers to the change between tonic and burst activation modes, which implies a different local computation mechanism: relaying feedforward information, or "forcing feedback", i.e., forcing a top-down hypothesis in the core thalamus and pseudo-"blockage" of the driver information (cf. Section 3.2 and Figure 1.9). Mixing may refer to topographically generate a current hypothesis in the matrix thalamus (read below), or simply to accumulate activations at a certain structure, as it happens with the *mixed* non-standard flow, that basically combines the different non-standard flows in a flattened version (cf. Section 3.2.1).

The core thalamus adapts the standard feedforward information flow depending on what the cortex is currently analyzing and on whether there is a mismatch (lack of correspondence) between the feedforward (from the core to cortical layer IV) and feedback (from cortical layer VI to core) information flows. The mismatch is computed in TRN and communicated to the core via the inhibitory connections.

On the other hand, the matrix part, sheltering the non-standard cells, signals the presence of an important stimulus in the scene, but also generates a modulating signal for the cortex to bias its treatment towards the possible existence of this (maybe dangerous) stimulus. In other words, by mixing the non-standard retinal output, the inhibition from the thalamic reticular nucleus, and the event/emergency information [41][43] received from SC

(layer 2a, cf. Section 3.2.4), the matrix thalamus generates a sort of "current hypothesis", that takes into account the alert information, to modulate cortical processing.

The computation carried out by the core thalamus writes

$$\mathbf{l_8} = \gamma_8 \times \mathbf{u_8} \tag{3.5}$$

while

$$u_8 = \begin{cases} & \mathbf{l_1} & (1 + (a_8\,\mathcal{L} * \mathbf{l_9} - \mathbf{l_{10}}) & \overline{H}(\mathbf{l_{10}})\,\overline{H}(l_{12}) + & \#\text{tonic} \\ & & (d_8\,\mathbf{l_1} + e_8\,\mathbf{l_9}) & H(\mathbf{l_{10}})\,\overline{H}(l_{12}) + & \#\text{burst} \\ (\mathbf{m_8} & \mathbf{l_1}) & (1 + (a_8\,\mathcal{L} * \mathbf{l_9} - \mathbf{l_{10}}) & \overline{H}(\mathbf{l_{10}})\,H(l_{12}) + & \#\text{tonic+alert} \\ \mathbf{m_8} & & (d_8\,\mathbf{l_1} + e_8\,\mathbf{l_9}) & H(\mathbf{l_{10}})\,H(l_{12}) & \#\text{burst+alert} \end{cases} \tag{3.6}$$

where the spaces are just included to show which parts are comprised within the parts of the equation, besides the differentiation for the cases. For instance, for each alert case, m_8 is present, and $\mathbf{l_1}$ is considered in the tonic computation.

The current values were hand-tuned without looking for optimality (cf. Section 4.2.2), and are present in Table 3.1. Here, $\mathcal{L}$ is an edge-detect-like kernel because information corresponds to differential motion, and thus such kernel allows to emphasize higher values inside the map while removing lesser variations of motion (thus making information finer).

Table 3.1: **Handpicked values for the computations on Core Thalamus**

Name	Constant	Value
Tonic feedback gain	a_8	0.4
Burst feedforward gain	d_8	0.25
Burst feedback gain	e_8	0.4
Alert amplification	m_8	1.5

This means that if TRN sets the core thalamus in tonic mode, normal (driver, modulation and inhibition) interaction takes place, where the excitatory alert connection will increment the numerical values of the alert region, so as to notify the standard pathway of the presence of an alert. Else, i.e. if TRN sets the core thalamus in burst mode, a linear combination of the feedforward and feedback flows is considered, so as to allow for a "forced feedback". This occurs as the information transmitted in tonic mode is mainly driving, whereas in burst mode the "gating" mechanism of the core thalamus passes to

"blocking mode", and the driving information becomes secondary, while feedback information becomes primary. Also, in these circumstances, the core thalamus keeps notifying about the presence of an alert.

The computation carried out by the matrix thalamus writes

$$l_7 = \gamma_7 \times u_7 \tag{3.7}$$

while

$$u_7^t = \begin{cases} l_7^{t-1} & \overline{H}(l_4)\,\overline{H}(l_{13} - s_d) + & \#\text{tonic} \\ {}_{c^{t+1}}l_2^t & H(l_4)\,\overline{H}(l_{13} - s_d) + & \#\text{burst} \\ 1 & \overline{H}(l_4)\,H(l_{13} - s_d) + & \#\text{tonic+alert} \\ 1 & H(l_4)\,H(l_{13} - s_d) & \#\text{burst+alert} \end{cases} \tag{3.8}$$

where the spaces are just included to show which parts are comprised within the parts of the equation, besides the differentiation for the cases. Here, $s_d = 0.01$ is a threshold to remove the delay effect on the binary information, and

$$c^{t+1} \equiv (c^t + 1) \mod C \tag{(3.8)bis}$$

where C is the set of pre-wired stimuli in l_2, and c^t is the particular pre-wired stimuli currently considered. Equation (3.8) means that in alert mode, the values are computed so as to inform the rest of the system (also via this pathway, by a linear combination of flows) of the presence of the alert (so it may be analyzed promptly if needed). Equation ((3.8)bis) simply states that the system follows on the next pre-wired stimulus in modulo integer. This is an oversimplification since we expect the system to select the most "salient" pre-wired stimulus, but it does not affect the behavior we study here, and it is a trivial extension of our present work.

Thalamic reticular nucleus

The thalamic reticular nucleus (TRN) regulates the feedforward information from the thalamus to the cortex [90]. We implement it by computing the mismatch (or lack of synchronization) between the feedforward and feedback information flows, and communicating it to the thalamus via inhibitory flows. The mismatch is here defined as the absolute variation between thalamic and cortical core information. If this variation exists and is weak, it will generate a mild inhibition, while if the variation exists and is strong enough, it will not

only inhibit, but also trigger a burst, allowing the thalamus to generate a new hypothesis (cf. Section 1.4).

Here, we should explain the thalamic "forced-feedback", and the role of TRN regarding this mechanism. The idea of "forced feedback" is similar to the one of Figure 1.9. Here, information is forced into a unit in order to analyze a current hypothesis. Similar to the one generated in the matrix thalamus from non-standard retinal information, the core thalamus can be inhibited by TRN to prioritize a non-winning (because of the DNF, cf. Section 2.1.5) information at the cortical level, while this can also happen globally to focus the cortical analysis in a particular area. Eventually, with the inclusion of higher-cortical areas, TRN will carry out the inhibition shown in Figure 1.9.

The computation carried out by TRN may be described by

$$\mathbf{l_{10}} = \gamma_{10} \times \mathbf{u_{10}} \tag{3.9}$$

$$l_4 = \gamma_4 \times u_4 \tag{3.10}$$

where

$$\mathbf{u_{10}} = \max(\widehat{\mathbf{u_{10}}}, s_{10}) \tag{3.11}$$

with

$$\widehat{\mathbf{u_{10}}} = |\mathcal{Z} * (\mathbf{l_9} - \mathbf{l_8})| \tag{3.12}$$

$$u_4 = H\left(\sum \mathbf{u_{10}} - s_4\right) \tag{3.13}$$

where $\widehat{\mathbf{u_{10}}}$ computes the absolute value of the mismatch smoothed by $\mathcal{Z}$ and $\mathbf{u_{10}}$ is the rectification of the mismatch. On its side, l_4 simply sums these thresholded values. Again, here we choose a minimal non-linear representation of the expected function. The current values were hand-tuned without looking for optimality, and are present in Table 3.2.

Table 3.2: **Handpicked values for the computations on TRN**

Name	Constant	Value
Rectification of mismatch	s_{10}	0.1
Lower bound for l_4	$s_4 = s_d$	0.01

3.2.3 Primary visual cortex

Here, the (primitive) visual cortex represents a single gathering structure. This means it is not separated in the six classical layers, but instead it gathers all their functions in a dynamic neural field (DNF) [133][135]. As the main function is to analyze the current hypothesis and to communicate the modulated standard information to the superior colliculus, TRN and the core thalamus, so as to complement the processing of the system via more developed information, a DNF is simple and complex enough for the tasks here studied. Since there are no higher-order cortical areas, and thus their feedback flows, the cortical mixture between Parvo and Magno flows is not considered at this level. However, one could directly implement an ad-hoc computation to account for this treatment, which would only require modifying the cortex module.

The computation carried out by the cortex writes

$$\mathbf{l_9} = \max(\mathbf{u_9}, 0) \tag{3.14}$$

with

$$\mathbf{u_9} = \gamma_9 \times (\mathbf{i_9} + \mathbf{j_9}) \tag{3.15}$$

and

$$\mathbf{i_9} = g_9\, \mathbf{l_8}\, (1 + \mathcal{Z} * l_7) \tag{3.16}$$

$$\mathbf{j_9} = \mathcal{K} * \mathbf{l_9} \tag{3.17}$$

where $\mathcal{K}$ is a convolution kernel, typically a difference of Gaussians (DoG) of the form

$$\mathcal{K} = \frac{a}{2\pi\sigma_a^2} e^{-(x^2+y^2)/(2\sigma_a^2)} - \frac{b}{2\pi\sigma_b^2} e^{-(x^2+y^2)/(2\sigma_b^2)} \tag{3.18}$$

where $(x, y) = \mathbf{s}$ (spatial coordinates). The current values were hand-tuned without looking for optimality, and are presented in Table 3.3.

3.2.4 Superior colliculus

As for the superior colliculus, we consider layers 2a and 2b of the superficial superior colliculus (sSC), and the deep superior colliculus (dSC).

The layer 2a of the superficial superior colliculus (sSC-2a) is the gathering point for early (non-standard retinal) information about targets with later (cortical) information of the

Table 3.3: **Handpicked values for the computations on the integrative cortex**

Name	Constant	Value
Gain of Gaussians	(a, b)	(0.83 , 0.415)
Var of Gaussian (+)	σ_a	0.1
Var of Gaussian (-)	σ_b	1
Input gain	g_9	0.4

current treatment. Its output serves as the modulating information for the deeper superior colliculus (via $\mathbf{l_6}$), while also being a relay of emergency information and an adapter of event information [41][43] for the Thalamus (via both l_{12} and l_{13}).

The computation here carried out writes

$$\mathbf{l_6} = \gamma_6 \times \mathbf{u_6} \tag{3.19}$$

where

$$\mathbf{u_6} = \begin{cases} k_6 + a_6(\mathbf{l_9} + {}_{mix}l_3) & H({}_{alert}l_3) + \quad \#\text{alert} \\ c_6\,\mathbf{l_9} + d_6\,{}_{mix}l_3 & \overline{H}({}_{alert}l_3) \quad \#\text{no-alert} \end{cases} \tag{3.20}$$

$${}_{mix}l_3 = \sum_C {}_cl_2 \tag{3.21}$$

The current values were hand-tuned without looking for optimality, and are shown in Table 3.4.

Table 3.4: **Handpicked values for the computations on layer 2a of the superior colliculus**

Name	Constant	Value
Alert offset	k_6	0.2
Gain in alert	a_6	0.4
Cortical gain without alert	c_6	0.3
Retinal gain without alert	d_6	0.7

Also, l_{12} and l_{13} are the alert information for the core and matrix thalamus, respectively. In our case, they are simple relays of the retinal alert information, though we are aware that such signal should also consider cortical information in an extended model. Thus, we write

$$l_{12} = l_{13} = {}_{alert}l_3 \tag{3.22}$$

while a more elaborated equation might be considered.

The layer 2b of the superficial superior colliculus (sSC-2b) is the converging point for early (retinal) and later (cortical) Magno-like (standard) information. Retinal Parvo-like information (from midget cells) does not reach the superior colliculus directly. Its output is the driver information for the dSC. Its main function is to integrate the early and late information for computing the saccadic output afterwards in the dSC.

The computation carried out by sSC-2b thus writes

$$\mathbf{l_5} = \gamma_5 \times \mathbf{u_5} \tag{3.23}$$

where

$$\mathbf{u_5} = g_5 \ \max(\widehat{\mathbf{u_5}}, s_5) \tag{3.24}$$

where

$$\widehat{\mathbf{u_5}} = a_5 \, \mathcal{Z} * \mathbf{l_1} + b_5 \, \mathcal{Z} * \mathbf{l_9} \tag{(3.24)bis}$$

introducing a thresholded rectification again.

The current values were hand-tuned without looking for optimality, and are shown in Table 3.5.

Table 3.5: **Handpicked values for the computations on layer 2b of the superior colliculus**

Name	Constant	Value
Output gain	g_5	0.8
Retinal gain	a_5	0.35
Cortical gain	b_5	0.65
sSC-2b threshold	s_5	0.1

The deep superior colliculus is in charge of computing the saccadic output –via a DNF– and deploying the motor resources linked to this saccade (not-implemented as we are not yet working with hardware). We consider the saccadic output to be a set of coordinates, for the moment, basically to guide the attentional focus towards it. Eventually, when being able to have a mobile system (e.g. a robot) depending on the classification of the detected and analyzed stimulus, the output will also indicate whether to approach or to escape.

The computation carried out by the dSC writes

$$\mathbf{l_{11}} = \max(\mathbf{u_{11}}, 0) \tag{3.25}$$

while

$$\mathbf{u_{11}} = \gamma_{11} \times (\mathbf{i_{11}} + \mathbf{j_{11}}) \tag{3.26}$$

where

$$\mathbf{i_{11}} = g_{11} \langle \mathbf{l_5} (1 + \mathbf{l_6}) \rangle \tag{3.27}$$

$$\mathbf{j_{11}} = \mathcal{K} * \mathbf{l_{11}} \tag{3.28}$$

where the angular brackets represent the average of this computation for the Parvo-like and Magno-like information, when these two systems are coexisting in a simulation, i.e.

$$\langle \mathbf{l_5} (1 + \mathbf{l_6}) \rangle = 0.5 \left([\mathbf{l_5} (1 + \mathbf{l_6})]_{parvo} + [\mathbf{l_5} (1 + \mathbf{l_6})]_{magno} \right)$$

.

The current values were hand-tuned without looking for optimality, and are shown in Table 3.6.

Table 3.6: **Handpicked values for the computations on the deep superior colliculus**

Name	Constant	Value
Output gain	g_{11}	0.6

3.2.5 Summary

Here, we have described the implementation of the local computations to be used in our simulations. It is from this local computations that complex functions will emerge, and this will be shown in the next chapter.

The computations we propose are biologically plausible, in term of structure and functional properties. Here, we reuse other scientific work for the standard (Magno and Parvo) pathways, while the novelty of this work is the inclusion of the non-standard (Konio) pathway: its interactions with the Magno and to some extents Parvo pathways, and how connections with the thalamus leads to interesting computational properties.

With respect to works like [124] or [67], we propose a minimal modeling as developed in the previous chapter (less parameters, minimal computational operator). We however, will not only test the result on a toy data set, but on real and realistic natural images, thus allowing to obtain simulation results at the behavioral level.

These behavioral results, will correspond to attentional shift in the deep superior colliculus, as a result of the different interactions and processing of the different pathways. They thus correspond to the emerging algorithmic mechanisms discussed in this chapter. More precisely, simulations correspond to stimuli where there is at least one distractor, while the attentional focus should be directed towards the "critical stimulus".

During these numerical experimentation, tuning is restricted to adapt the model to its environment class (e.g. either artificial or natural images) or a change in the system architecture (e.g. when adding the Parvo pathway in the loop), but no more.

Let us analyze the different simulations in the next chapter.

Chapter 4

Our minimal model in the real world: Experimental results

Contents

4.1 First experimental result: using artificial images 87

4.1.1 Discrimination, selection and tracking 89

4.1.2 Numerical Robustness 89

4.2 Original experimental result: using natural images (M+K) . . 95

4.2.1 Discrimination, selection and tracking 97

4.2.2 Numerical robustness 102

4.3 Experimental result: using natural images (P+M+K) 104

4.4 About observed emerging properties 116

4.5 Open-access software 116

Summary

The different modules explained in the previous chapter are used to build different models of the early visual system. As previously discussed, different properties will emerge from their union: not because they have been modeled so, but because of the self-arrangement and organization of these modules and their treatment. It is now time to observe this experimentally.

In a nutshell: The models replicate the expected behavior of the attentional shifts tasks in presence of "critical" (fearful) stimuli (cf. Sections 4.1, 4.2 and 4.3). This is thanks to the different distributed local mechanisms, and the global mechanism, emergent. In addition, the results show numerical robustness and stability.

We first test the system with Magno and Konio sub-system, in a paradigm where artificial stimuli are used. A sequence of full-contrast, noiseless images is created, and fed to the model. The simulations allow us to tune the system and experiment that only a relatively large modifications of the key parameters affect the overall processing. Using a fully controlled situation yields a quantitative analysis of these aspects.

The main goal of the numerical experimentation was to use natural images, and the three (Magno, Parvo and Konio) systems. To this end, the second simulations were carried out with natural images, first with the same Magno+Konio model. Before including the Parvo pathway, a battery of numerical tests was performed, to ensure numerical robustness, stability and parameter sensitivity.

Finally, we show how our model is extended to include the Parvo pathway, reusing most of the algorithms, and only applying a slight tuning to a few parameters for this change of architecture. Similar stable, robust and efficient results.

Keywords: Model, Result, Artificial image, Natural image, Robustness

Organization of this chapter:

This chapter starts with a brief introduction to the experimental process. First, results obtained with very simple artificial stimuli are shown. These consist on the very first approach to a visual system, where the interactions between Magno and Konio pathways are studied, together with giving a first view at the numerical robustness the model offers. Then, natural images are used in the following experiments, where the first one stays with the Magno and Konio system, whereas the second one includes the Parvo pathway. Here,

an in-depth numerical robustness study is undertaken for the Magno and Konio system, where the stability and robustness properties are kept. Then, when the Parvo pathway is added, the system reuses many algorithms and works as expected. To end this chapter, information of the open-access software is given.

Our contribution is to numerically experiment with a computational systemic model of the primitive early visual system, including the non-standard (Konio) stream. This model implements a coordinating thalamus, which allows to influence cortical processing with contextual information of a fearful stimulus, if detected. This detection and bias towards the fearful stimulus has to modify the response from the superior colliculus, making it faster (as this "critical" stimulus will be prioritized). Here, we also include the simulation of biological mechanisms, such as the burst and tonic activation modes for thalamocortical communications, or the driver and modulator information flows duality.

This model, shown in Figure 3.1, is formed by local computations (i.e. modular) and thanks to the synergy between its components, we observe emergent behaviors, such as stability or synchronization. It is also a reduced model, with few parameters, and easily modifiable. Thanks to this, it is experimentally robust, while showing genericity in the computation.

Other experiments have been conducted, but not presented here as results are similar and do not modify the illustrations. They are available as supplementary material (cf. Section 6), allowing to see that we not only show the "best" results but that these illustrative results are reproducible.

The principles used in these different protocols have been presented in Chapter 2, and the implementation described in Chapter 3.

The goal of this chapter is to verify the expected behavior of the system in different scenarios, while analyzing the inner mechanisms and interplay between the different submodules.

4.1 First experimental result: using artificial images

In order to test the first version of our work, we sought to use really simple stimuli, for which the results could be easily predicted. We start with a version of only the Magno and Konio systems.

Here, we use the video of two circular stimuli with different sizes and speed, as shown in Figure 4.1. The larger circle will, in this case, be considered as the fearful stimulus. Here, the smaller circle can be considered as any neutral stimulus, in the sense that its detection is not wired in the Konio pathway, and would not trigger any behavior higher in the hierarchy.

The task is to detect and follow the fearful (pre-wired) stimulus. In the first part, only

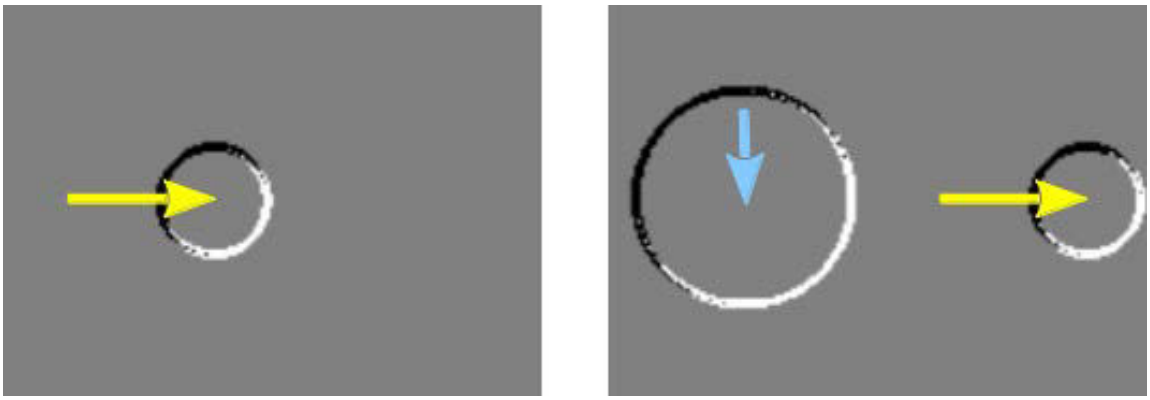

Figure 4.1: **Sample of artificial stimuli used.** First, a single target advances rightwards (left) when, suddenly, a second, larger target, appears moving downwards at a slower speed (right). The detection of this second stimulus is pre-wired in the Konio system and should thus trigger a faster response. The arrows are not part of the stimulus. They are added so as to understand the different movements, where the longer yellow arrow means horizontal movement, quicker the blue vertical arrow.

one neutral stimulus is present, without noise nor distractors, thus the system will easily detect and follow this stimulus. However, when a fearful, but slower, stimulus, moving in a perpendicular direction (as vertical opposed to horizontal) appears, rather than keeping the attentional focus on the faster stimulus, thanks to the modulation and alert of the non-standard system, the attentional focus will switch towards the slower –fearful– stimulus.

Our results in this detection, selection and tracking task (attentional shift) follow the prediction that by the inclusion of the Konio pathway, these actions are done faster than with a purely Magno system, when the existence of the fearful stimulus is acquainted for in the non-standard information flows. We also test the numerical robustness of the model, as another objective of this work is to develop a stable model without many parameters. We realize that variations of up to +100% lead mainly to violate bio-plausibility, rather than to provoke numerical instability. In addition, when doubling ($\mathcal{K}$) the DNF simply stays fixed in a point, but numerical instability was not found. We remind that no saturation mechanism is applied at the output of any structure (cf. Section 2.2.4), and thus that avoiding numerical instability is an emergent property of the system.

4.1.1 Discrimination, selection and tracking

To draft a comparison between the simulation results, and the expected results, we propose two indicators:

- The distance between the center of mass of the stimulus supposed to be attended and the center of the obtained response in dSC, which we denote "d". The location of the "supposed to be attended" stimulus is artificially generated by hand, as we create the stimuli and its shape allows to need just a simple computation to obtain it. These results are shown in Figure 4.2.
- The percentage error between surfaces of the dSC generated image (from the obtained response) and the retinal image, which we denote "Se". These results are shown in Figure 4.3.

The relatively better performance of the purely Magno system in the beginning of the simulation is explained as the activation levels are smaller –absence of Konio modulation as fearful stimulus is not present– and thus the DNF may follow more quickly. However, in the second part, i.e. when the pre-wired stimulus appears, the Magno+Konio system quickly overtakes in performances and converges in a quicker manner, with a better ongoing pursuit.

4.1.2 Numerical Robustness

One of the goals of this work is to develop a minimal simple model. The values chosen for the parameters are hand picked and are based on other studies (e.g. delays based on latencies) or biologically plausible numerical needs (e.g. a small threshold as a minimal amount of activation needed for a unit to respond). One of our goals is to provide a numerically robust model. Here, we test for positive differences of 1, 5, 10, 20, 50, and 100% of the values of: (i) a_9, the cortical matrix gain, as one of the interesting points in this study is the influence of the Konio pathway on standard information processing (Figure 4.4); (ii) g_9, the cortical input gain, as we state that the coarse interpretation done by the colliculus with retinal information will be later reinforced by this "more developed" (in terms of detail) information flow (Figure 4.5); (iii) $\mathcal{K}$, the amplitude of the difference of Gaussians used for the DNFs, as it is these DNFs that will allow to detect, select and track the most salient stimulus in the visual scene, and this parameter regulates the local feedback of the DNFs (Figure 4.6). Specially, it is the only case where variations over

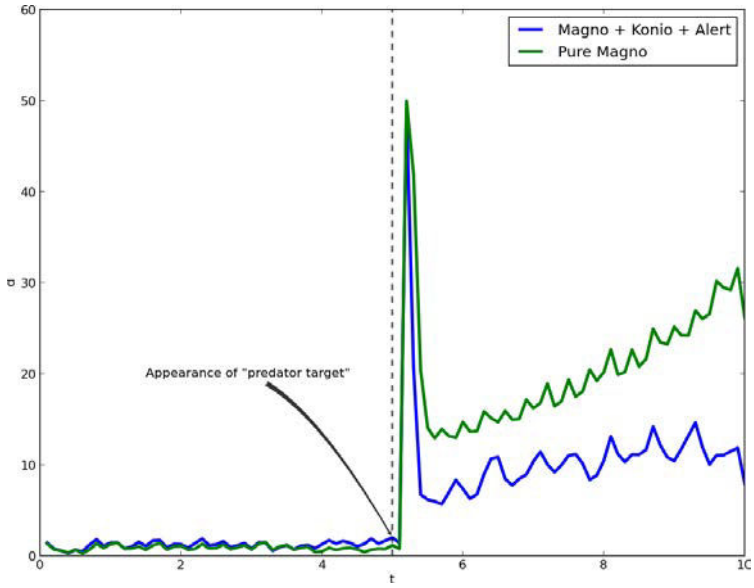

Figure 4.2: **Simulation results: Euclidean distance of center of mass of attended stimulus to center of the dSC generated image** (from the obtained response), in arbitrary units. While for the small stimulus a purely Magno system tracks slightly better the target, when the large stimulus appears (t=5s) it is the mixed system that fairly quickly shows a better tracking response. The peak is because we manually set the reference point at the "predator target" when it appears, thus because of the geometrical location of the attentional focus, the distance to the "correct" target becomes suddenly big.

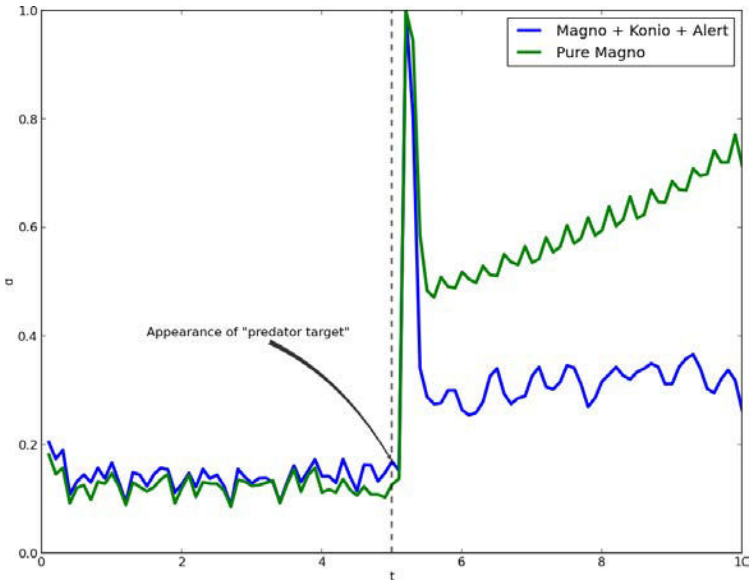

Figure 4.3: **Simulations results: Percentage error between surfaces of the dSC generated image** (from the obtained response) and the retinal image. Results are similar to the distance test, showing that the mixed system converges quicker towards the attended stimulus (appearance of the second stimulus at t=5s).

20% provoke an abnormal behavior from the systen, this behavior being still numerically stable; (iv) $\tau_1 1$, the time constant of the dSC, as it is here that the decision should be made, whether to follow or to flee in the case of a predator [19] (Figure 4.7).

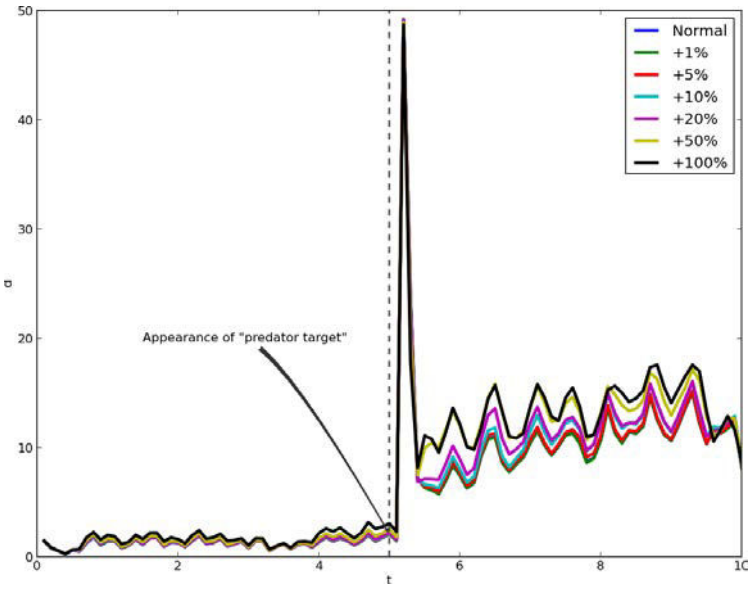

Figure 4.4: **Simulations results. Variation of center-of-mass test (Figure 4.2) by varying the cortical matrix gain in 1, 5, 10, 20, 50 and 100%**. As a_9 increases, the system takes longer to converge. A more notorious difference is made after a +20% increment.

These results show that, in an artificial scenario, the responses of the system are similar to what is expected, while at the same time being robust enough to changes in its parameters.

While the sequence has only one stimulus, the attentional focus is following it, and when the fearful stimulus comes into scene, the attentional focus switches towards it because of the action of the non-standard pathway. This provides a good first result to move towards natural images. The performance of the system is lowered after relatively big modifications (e.g. +50% of g_9), and this is a good starting point for the re-usability of the modules with natural images, and eventually the Parvo pathway.

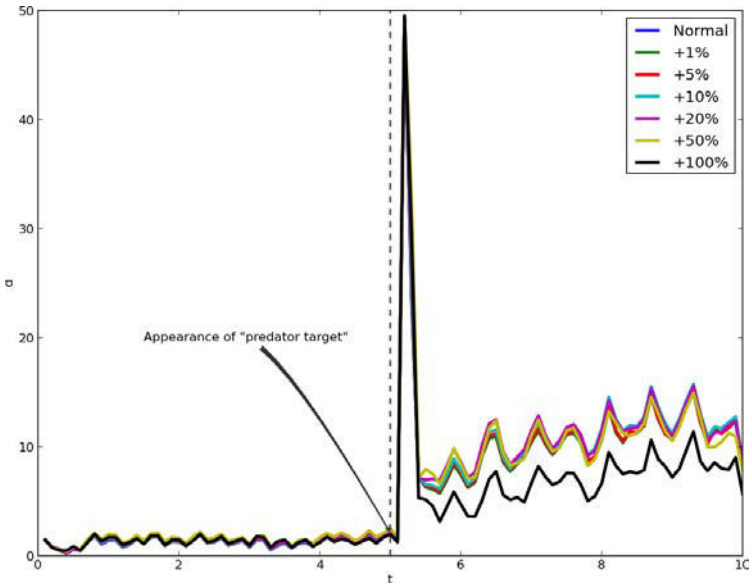

Figure 4.5: **Simulations results. Variation of center-of-mass test (Figure 4.2) by varying the cortical input gain in 1, 5, 10, 20, 50 and 100%**. As g_9 increases, the system converges faster, showing that the hand-picked values can be improved. A +100% variation generates a more notorious improvement (smaller error), but violates the range of action (up to 100% activation for units; not shown here).

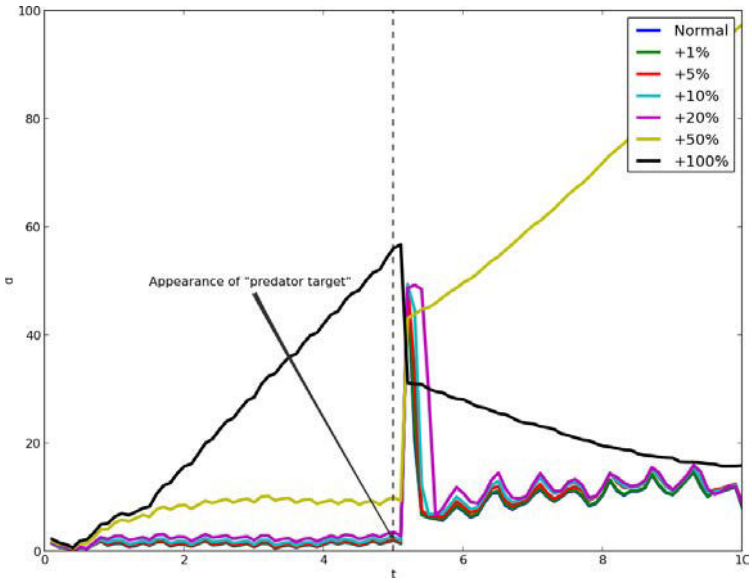

Figure 4.6: **Simulations results. Variation of center-of-mass test (Figure 4.2) by varying the DoG amplitudes (a,b) in 1, 5, 10, 20, 50 and 100% at the same time**. The system handles fairly well variations up to 20%, but larger variations don't allow for correct tracking. With a +50% variation the system does not change attention to the stimulus under alert, and with +100% variation the DNF simply stays fixated at a point, and as the small stimulus continues its path the distance increases, while when the second stimulus arrives, as it approaches this fixation point, the distance reduces itself gradually (both increase and decrease proportional to the speed of the stimulus that should be attended).

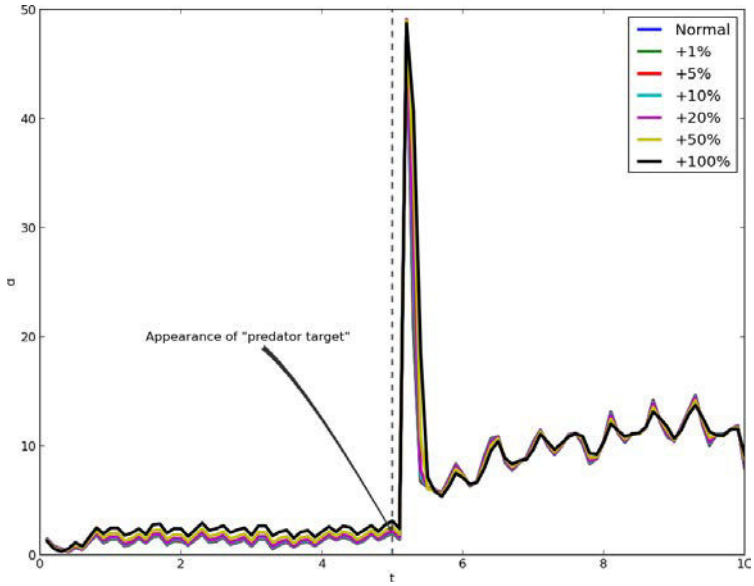

Figure 4.7: **Simulations results. Variation of center-of-mass test by varying the dSC time constant in 1, 5, 10, 20, 50 and 100%**. No important changes are noticed, as these percentage variations keep it under biologically plausible values.

4.2 Original experimental result: using natural images (M+K)

In order to extend the first version of our work, we use natural stimuli, as our system is particularly dedicated to these kinds of stimuli. An important characteristic of natural images is the difficulty to work with them, as they are noisy, contain several stimuli at times and may contain close distractors. They also have spectral characteristics that are very different from the previous artificial stimuli: instead of maximum contrast, the whole range of contrasts is allowed; instead of stimuli with opposed movements (horizontal and vertical), our sequences here use complex movements (including approaching motion), among others. Because of these characteristics, the stimuli are pre-treated, filtered and overall "adapted" before being used as input for our model (cf. Chapter 2). We start with a version of only the Magno and Konio systems, and we will include the Parvo pathway in the next experiment.

Here, we use the video of a kitten approaching a camera[1], as if to pounce on it, as shown in Figure 4.8. The kitten will, from now on, be considered as the fearful stimulus. We

Figure 4.8: **Sample of naturalistic stimuli used.** The sequence corresponds to a video of a kitten approaching and pouncing at a camera, and it is used with permission. The sliding text at the bottom was added as a distractor, to test the performances in competition, similar to the scenario with artificial images with the "predator" and "distractor" stimuli.

added a sliding text at a constant speed (faster than the kitten) to test the response of the system in a scenario where, being a classically more salient stimulus present –sliding text faster, and thus it would win the DNF competition if only the Magno stream were present–, the Konio stream allows i) the thalamus to influence cortical processing with the fearful contextual information, and ii) the superior colliculus to trigger an autonomic response (in

[1]Cf. `http://youtu.be/y_hikLJ7iB8`

this case, focus of attention) faster than expected using solely retinal information.

Our results in a detection, selection and tracking task are qualitatively similar to those of human observation (cf. Figure 4.9). We also test the numerical robustness of the model, as another objective of this work is to develop a stable model without many parameters. We realize that variations of up to +100% lead mainly to violate bio-plausibility, rather than to provoke numerical instability. However, this property is challenged only by one parameter when doubled ($\mathcal{K}$). We remind that no upper thresholding/saturation is applied at the output of any structure, precisely so avoiding numerical instability results as an emergent property of the system.

4.2.1 Discrimination, selection and tracking

We qualitatively draft a comparison between the simulation estimations and the targets. An overview of this process is shown in Figure 4.9. Here, we use a video with a fearful stimulus (kitten) and a distractor (sliding text) as stimulus. The distractor has a constant, faster speed than the fearful stimulus, and thus will attract the attention of a Magno-only system, which is represented by the red marker. The fearful stimulus is on the hunt, approaching smoothly and preparing to pounce on its target (the video camera), and because of these irregular motion behaviors a Magno-only system, while the distractor is present, will not be able, solely, to focus its attention on it. With the addition of the Konio pathway (system represented by the green marker), we observe a change in attention, which comes from the influence of the non-standard detection on the thalamic, cortical and collicular areas. Moreover, with the addition of the alert mechanism to the Magno and Konio system, this case represented by the blue marker, we observe a correct, or at least faster, positioning of the attentional focus on the fearful stimulus. This is due to several factors, and we can observe, also in Figure 4.9, their influence and importance to the outcome.

The situation here is the following:

1. The standard system detects motion (cf. Figure 4.10)

2. The non-standard system detects the fearful stimulus, and the alert information is sent towards SC (and relayed to LGN). Then, the cortex is biased towards the kitten, rather than keeping its focus at the sliding text (distractor) (cf. Figure 4.11)

3. TRN computes the mismatch and inhibits the text and extra motion in the scene (so

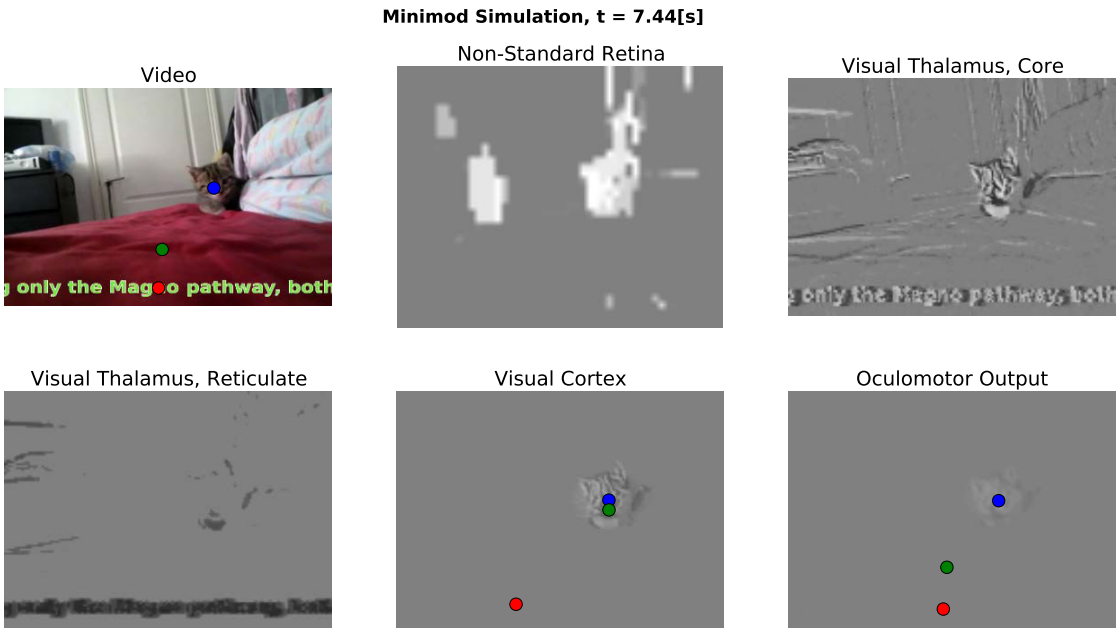

Figure 4.9: **Overview of results with natural stimuli.** Here, the pre-wired target (kitten) moves and stays still, and thus continuous competition is tested. The red marker is the equivalent of the fixation point for an only-Magno system, while the green marker represents a system including the Konio pathway. The blue marker corresponds to a system including also the alert mechanism.

the cortex focuses on the fearful stimulus) (cf. Figure 4.12)

4. Topographic tonic/burst information is sent to the cortex
5. Matrix, modulating information is processed by the cortex (cf. Figure 4.12)
6. Cortical output generates forced feedback if needed, and helps the decision at the SC (cf. Figure 4.12)

In addition, this system can easily simulate any "lesions" by simply deactivating a connection. The maps shown in Figure 4.9 are obtained from the Magno+Konio+Alert system (blue marker), and the other two markers are added for comparison. As shown, and thanks to the combined action of the different mechanisms and interactions mentioned, the system including the alert mechanism responds more rapidly.

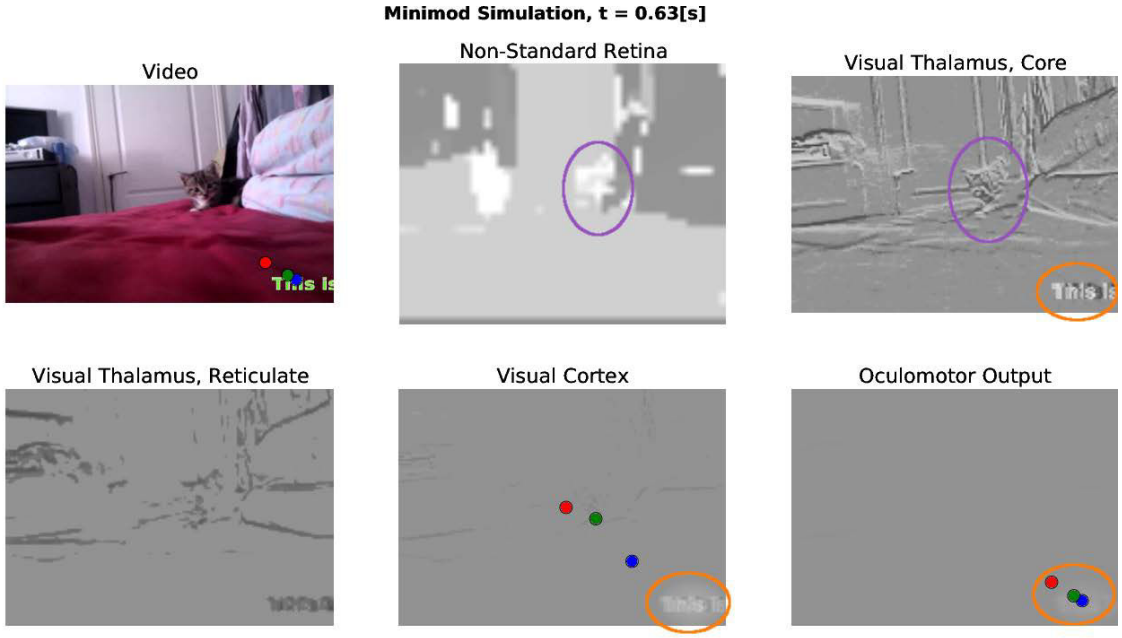

Figure 4.10: **Retinal detection (standard)**. Here, the non-standard retina does not clearly identify the fearful stimulus, and the system responds to the most salient movement, coming from the sliding text.

To be able to compare the performances of the three systems we measured, for the sliding text, the minimal distance to the line where it is moving; whereas for the kitten

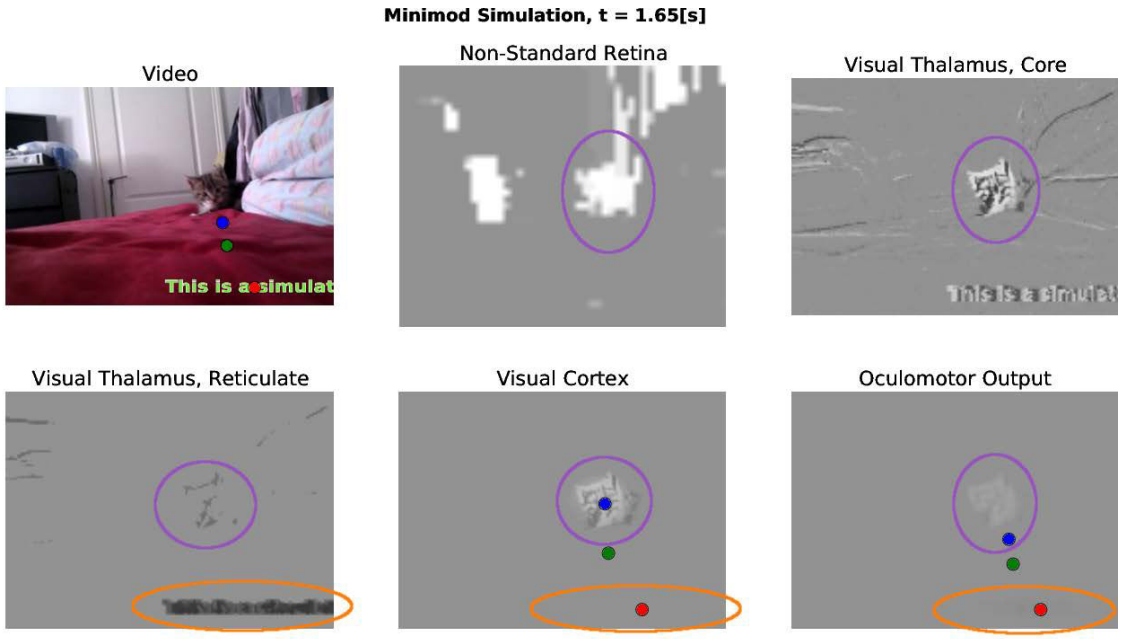

Figure 4.11: **Retinal detection (non-standard)**. This time, the non-standard retina does identify the fearful stimulus, and thus communicates this information to the SC and LGN, to bias posterior treatment towards this important target, here shown faster by the cortex, but very tightly followed by the SC.

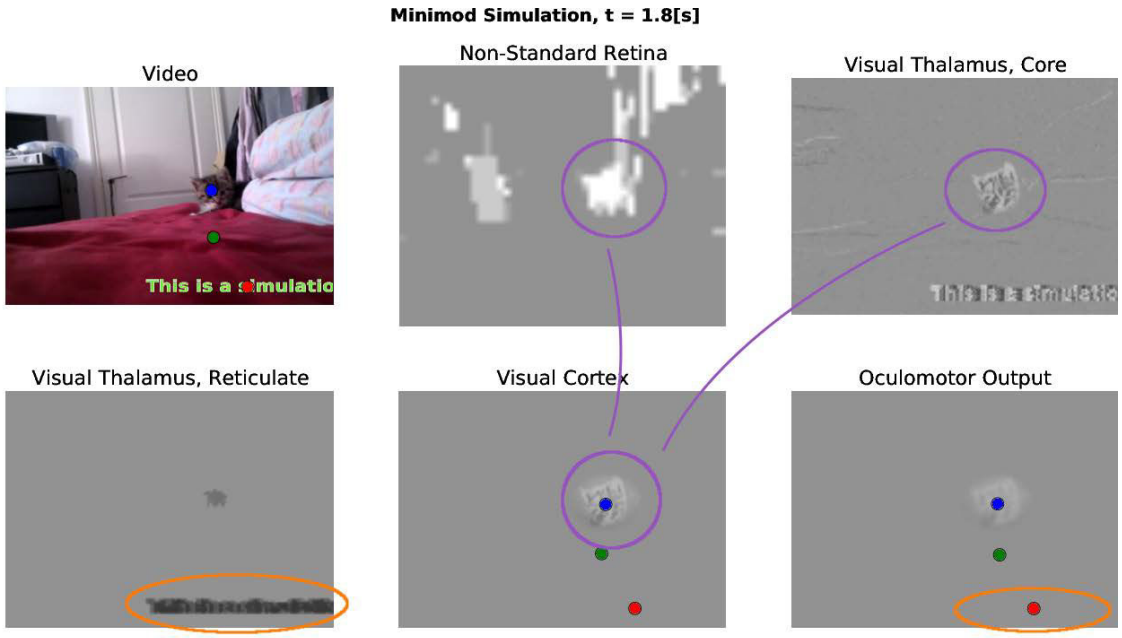

Figure 4.12: **TRN and mismatch in action**. When TRN checks for the mismatch between feedforward and feedback information, while the system being modulated/biased by the non-standard information, the sliding text must be inhibited to allow for proper treatment of the fearful stimulus, and this is why we see it darker in the image (darker means larger inhibition for this map).

we manually select the fixation points at its head. We then measured the euclidean distance between the simulated estimation and the two targets, and plotted these values as simulation errors, as shown in Figure 4.13, for the three studied systems, where the line colors correspond to those of the markers of Figure 4.9. We can see in Figure 4.13 that, despite being in a complex situation, the behavior of our system roughly corresponds to an usual human observation, when considering attentional shifts. As a pure Magno early visual system, its attention will focus on the fastest stimulus present in the scene, and we can see this specially in Figure 4.13 (bottom), where the error is practically a low constant value, because the text is faster at almost all times. However, when adding the Konio system, and particularly with its alert mechanism, we observe that, thanks to the different interactions between pathways, the system is able to switch its attentional focus towards the fearful stimulus (kitten), when it moves (i.e. when detected, as we consider only motion information). This is all thanks to the addition of the non-standard pathway: the matrix flow to the cortex, regulated by TRN, will communicate modulating information of the important stimulus, while the superficial SC transmits the alert signal to the (core and matrix) thalamus and the deep SC, so their processing is biased towards this "extremely relevant stimuli".

What happens is that when the "predator" is not moving, the DNF will only use the environmental information from camera movements (i.e. noise) and its internal feedback, but as the moving text is present, it switches its attention towards it. However, then the predator moves, the system detects it and reacts: the standard pathway transmits feedforward specific information, while the non-standard pathway transmits the alert and modulatory information to the matrix thalamus and the superficial superior colliculus. Here, the SC is already able to trigger a reaction, while the cortex will quickly validate its decision thanks to the action of the thalamocortical processing regulated by TRN: the presence of the fearful stimulus is transmitted to the cortex, which will allow for the predator to be prioritized, and the mismatch will allow TRN to inhibit other regions, such as the distractor (sliding text) and environmental noise.

4.2.2 Numerical robustness

This minimal simple model uses hand-picked values for its parameters. These are based on other studies (e.g. delays based in latencies) or biologically plausible numerical needs (e.g. a small threshold as a minimal amount of activation needed for a unit to respond). Here, we tested certain values for negative and positive differences of 1, 5, 10, 20, 50, and 100%.

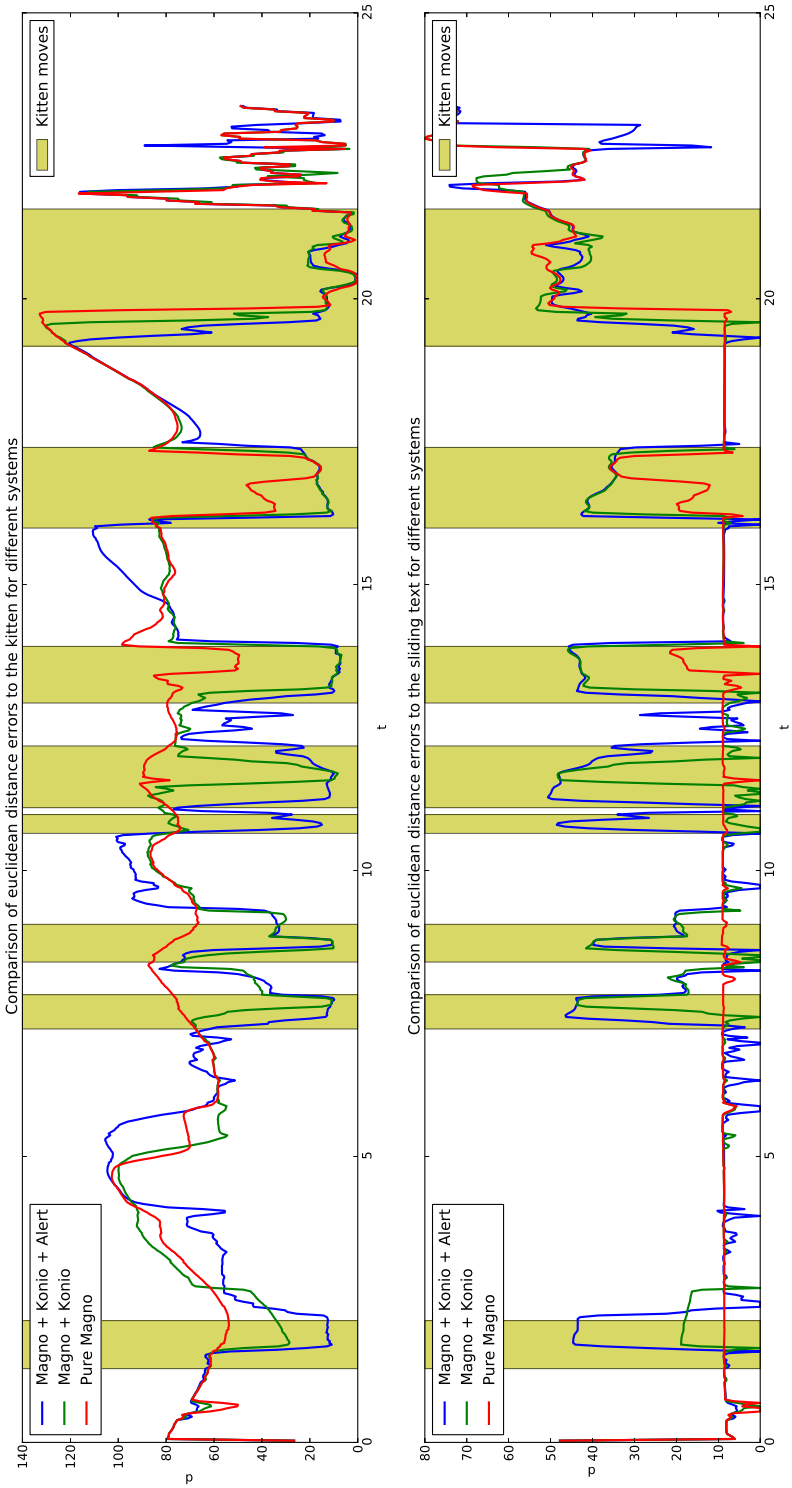

Figure 4.13: **Simulation results for all three systems with natural images.** The error is computed as the euclidean distance to target, and the yellow areas represent periods at which the kitten moves. (Top) Error against the head of the kitten. (Bottom) Minimal error against the sliding text.

Only the case of $\mathcal{K}+100\%$ led to numerical instability after 16.29 simulated seconds, which represents roughly 66% of the duration of the input video. To exemplify, Figure 4.14 shows the variations for g_9, Figure 4.15 shows the variations for $\mathcal{Z}$, and Figure 4.16 shows the variations for $\mathcal{K}$. In these figures we can observe certain improvements when modifying parameters, but some of them are not biologically plausible, which is represented by the dashed lines. These values usually mean an activation level of over 100% in a particular structure (not necessarily the one where the modified variable is used). All these results, and the results for the rest of the parameters of the system, are compiled in Table 4.1.

In Table 4.1, we observe again the numerical instability of $\mathcal{K}+100\%$, two cases where there would be no output –when g_5 or g_{11} have zero value–, the case of complete input annihilation if we nullify the rectification parameter (provoking a constant input), and the case of instantaneous effect, which besides unrealistic, numerically would imply dividing by zero in the differential equations.

4.3 Experimental result: using natural images (P+M+K)

In this experimental result, we add the Parvo pathway, and its contrast analysis capabilities. Another video[2] is used here to better illustrate how contrast information is used within the early visual system. The real early visual system processes also color information through this pathway, but as we build our models incrementally (adding one thing at a time), at the current stage color is not used in our model. In this video, a blackish dog receives a yellow tennis ball that has been thrown by an unseen thrower, while on the background one can see grass, bushes and trees. In the beginning, one can only see the dog moving, while after some time the ball, which will be considered as the fearful stimulus, appears from the top of the image. The usage of the ball as fearful stimulus is an artificial scenario, made up to illustrate the addition of the Parvo pathway. The Magno+Konio system shown in the previous section is already capable of switching its attention focus to the ball, but we wanted to see whether we could also use the Parvo pathway to help using the contrast information.

In this illustration we also look at a detection, selection and tracking task. However, there are four differences. One is the fact that the standard midget cells do not project to the superior colliculus. The second one is the mixing done at the deep superior colliculus, where at the time a simple average of the saliency maps has been done, and this result

[2]Cf. `http://youtu.be/iemfTNSe8s4`

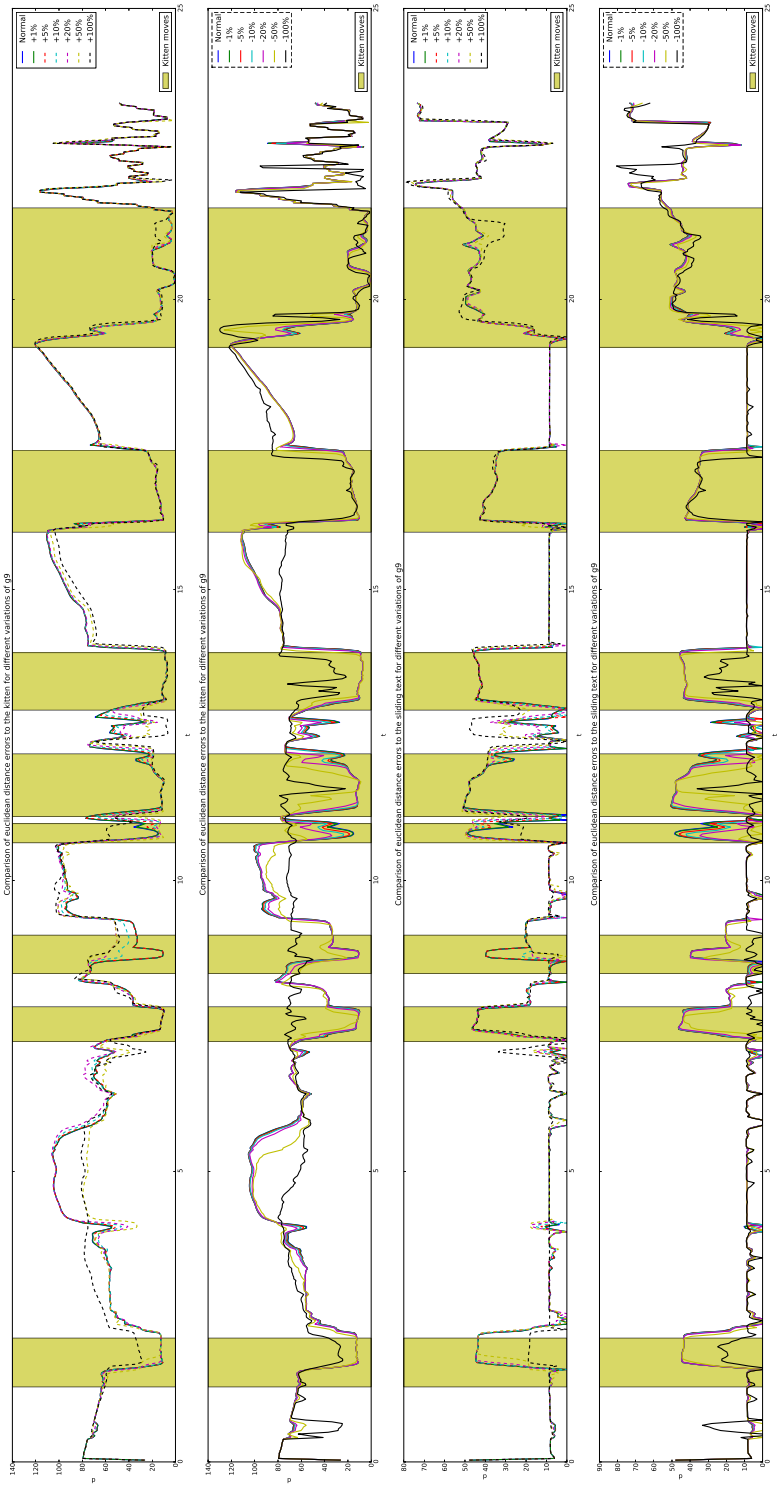

Figure 4.14: **Variation of the simulation results for g_9.** Simulation results for a Magno+Konio+Alert system, as in Figure 4.13, when the gain of cortical input (g_9) is varied from -100 to +100%, contrasted to the normal value, present in Table 4.1. The dashed lines represent the violation of bio-plausibility. (Top and middle top) Results for the kitten. (Bottom and middle bottom) Results for the sliding text. Image and caption taken from [23].

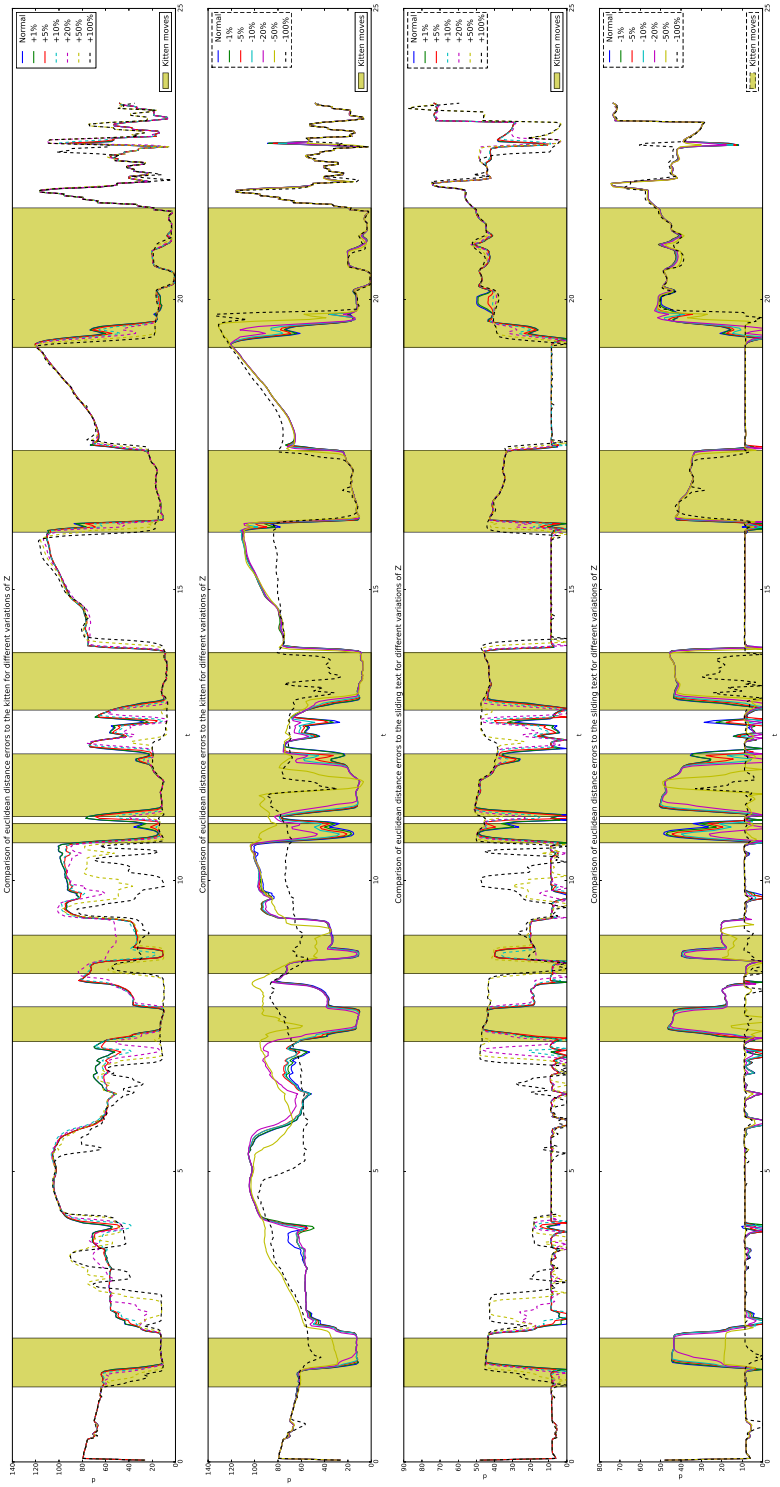

Figure 4.15: **Variation of the simulation results for $\mathcal{Z}$.** Simulation results for a Magno+Konio+Alert system, as in Figure 4.13, when the 2nd-order Gaussian-blur-like integrator ($\mathcal{Z}$) is varied from -100 to +100%, contrasted to the normal value, present in Table 4.1. The dashed lines represent the violation of bio-plausibility. (Top and middle top) Results for the kitten. (Bottom and middle bottom) Results for the sliding text.

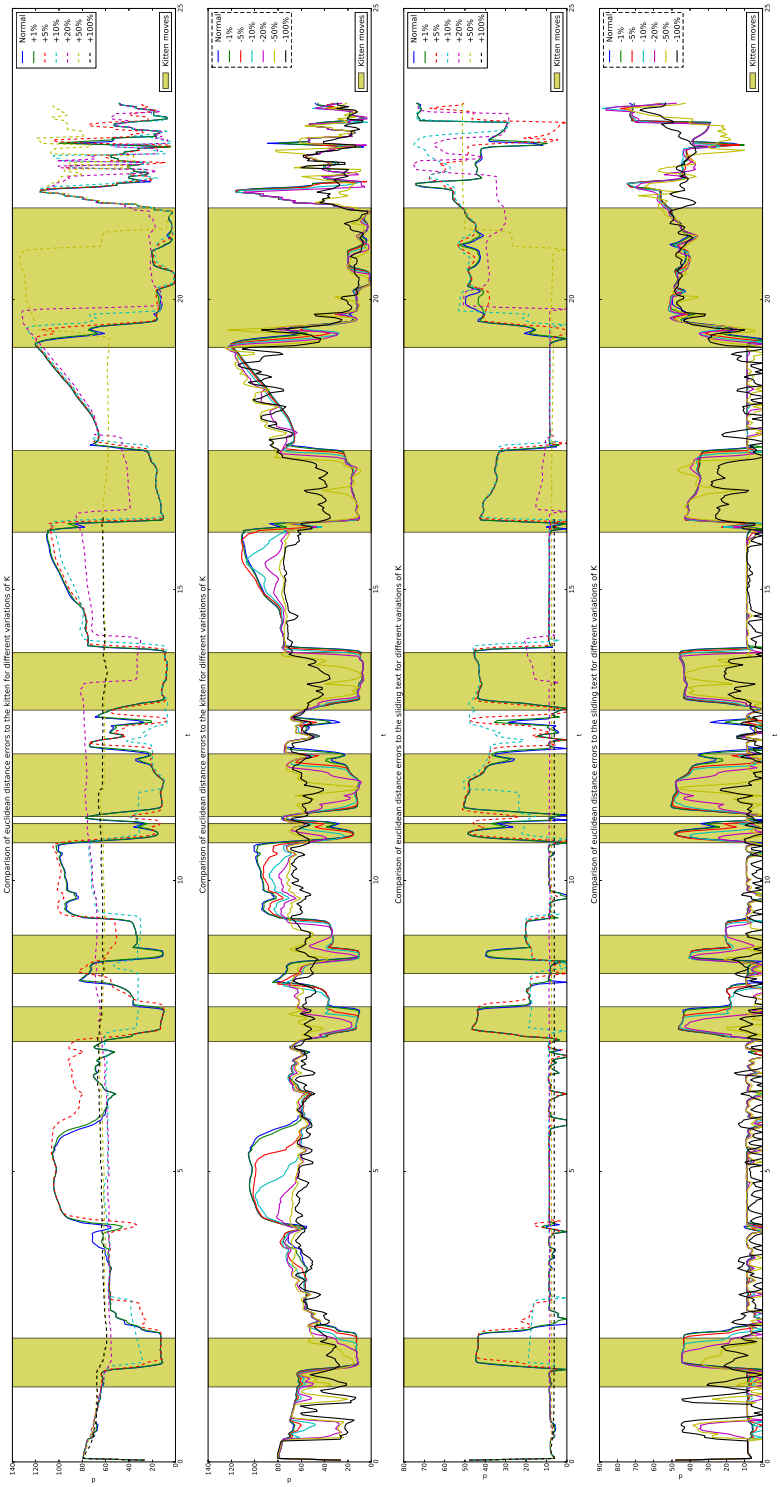

Figure 4.16: **Variation of the simulation results for $\mathcal{K}$.** Simulation results for a Magno+Konio+Alert system, as in Figure 4.13, when the amplitude of the DNF kernels ($\mathcal{K}$) is varied from -100 to +100%, contrasted to the normal value, present in Table 3.3. The dashed lines represent the violation of bio-plausibility. (Top and middle top) Results for the kitten. (Bottom and middle bottom) Results for the sliding text.

fed as input to the DNF. The third is that certain values (e.g. retinal time constant) are changed for the Parvo pathway. These numerical modifications are presented in Table 4.2, and the ensuing numerical analysis for robustness has not been considered as these modifications are only reductive ("lowering" a value).

Table 4.2: Variations from Magno to Parvo values

Variable	Value in Magno	Value in Parvo
τ_1	25ms	45ms
a_8	0.4	0.38
d_8	0.25	0.2375
e_8	0.4	0.38
m_8	1.5	1.425

An overview of the results is shown in Figure 4.17, where the marker represents the attentional focus at that stage.

Here, what happens is the following:

1. The parasol cells detect motion, while the midget cells do the contrast analysis (cf. Figure 4.18)

2. The ball (fearful stimulus) appears, and while the Magno system detects it (and is already modifying its focus), the Parvo system takes longer to do this (cf. Figure 4.19)

3. When the Parvo system finishes switching the focus, the Magno system seems to still hesitate between stimuli. This could be because of the similar speeds at that instant, and the internal connection of the DNF used (cf. Figure 4.20)

4. Both systems converge at the fearful stimulus after some more time passes (cf. Figure 4.21)

In addition to the previous results, the system has been simulated with a lesion on the connection between parasol and Magno cells. The parasol projections to the superior colliculus have been left intact. This is done to show with more detail the importance of the Parvo pathway, and how the Parvo+Konio interactions would allow for a proper attentional

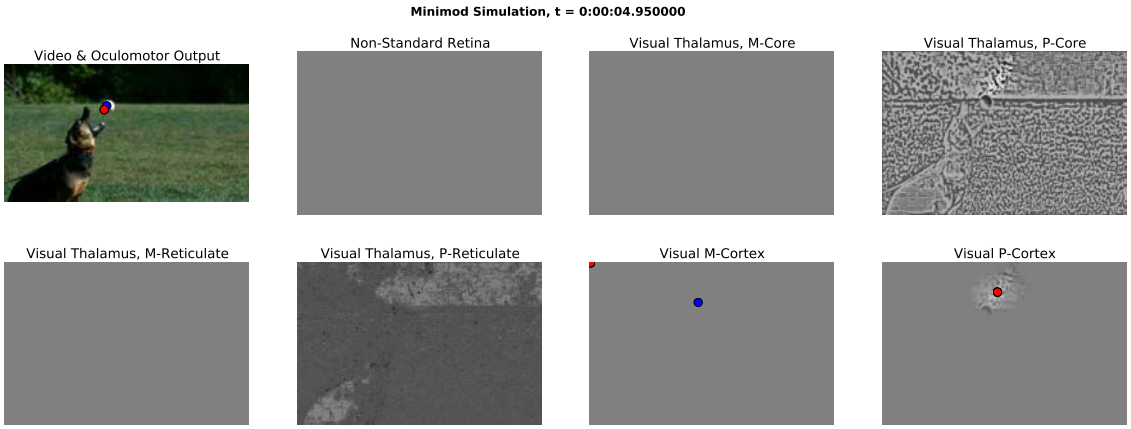

Figure 4.17: **Overview of results with natural stimuli in the P+M+K system.** Here, the pre-wired target (ball) appears after the dog starts moving. The markers are equivalent to the fixation point for the systems. The blue marker represents a normal system, i.e., a system composed of all three pathways in a healthy situation. The red marker, however, presents a lesion between the retina and LGN, where the parasol cells cannot communicate to the Magno cells, thus depriving LGN and cortex of motion information. This system already includes the alert mechanism, and the simulation images correspond to the unhealthy system with the healthy marker added from the same point of time in the healthy simulation. Here, the conclusion can be seen in the upper left figure, where the blue marker is closer to the fearful stimulus than the unhealthy one. Also, we observe that the healthy system changes much faster (not shown here), and we infer this is due to the action of the Magno-like system, which is able to process information faster than the Parvo-like system, and thus will help deciding and reacting in a shorter amount of time.

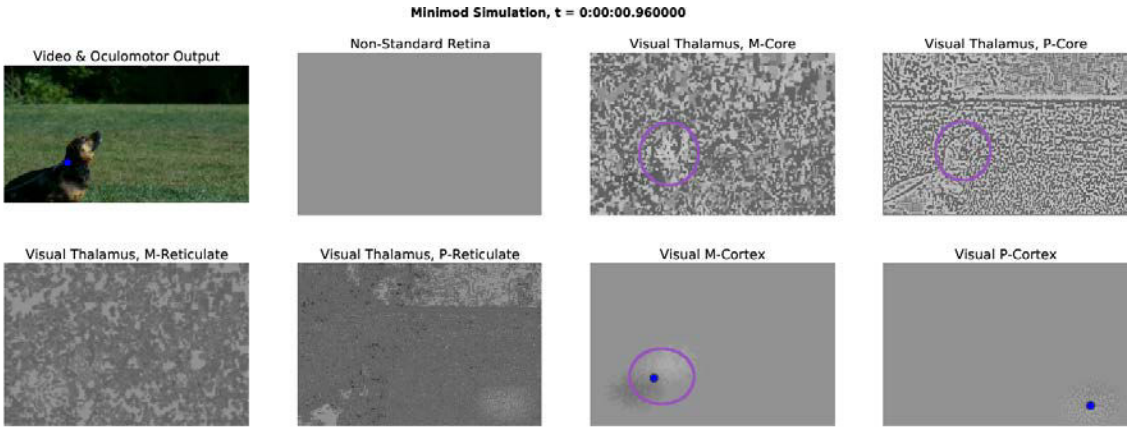

Figure 4.18: **Parasol cells detect motion**. Here, the parasol cells –part of the Magno pathway– have detected motion coming from the dog, while the midget cells –part of the Parvo pathway– analyze the region they found to contain maximum contrast in the image.

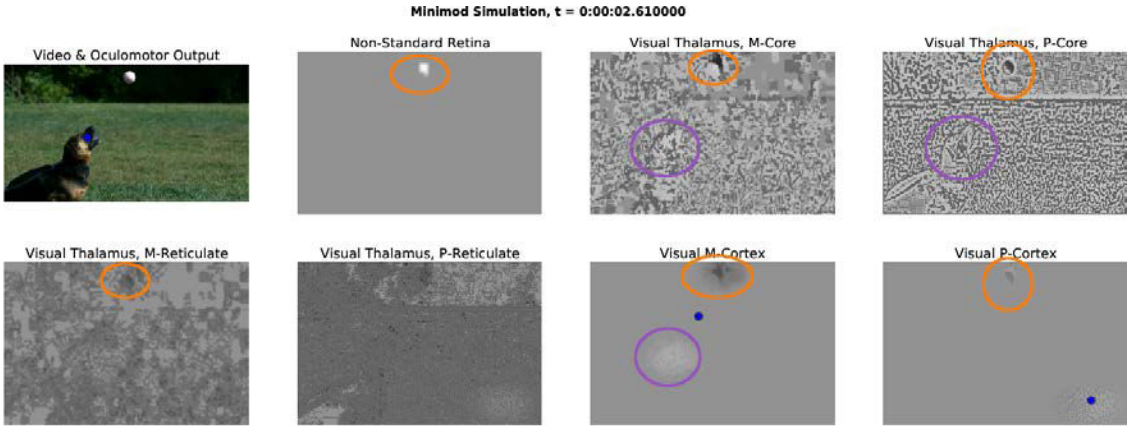

Figure 4.19: **Appearance of the fearful stimulus**. After some time, the fearful stimulus (tennis ball) appears, and the Magno system reacts faster than the Parvo system (while both are influenced by the Konio system).

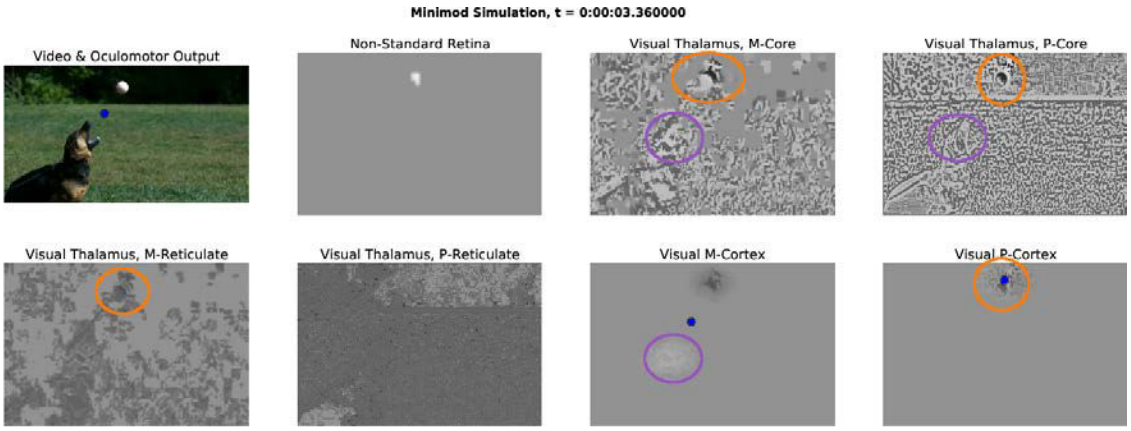

Figure 4.20: **Focus switch occurs**. After little time, both systems change their focus towards the fearful stimulus. Here, the Parvo system seems to be more accurate than the Magno system, despite the latter changing faster. This sort of "hesitation" from the Magno system could be because of the internal connection of the corresponding DNF, together with the similar motion obtained from the distractor.

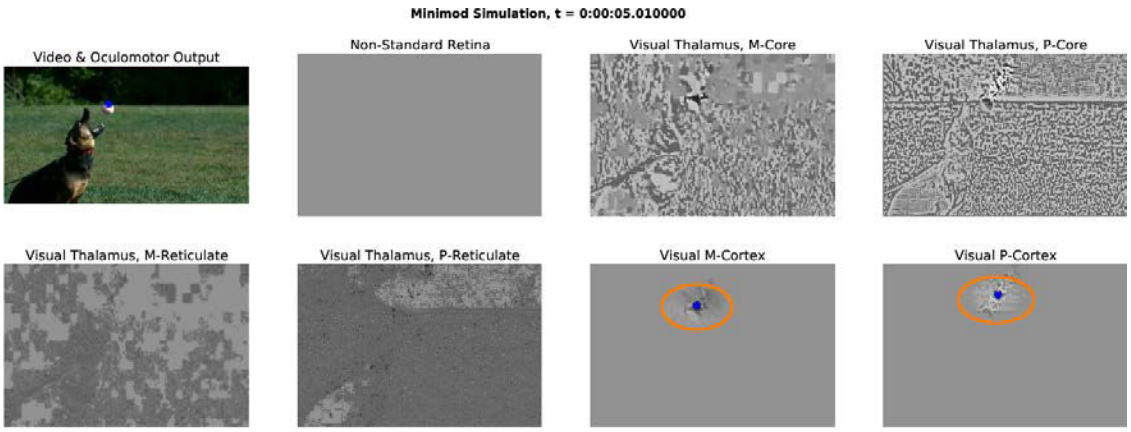

Figure 4.21: **Parvo and Magno convergence**. After some time, both systems are focused at the fearful stimulus, and this is possible thanks to the action of the Konio system. Notice that in this frame the non-standard retina does not show the fearful stimulus, and this could be because of how the stimulus was learned: isolated, not in the snout of a dog.

shift; similar to what was done with the M+K system. Also, this simulation allows to pay more attention at the way of working of the Parvo pathway. No other parameters (than the lesion) have been changed from the previous simulation. The lesion on the midget cells is equivalent to presenting other example of the M+K system shown previously, so it has been omitted.

Here –and using the same time points as for the previous simulation–, what happens is the following:

1. The parasol cells detect motion, while the midget cells do the contrast analysis. Notice that since the lesion is for the parasol output towards Magno cells (no data neither in the thalamus, nor in the cortex), the SC still receives the motion information, which allows the focus to be at the dog (cf. Figure 4.22)

2. The ball (fearful stimulus) appears, and this is already visible in the Parvo-like cortex, which starts changing its focus (cf. Figure 4.23)

3. When the Parvo system finishes switching the focus, this information is communicated to the SC. Here, the collicular DNF still does not change its focus (cf. Figure 4.24)

4. The system converges at the fearful stimulus after some more time passes (cf. Figure 4.25)

The performance of the system is measured by simply comparing its attentional focus to a man-made focus at the ball, the fearful stimulus. The results, though still illustrative, are shown in Figure 4.26. Here, we see that the system converges, despite the different timings for the driving pathways, and the Magno and Parvo pathways working independently only till the deep superior colliculus. This is thanks to the action of the Konio pathway, the regulation from TRN, and the different interactions throughout the whole system, for both the healthy system and the unhealthy one. We notice, however, the difference in speed between them, where the healthy one (containing the standard feedforward Magno-like information) performs better than its unhealthy counterpart.

We thus illustrate how to reuse the thalamocortical computations (modules) proposed for the Magno pathway, now for the Parvo pathway. The system is easily modified to include another pathway, keeping its properties when already stable parameters are lowered. In addition, we can easily study certain failures inside the system, where diminished or nullified connections is only a single example of the full potential of this model.

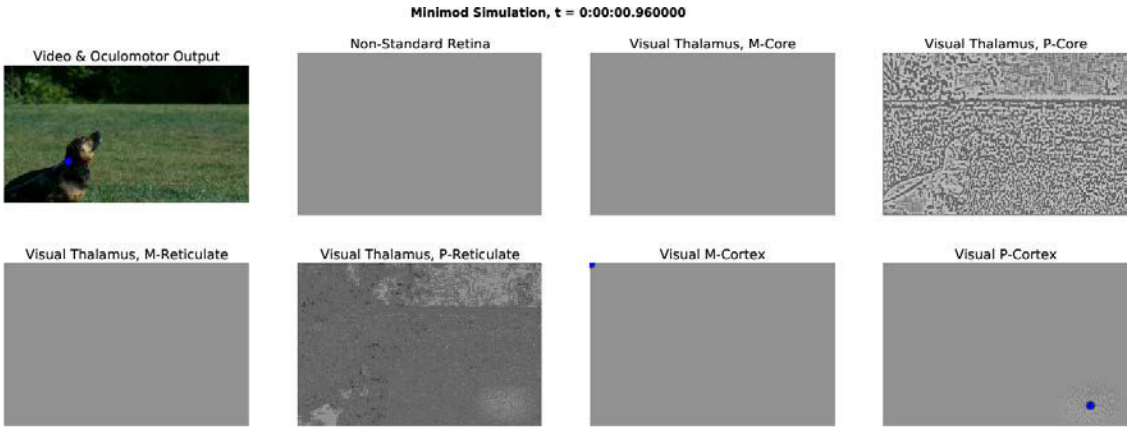

Figure 4.22: **Parasol cells detect motion, but do not transmit it to LGN**. As in Figure 4.18, the parasol cells detect motion coming from the dog, while the midget cells analyze the region they found to contain maximum contrast in the image. Here, the difference is the lesion in the link between parasol and Magno cells, where the Magno-related collicular links are responsible for the selection of the dog.

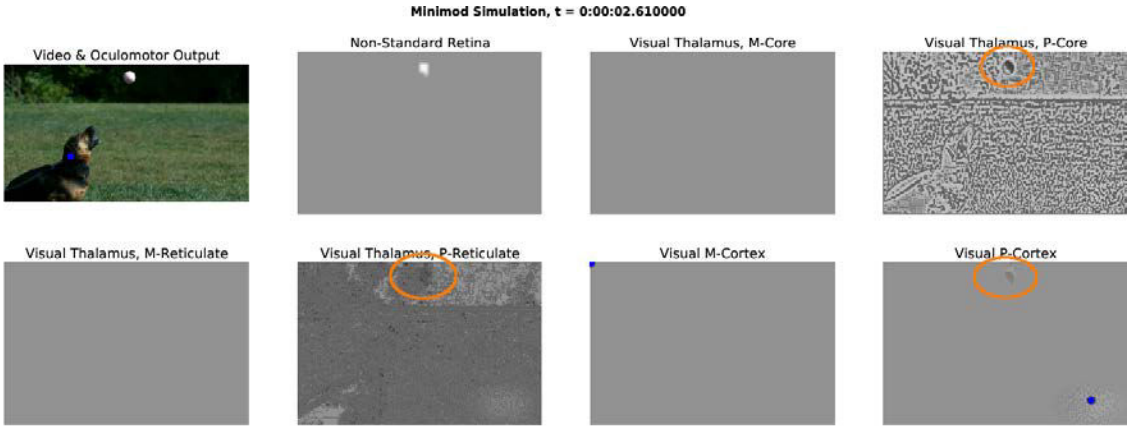

Figure 4.23: **Appearance of the fearful stimulus**. After some time, the fearful stimulus (tennis ball) appears, and despite noticing this in the cortical map, the Parvo-like cortical DNF has only started switching the focus. This is already a proof of the slower processing, when compared to the Magno system, as we use the same time points as in the previous simulation.

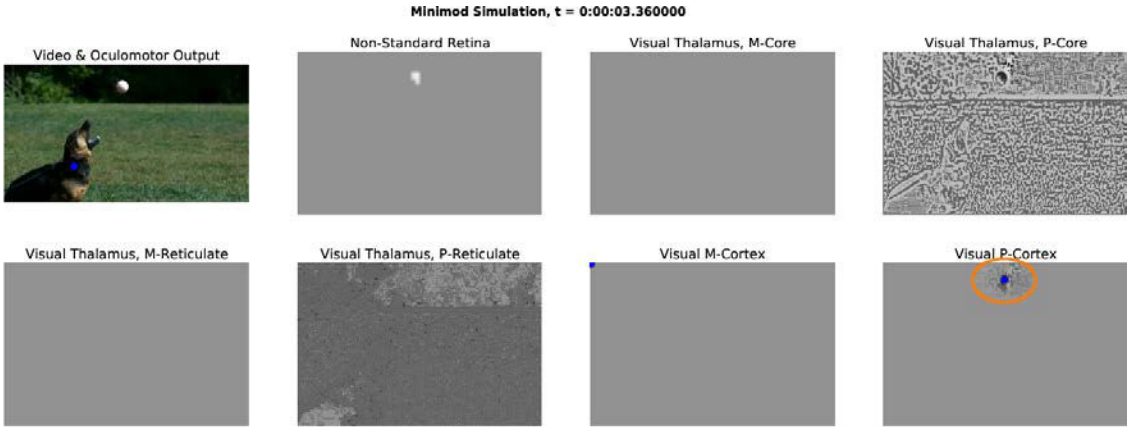

Figure 4.24: **Focus switch occurs cortically, but it is not yet reflected collicularly**. After little time, the Parvo system changes its focus towards the fearful stimulus. However, this has just happened cortically, while the colliculus stays at the dog position. This follows the fact of slower Parvo treatment when compared to Magno treatment.

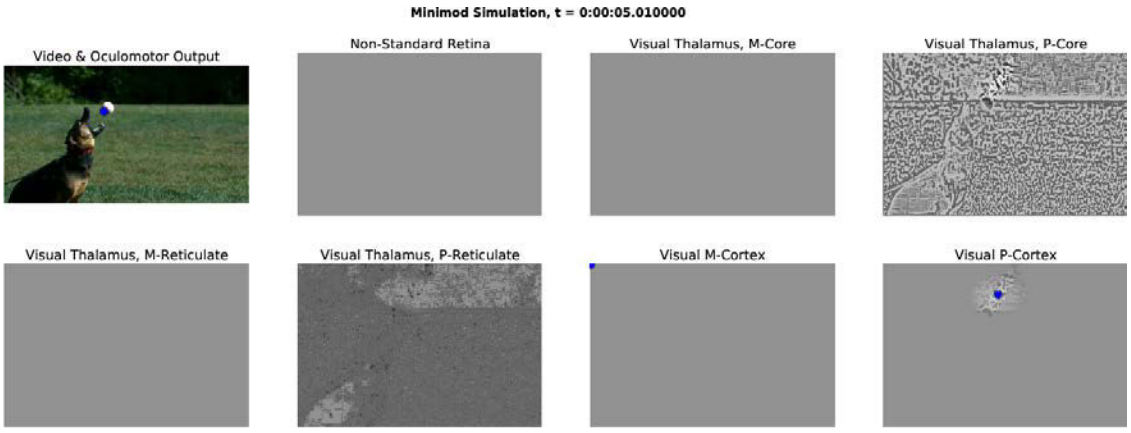

Figure 4.25: **Convergence of the lesioned system**. After some time, the system is focused at the fearful stimulus.

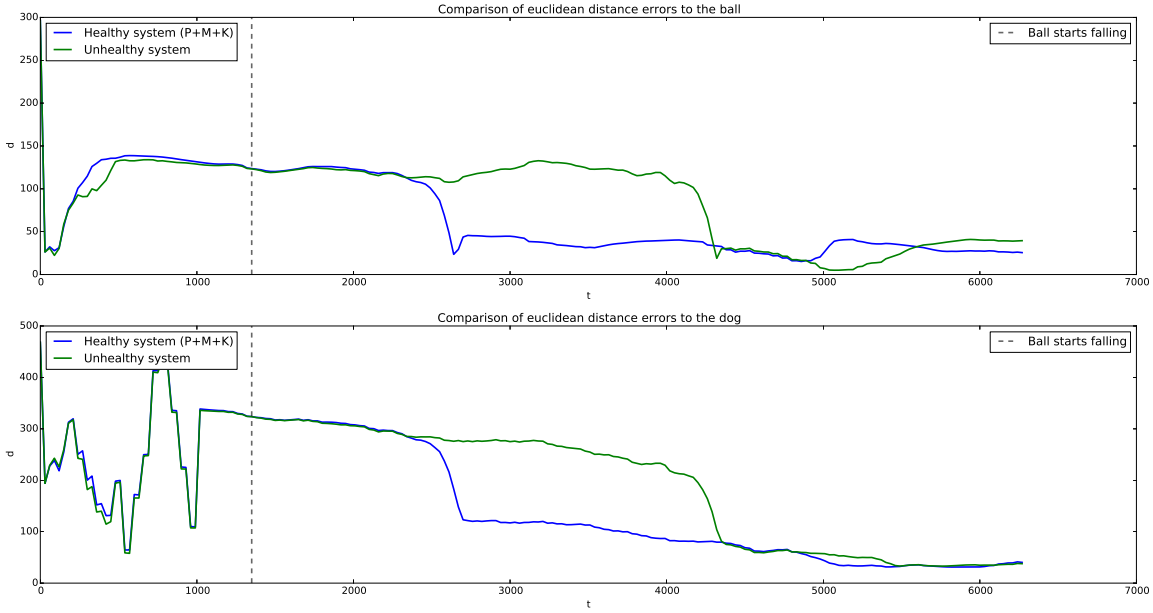

Figure 4.26: **Simulation results for the P+M+K systems**. As for the M+K system, the error is computed as the euclidean distance to target, where the reference point has been built by hand. For simplicity, as this is only an illustration, only the full system has been analyzed in both healthy and unhealthy –broken connection between parasol and Magno cells– cases. The lower error to both targets is explained because the distractor is approaching towards the fearful stimulus (dog catching the tennis ball). We notice that the green curve (unhealthy system) reacts slower when compared to the blue one, and we infer this is because of the lack of the standard Magno-like information towards LGN, the cortex and ultimately the SC, because of the disability in the parasol-Magno connection.

4.4 About observed emerging properties

"The strategy, as we have said, is to build a cognitive system, not from symbols and rules, but from simple components that can be dynamically linked between each other in a very dense manner. Here, each component works in its *local* environment so as that the system cannot be operated by an external agent that would pull the lever, in a sort of way. But thanks to the nature of the configuration of the system, a *global* cooperation *emerges* spontaneously when the states of each concerned neuron yield a satisfactory global performance. Such a system does not require a central processing unit to control its operation. This transfer of local rules to the global coherence is the heart of what was agreed to be called self-organization during the years of cybernetics. Today, one prefers to talk about emerging or global properties, of dynamical networks, or nonlinear, of complex systems, or even of synergy." (Translated to English from [178]).

The previous paragraph encompasses the spirit of our systemic approach and its properties.

Furthermore, our simulation allows us to make two predictions about some neural properties of the system:

- On the one hand, the adaptation following target selection in the thalamocortical loop, involves the inhibition by TRN, independently of the existence of an alert
- On the other hand, the numerical stability in the range of bio-plausible values, makes us predict that no saturation mechanisms are in action

These are not the only possible predictions but we propose to make them explicit and make the bet that they are verified experimentally.

4.5 Open-access software

All the software used for obtaining these results is accessible at `http://www.loria.fr/~ccarvaja/earlymod`, or by demand to the author.

Table 4.1: **Numerical Robustness for parameters used with natural stimuli**

Parameter	Original Value	Bio-plausible Variation(%)	Non Bio-plausible Variation(%)
τ_1	25[ms]	*[-50,+100]	∅
τ_2	45[ms]	*[-50,+100]	∅
τ_3	45[ms]	*[-50,+100]	∅
τ_4	4[ms]	*[-50,+100]	∅
τ_5	15[ms]	*[-50,+100]	∅
τ_6	15[ms]	*[-50,+100]	∅
τ_7	10[ms]	*[-50,+100]	∅
τ_8	8[ms]	*[-50,+100]	∅
τ_9	12[ms]	[-10,+100]	*[-50,-20]
τ_{10}	4[ms]	*[-50,+100]	∅
τ_{11}	30[ms]	*[-50,+100]	∅
τ_{12}	15[ms]	*[-50,+100]	∅
ψ	0.06	**[-50,+20]	[+50,+100]
s_{alert}	0.6	[-100,+100]	∅
g_5	0.8	***[-50,+20]	[+50,+100]
a_5	0.35	[-100,+100]	∅
b_5	0.65	[-100,+50]	+100
s_5	0.1	[-100,+100]	∅
k_6	0.2	[-100,+100]	∅
a_6	0.4	[-100,+100]	∅
c_6	0.3	[-100,+20]	[+50,+100]
d_6	0.7	[-100,+10]	[+20,+100]
s_d	0.01	[-100,+100]	∅
$\mathcal{L}$	$\begin{bmatrix} 0 & 1 & 0 \\ 1 & -4 & 1 \\ 0 & 1 & 0 \end{bmatrix}$	[-100,+100]	∅
a_8	0.4	[-100,+100]	∅
d_8	0.25	[-100,+100]	∅
e_8	0.4	[-100,+100]	∅
m_8	1.5	[-100,+100]	∅
g_9	0.2	[-100,+1]	[+5,+100]
$\mathcal{Z}$	$\frac{1}{16}\begin{bmatrix} 1 & 2 & 1 \\ 2 & 4 & 2 \\ 1 & 2 & 1 \end{bmatrix}$	[-50, +5]	-100,[+10,+100]
$\mathcal{K}\ (a, b)$	(0.83 , 0.415)	[-100,+1]	[+5,+50],+100****
s_{10}	0.2	[-100,+20]	[+50,+100]
g_{11}	0.2	***[-50,+100]	∅

(*) -100% would imply dividing by zero

(**) -100% would imply a constant input in all retinal links

(***) -100% generates no output for these variables

(****) Provokes numerical instability

Chapter 5

Conclusion

"Great is the art of beginning, but greater is the art of ending"
– Henry Wadsworth Longfellow

This study was set up to explore the role of the thalamus and the non-standard visual pathway in the behavioral responses of the early visual system. This work also sought to develop a computational model to test our hypotheses using simulations of real-world scenarios, with natural image sequences. The general theoretical and experimental literature on this subject explores the roles and interactions between the so-called "standard" visual pathways: Parvocellular and Magnocellular, with a particular emphasis on what happens in the brain. Our study reuses the core ideas of this literature, together with newer sources regarding non-standard visual streams. We consider the early visual system and its processing, in order to answer the questions:

1. How does this non-standard visual system aid behavioral processes, more specifically visual event detection?

2. How do these standard and non-standard information flows interact in the early visual system?

3. What is the role of the thalamus in the regulation and synchronization of the different feed-forward and feedback information flows?

4. Can one put all this into a piece of software and use it for simulations, and eventually for applications beyond brain understanding?

The main findings of this study are shown and discussed in Chapter 4: *Our minimal model in the real world: Experimental results*. This section synthesizes these findings to make explicit the answer we can offer regarding the four issues proposed here.

1. *How does this non-standard visual system aid behavioral processes, more specifically visual event detection?*

   Through the coarse detection mechanisms present in the non-standard ganglion cells, its output is able to communicate, via a direct connection, to the superior colliculus, allowing rapid event/emergency behavior. The non-standard visual system thus allows the superior colliculus to initiate an action without the need for cortical processing.

   Furthermore, the modulation imposed by the Konio cells to the cortex afferences –in both Parvo and Magno information flows–, biases the response towards the detected visual event. However, this bootstrapping information, fast but coarse when not spurious, is regulated by the cortex to prevent a critical response to a "ghost" stimulus, i.e. a stimulus not really present in the scene.

2. *How do these standard and non-standard information flows interact in the early visual system?*

   Even if these streams travel in parallel along most of the early visual system, they do not interact at each step. On the contrary, clear interactions between them exist at the primary visual cortex, and the superior colliculus, as implemented in our model.

   In V1, both standard information flows (Parvo and Magno) are separately modulated by the non-standard (Konio) pathway. In the SC, not only cortical and retinal information are meshed. Both standard pathways are mixed, and ultimately the dSC computes the final behavioral decision.

3. *What is the role of the thalamus in the regulation and synchronization of the different feed-forward and feedback information flows?*

   The thalamus is at a first glance a smart "relay" for the retinal information to the cortex, when working in the tonic mode. It is a smart relay because its core part also processes this information, while non-standard collicular information and cortical feedback are taken into account. This feedback influences the core treatment both directly and through TRN.

The matrix part of the thalamus is also regulated by TRN (who serves as the thalamic regulator at all levels), but seems to lack a cortical connection. Though this last statement is sometimes contradicted in the literature, we have opted for the classical approach.

The TRN regulates the thalamus, and thus all three information flows, through selective inhibition. This inhibition is the result of the thalamocortical mismatch: feedforward thalamic versus cortical feedback flows. The result of this mismatch helps switching into the burst mode (or back to the tonic mode), and to regulate what information should pass, or simply how much of it, as it can be fully inhibited, partially inhibited, or not inhibited. This inhibition is topographic (one to one mapping on the retinotopic map).

4. *Can one put all this into a piece of software and use it for simulations, and eventually for applications beyond brain understanding?*

   Yes, and possibly yes. We present in this work a computational model where we have studied our hypotheses and reused the main ideas present in the literature, where we can easily study lesions too, and with relatively simple algorithms that could be used in simple, and eventually more developed, robots.

   For prosthetics, we have shed some light on the *"why/what-for"* the retinal information is used. The main message here is that a complete artificial retina can by no mean be "a camera connected to the thalamus", whereas it must include visual preprocessing at the edge of the state of the art of computer vision. This does not mean that a visual sensor that only provides standard contrast and motion information to the visual cortex is not already a useful prosthesis for visual observation tasks. This means that this is not going to help for embedded vision (i.e. vision in action).

This work focuses on the early visual system, considering local computations and emergent global properties. However, this is only one aspect, and much is to be studied regarding higher cortical areas, and other structures that are involved in the behavioral responses considered here. Here are a few issues regarding next steps, beyond this work:

- Study and inclusion of the core and matrix pulvinar, in order to incrementally add other cortical areas to the system, and exploit more sophisticated thalamocortical processing

- Study and inclusion of thalamocortical learning (related to the pulvinar), to provide the system with adaptability and memory, in order to learn new scenarios that are not pre-wired, but acquired through time
- Addition of multi-order synchronization by the inclusion of gap junctions in TRN This would allow us to better understand the thalamocortical regulation and synchronization
- A more detailed study of the different lesions that can be operated, and the related performance impairment
- An improvement in speed of processing for the current development so it can be used in real time circuits, essential point for robotics
- The modification of the DNF mechanism used for V1, where instead of a DNF, competing orientation maps should be implemented

The mystery of vision is still a work in progress. It will take many more studies, and the combined efforts of many people to work it out. Through our results studying the early visual system, and the developing of our simulating environment, we have given one step further into unraveling this mystery.

Chapter 6

Conclusion (Français)

"Great is the art of beginning, but greater is the art of ending"
– Henry Wadsworth Longfellow

Cet étude a été réalisé pour explorer le rôle du thalamus et de la voie visuelle non-standard dans les réponses comportementales du système visuelle précoce. Ce travail a aussi cherché à développer un modèle computationnel pour tester nos hypothèses en simulant des scénarios du monde réel, avec des séquences d'images naturelles. La littérature dans ce sujet explore généralement les rôles et les interactions entre les voies dites "standard": Parvocellulaire et Magnocellulaire, avec une accentuation particulière sur cela qui se passe au niveau du cerveau. Notre étude réutilise les idées principales de cette littérature, en ajoutant des nouvelles sources qui ont étudié les voies visuelles non-standard. Nous considérons le système visuelle précoce et son traitement, pour répondre à ces questions:

1. Comment ce système visuelle non-standard aide des processus comportementaux, plus spécifiquement de détection visuelle d'événements ?

2. Comment ces flux d'information non-standard interagissent dans le système visuelle précoce ?

3. Quel est le rôle du thalamus dans la régulation et synchronisation des différents flux d'information montants et descendants ?

4. Peut-on compacter tout cela dans un logiciel et l'utiliser pour faire des simulations, et éventuellement pour des applications au delà de la compréhension du cerveau ?

Les résultats principaux de cet étude sont montrés et discutés dans le chapitre 4: *Our minimal model in the real world: Experimental results.* Cette section synthétise ces résultats pour faire explicite la réponse que nous donnons aux quatre questions posés ici.

1. *Comment ce système visuelle non-standard aide des processus comportementaux, plus spécifiquement de détection visuelle d'événements ?*

   Through the coarse detection mechanisms present in the non-standard ganglion cells, its output is able to communicate, via a direct connection, to the superior colliculus, allowing rapid event/emergency behavior. The non-standard visual system thus allows the superior colliculus to initiate an action without the need for cortical processing.

   Furthermore, the modulation imposed by the Konio cells to the cortex afferences –in both Parvo and Magno information flows–, biases the response towards the detected visual event. However, this bootstrapping information, fast but coarse when not spurious, is regulated by the cortex to prevent a critical response to a "ghost" stimulus, i.e. a stimulus not really present in the scene.

2. *Comment ces flux d'information non-standard interagissent dans le système visuelle précoce ?*

   Même si ces flux se déplacent en parallèle tout au long de la majeure partie du système visuel précoce, ils n'interagissent pas à chaque étape. Au contraire, des claires interactions existent entre eux au niveau du cortex visuel primaire, et du colliculus supérieur, comme implémenté dans notre modèle.

   En V1, les deux flux d'information standard (Parvo et Magno) sont modulés séparément par la voie non-standard (Konio). Dans le SC, non seulement l'information corticale et de la rétine sont prises en compte. Les deux voies standard sont mélangés, et, finalement, le dSC calcule la décision comportementale finale.

3. *Quel est le rôle du thalamus dans la régulation et synchronisation des différents flux d'information montants et descendants ?*

   Le thalamus est, à première vue, une "relais" intelligent pour l'information de la rétine au cortex, lorsque l'on travaille en mode tonique. Il est un relais intelligent parce que sa partie centrale traite également cette information, alors que l'information colliculaire non-standard et le retour corticale sont pris en compte. Ce retour influe sur le traitement core à la fois directement, et indirectement par TRN.

La partie de la matrix du thalamus est également régulée par TRN (qui sert de régulateur thalamique à tous les niveaux), mais semble manquer une connexion corticale. Bien que cette dernière affirmation est contredite parfois dans la littérature, nous avons opté pour l'approche classique.

Le TRN régule le thalamus, et donc cela est vrai pour tous les trois flux d'information, par inhibition sélective. Cette inhibition est le résultat de la disparité thalamocortical: flux thalamiques montants contre les flux des retours corticales. Le résultat de cette disparité aide à basculer en mode rafale (ou revenir au mode tonique), et de réguler quelle information devrait passer, ou tout simplement combien d'elle, car il peut être totalement inhibée, partiellement inhibée, ou pas inhibée. Cette inhibition est topographique (cartographie un-à-un sur la carte rétinotopique).

4. *Peut-on compacter tout cela dans un logiciel et l'utiliser pour faire des simulations, et éventuellement pour des applications au delà de la compréhension du cerveau ?*

   Oui, et peut-être oui. Nous présentons dans ce travail un modèle informatique où nous avons étudié nos hypothèses et réutilisé les principales idées présentes dans la littérature, où l'on peut aussi facilement étudier des lésions, et avec des algorithmes relativement simples qui pourraient être utilisés dans des robots simples, et éventuellement plus développés.

   Pour les prothèses, nous avons éclairé un peu les emph "pourquoi/pour-quoi" l'information rétinienne est utilisé. Le message principal est que une rétine artificielle complète ne peut en aucun cas être "une caméra connectée au thalamus", alors qu'elle doit inclure un prétraitement visuel à l'état de l'état de l'art de la vision par ordinateur. Cela ne signifie pas qu'un capteur visuel qui fournit uniquement des informations standard de contraste et de mouvement pour le cortex visuel n'est pas déjà une prothèse utile pour des tâches d'observation visuelle. Cela signifie que ce ne va pas aider à la vision embarquée (c'est à dire de la vision en action).

Ce travail se concentre sur le système visuel précoce, en considerant des calculs locaux et propriétés globales émergentes. Cependant, ce n'est qu'un aspect, et beaucoup doit être étudié en ce qui concerne les zones corticales supérieures, et d'autres structures qui sont impliquées dans les réponses comportementales considérées ici. Voici quelques questions concernant les prochaines étapes, au-delà de ce travail:

- Étude et inclusion des pulvinar core et matrix, afin d'ajouter progressivement d'autres

aires corticales du système, et d'exploiter des traitements thalamocorticaux plus sophistiqués

- Étude et inclusion de l'apprentissage thalamocortical (liée au pulvinar), pour fournir le système d'une capacité d'adaptation et d'une mémoire, afin d'apprendre de nouveaux scénarios qui ne sont pas pré-câblés, mais acquis à travers le temps
- Ajout de la synchronisation multi-ordre par l'inclusion des jonctions dans TRN Cela nous permettrait de mieux comprendre la régularisation et la synchronisation thalamocorticales
- Une étude plus détaillée des différentes lésions qui peuvent être exploités, et la perte de performance liée à telle lésion
- Une amélioration de la mise au point actuelle de sorte qu'elle puisse être utilisé dans des circuits en temps réel, comme dans la robotique, par exemple
- La modification du mécanisme du DNF utilisé pour V1, où, au lieu d'un DNF, des cartes d'orientation en compétition doivent être implémentées

Le mystère de la vision est encore un travail en cours. Il faudra encore de nombreuses études, et les efforts combinés de nombreuses personnes pour s'en sortir. Grâce à nos résultats qui étudient le système visuel précoce, et le développement de notre environnement de simulations, nous sommes allés un peu plus loin pour éclairer ce mystère.

Appendix

Other illustrations (simulations)

Here we present a few results from other simulations, just to show that the results shown in the main text are not the only illustrative ones.

The markers have different colors than previously shown. This does not replace the previous markers. There is a difference: with natural images we use different systems, and present them with the markers; while with artificial stimuli the markers represent two different neural populations that collaborate to provide us with the green marker, used for the computation of the degree of goodness of the simulation.

Weizmann database: Eli P-jump

For this simulation, we used the jump in position, done by subject "Eli", from the Weizmann database [9].

Youtube video I: Puppy

For this simulation, we used a video of a corgi pup running to the camera and then sitting down in the position shown in the figure.

Youtube video II: Signature

For this simulation [3], we used a video of Britain's Got Talent: the first audition of the dancing group "Signature"[1].

[1] `http://youtu.be/5PtHsae0bEs`

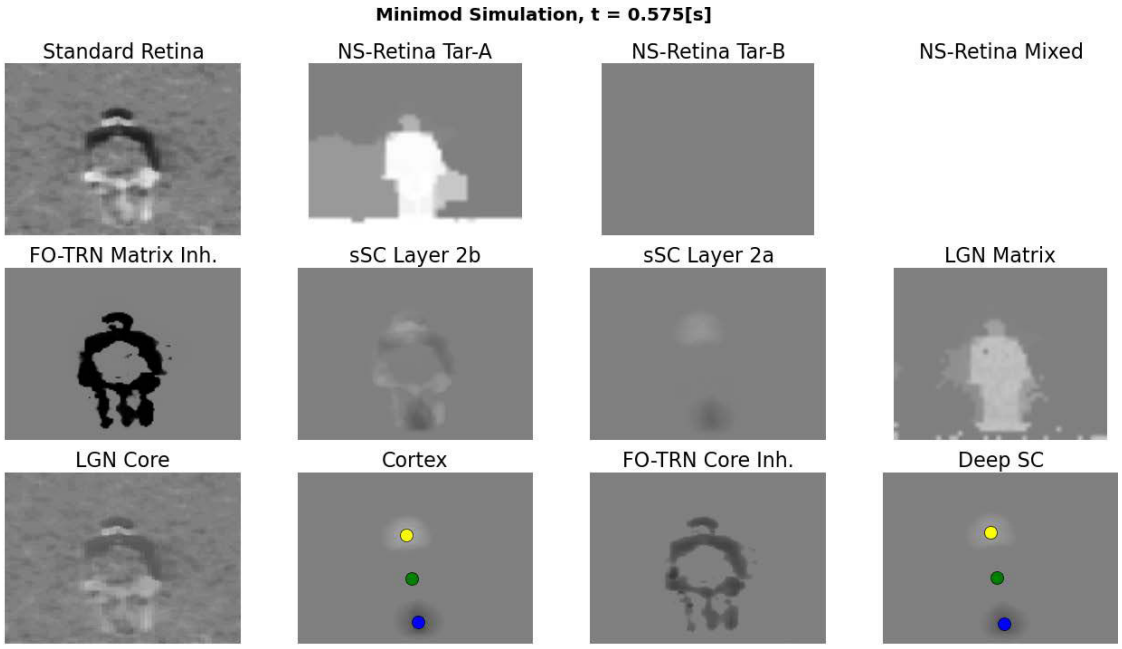

Figure 6.1: **Overview of simulation using Eli P-jump**. Here, the markers represent the average (green) and two DNFs (yellow and blue), representing two populations of neurons that follow positive and negative motion, as explained in 2.1.4. The target area shows only a white image as only one target was taught to the non-standard system.

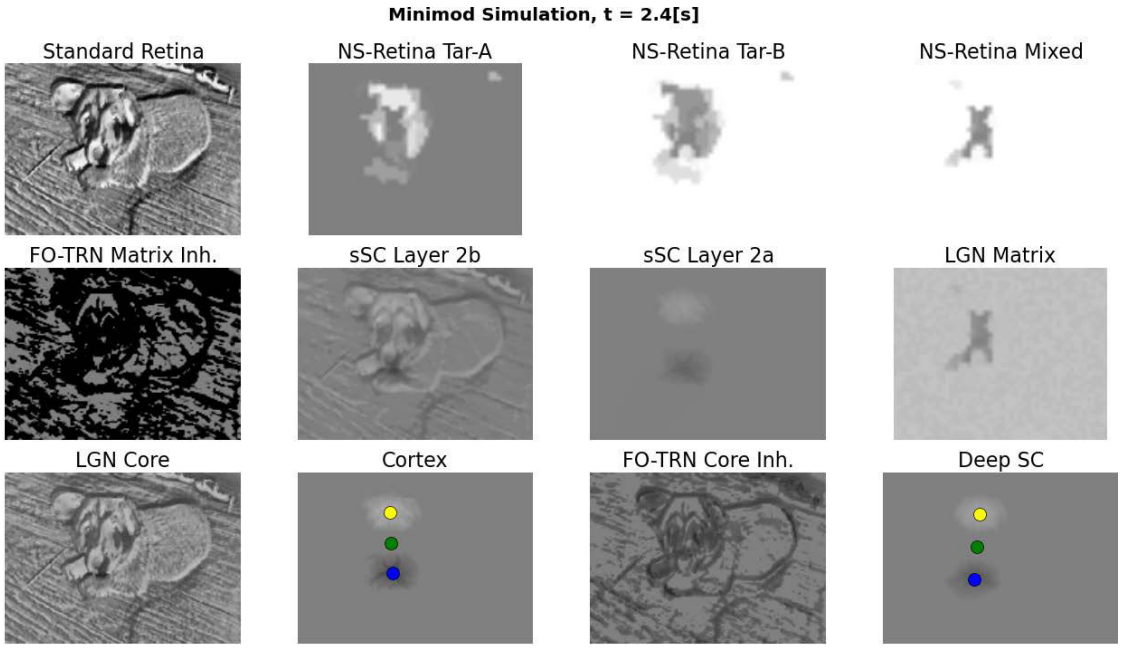

Figure 6.2: **Overview of simulation using the video of a puppy dog**. Here, the markers represent the average (green) and two DNFs (yellow and blue), representing two populations of neurons that follow positive and negative motion, as explained in 2.1.4. The training was done for the pup twice, thus both targets show its information.

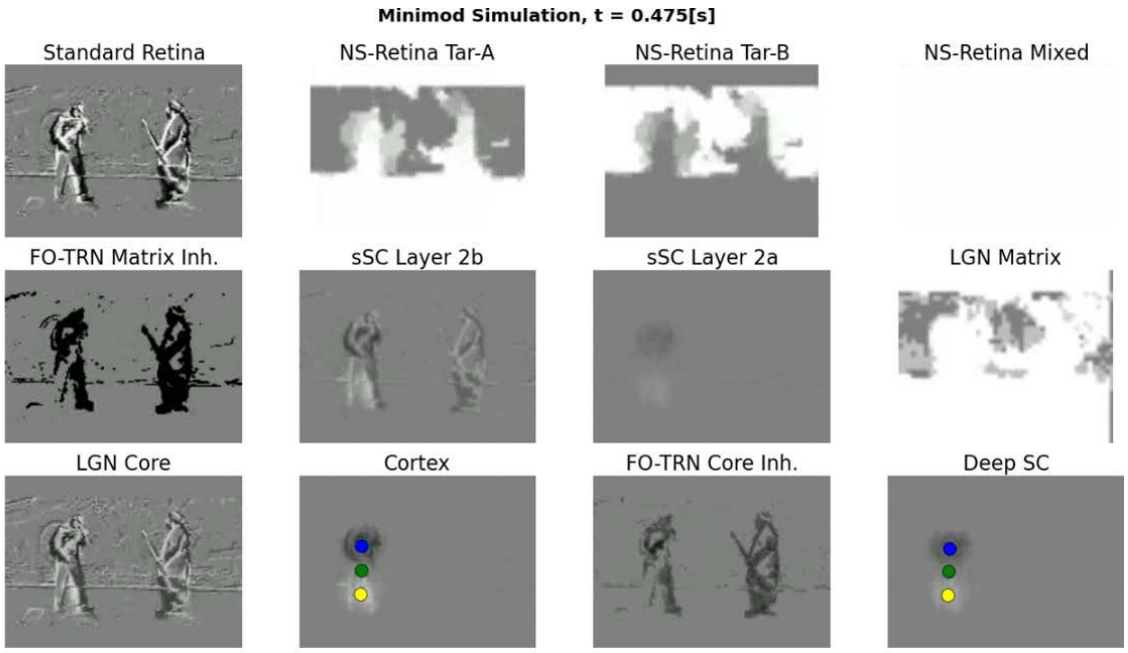

Figure 6.3: **Overview of simulation using the video of Signature**. Here, the markers represent the average (green) and two DNFs (yellow and blue), representing two populations of neurons that follow positive and negative motion, as explained in 2.1.4. The training was done for the dancers, thus both targets show its information, and because the data from two populations is opposed, their addition results in flat activation (homogeneously activated mixed signal).

Publications arising from this work

Scientific Outreach

- F. Alexandre, C. Carvajal, and T. Viéville. Comprendre le système le plus complexe de notre planète ? *Mathématique pour la planète Terre, Un jour une brève*, Dec. 2013.

International Conferences

- C. Carvajal, T. Vieville, and F. Alexandre. Impact of the Konio pathway in the thalamocortical visual system: a modeling study. *BMC Neuroscience*, 14(Suppl 1):P6+, 2013.
- C. Carvajal, T. Viéville, and F. Alexandre. To flee or not to flee? Neural Field dynamics shape information flows in a model of the thalamocortical visual system. In *Bernstein Conference 2013*, 2013.

Research Report

- E. Teftef, M.-J. Escobar, A. Astudillo, C. Carvajal, B. Cessac, A. Palacios, T. Viéville, and F. Alexandre. Modeling non-standard retinal in/out function using computer vision variational methods. Technical Report RR-8217, Inria, Jan. 2013.

National Conferences

- C. Carvajal, T. Viéville, and F. Alexandre. Konio Pathway: An Instinctive Visual Mechanism for Survival and Decision Making? In *NeuroComp/KEOpS'12 workshop beyond the retina: from computational models to outcomes in bioengineering. Focus on architecture and dynamics sustaining information flows in the visuomotor system.*, Bordeaux, France, Oct. 2012.

- E. Teftef, C. Carvajal, T. Viéville, and F. Alexandre. When early vision in the retina attempts to take decisions about visual motion events : the role of konio cells. In *Third International Symposium on Biology of Decision Making*, Paris, France, May 2013. Université Pierre et Marie Curie (Paris 6).
- C. Carvajal, T. Viéville, and F. Alexandre. A modeling study of the dynamic interplay between pathways in the thalamocortical visual system: The Magno and Koniocellular streams case. In *APIL 2014*, Nancy, France, Oct. 2013. Université de Lorraine.

Bibliography

[1] L. F. Abbott and F. S. Chance. Drivers and modulators from push-pull and balanced synaptic input. *Progress in brain research*, 149:147–155, 2005.

[2] B. Ahmed, J. C. Anderson, K. A. Martin, and J. C. Nelson. Map of the synapses onto layer 4 basket cells of the primary visual cortex of the cat. *The Journal of comparative neurology*, 380(2):230–242, Apr. 1997.

[3] F. Alexandre, C. Carvajal, and T. Viéville. Comprendre le système le plus complexe de notre planète ? *Mathématique pour la planète Terre, Un jour une brève*, Dec. 2013.

[4] S. Amari. Dynamics of pattern formation in lateral-inhibition type neural fields. *Biological cybernetics*, 27(2):77–87, Aug. 1977.

[5] A. Angelucci, J. B. Levitt, E. J. Walton, J.-M. M. Hupe, J. Bullier, and J. S. Lund. Circuits for local and global signal integration in primary visual cortex. *The Journal of neuroscience : the official journal of the Society for Neuroscience*, 22(19):8633–8646, Oct. 2002.

[6] G. Aubert and P. Kornprobst. Can the Nonlocal Characterization of Sobolev Spaces by Bourgain et al. Be Useful for Solving Variational Problems? *SIAM Journal on Numerical Analysis*, 47(2):844–860, Jan. 2009.

[7] D. H. Ballard, M. M. Hayhoe, P. K. Pook, and R. P. Rao. Deictic codes for the embodiment of cognition (with commentary). *Behavioral and Brain Sciences*, 20(4), Dec. 1997.

[8] J. Bergstra and Y. Bengio. Random Search for Hyper-parameter Optimization. *J. Mach. Learn. Res.*, 13(1):281–305, Feb. 2012.

[9] M. Blank, L. Gorelick, E. Shechtman, M. Irani, and R. Basri. Actions as space-time shapes. In *Computer Vision, 2005. ICCV 2005. Tenth IEEE International Conference on*, volume 2, pages 1395–1402 Vol. 2, Los Alamitos, CA, USA, Oct. 2005. IEEE.

[10] G. G. Blasdel and J. S. Lund. Termination of afferent axons in macaque striate cortex. *The Journal of Neuroscience*, 3(7):1389–1413, July 1983.

[11] W. H. Bosking, Y. Zhang, B. Schofield, and D. Fitzpatrick. Orientation Selectivity and the Arrangement of Horizontal Connections in Tree Shrew Striate Cortex. *The Journal of Neuroscience*, 17(6):2112–2127, Mar. 1997.

[12] R. Brette, M. Rudolph, T. Carnevale, M. Hines, D. Beeman, J. M. Bower, M. Diesmann, A. Morrison, P. H. Goodman, F. C. Harris, M. Zirpe, T. Natschläger, D. Pecevski, B. Ermentrout, M. Djurfeldt, A. Lansner, O. Rochel, T. Vieville, E. Muller, A. P. Davison, S. El Boustani, and A. Destexhe. Simulation of networks of spiking neurons: a review of tools and strategies. *Journal of computational neuroscience*, 23(3):349–398, Dec. 2007.

[13] C. Büchel and K. J. Friston. Modulation of connectivity in visual pathways by attention: cortical interactions evaluated with structural equation modelling and fMRI. *Cerebral cortex (New York, N.Y. : 1991)*, 7(8):768–778, Dec. 1997.

[14] J. Bullier. Integrated model of visual processing. *Brain research. Brain research reviews*, 36(2-3):96–107, Oct. 2001.

[15] E. M. Callaway. Local circuits in primary visual cortex of the macaque monkey. *Annual Review of Neuroscience*, 21:47–74, 1998.

[16] E. M. Callaway. Structure and function of parallel pathways in the primate early visual system. *Journal of Physiology*, 566:13–19, 2005.

[17] E. M. Callaway and A. K. Wiser. Contributions of individual layer 2-5 spiny neurons to local circuits in macaque primary visual cortex. *Visual neuroscience*, 13(5):907–922, 1996.

[18] M. Carandini. Area V1. *Scholarpedia*, 7(7):12105+, 2012.

[19] C. Carvajal, T. Viéville, and F. Alexandre. Konio Pathway: An Instinctive Visual Mechanism for Survival and Decision Making? In *NeuroComp/KEOpS'12 workshop beyond the retina: from computational models to outcomes in bioengineering. Focus on architecture and dynamics sustaining information flows in the visuomotor system.*, Bordeaux, France, Oct. 2012.

[20] C. Carvajal, T. Viéville, and F. Alexandre. A modeling study of the dynamic interplay between pathways in the thalamocortical visual system: The Magno and Koniocellular streams case. In *APIL 2014*, Nancy, France, Oct. 2013. Université de Lorraine.

[21] C. Carvajal, T. Vieville, and F. Alexandre. Impact of the Konio pathway in the thalamocortical visual system: a modeling study. *BMC Neuroscience*, 14(Suppl 1):P6+, 2013.

[22] C. Carvajal, T. Viéville, and F. Alexandre. To flee or not to flee? Neural Field dynamics shape information flows in a model of the thalamocortical visual system. In *Bernstein Conference 2013*, 2013.

[23] C. Carvajal, T. Viéville, and F. Alexandre. Primitive attentional shifting in a reduced thalamocortical computational model using natural images, in prep. for PLOS ONE.

[24] V. A. Casagrande, F. Yazar, K. D. Jones, and Y. Ding. The morphology of the koniocellular axon pathway in the macaque monkey. *Cerebral cortex (New York, N.Y. : 1991)*, 17(10):2334–2345, Oct. 2007.

[25] B. Cessac. A discrete time neural network model with spiking neurons. Rigorous results on the spontaneous dynamics, June 2007.

[26] B. Cessac, B. Doyon, M. Quoy, and M. Samuelides. Mean-field equations, bifurcation map and route to chaos in discrete time neural networks. *Physica D: Nonlinear Phenomena*, 74(1-2):24–44, July 1994.

[27] B. Cessac, H. Paugam-Moisy, and T. Viéville. Indisputable facts when implementing spiking neuron networks, Mar. 2009.

[28] B. Cessac, H. Rostro, J. C. Vasquez, and T. Viéville. How Gibbs distributions may naturally arise from synaptic adaptation mechanisms. A model-based argumentation, June 2009.

[29] B. Cessac and T. Vieville. Revisiting time discretisation of spiking network models. *BMC Neuroscience*, 8(Suppl 2):P76+, 2007.

[30] E. J. Chichilnisky and R. S. Kalmar. Temporal resolution of ensemble visual motion signals in primate retina. *The Journal of neuroscience : the official journal of the Society for Neuroscience*, 23(17):6681–6689, July 2003.

[31] S. Ciocchi, C. Herry, F. Grenier, S. B. E. Wolff, J. J. Letzkus, I. Vlachos, I. Ehrlich, R. Sprengel, K. Deisseroth, M. B. Stadler, C. Muller, and A. Luthi. Encoding of conditioned fear in central amygdala inhibitory circuits. *Nature*, 468(7321):277–282, Nov. 2010.

[32] R. Cofré and B. Cessac. Dynamics and spike trains statistics in conductance-based Integrate-and-Fire neural networks with chemical and electric synapses. *BMC Neuroscience*, 14(Suppl 1):P58+, Dec. 2012.

[33] S. Coombes. Neural fields. *Scholarpedia*, 1(6):1373+, 2006.

[34] A. Cowey. Visual System: How Does Blindsight Arise? *Curr Biol*, 20(17):R702–R704, Sept. 2010.

[35] F. Crick and C. Koch. Constraints on cortical and thalamic projections: the no-strong-loops hypothesis. *Nature*, 391(6664):245–250, Jan. 1998.

[36] J. D. Crook, C. M. Davenport, B. B. Peterson, O. S. Packer, P. B. Detwiler, and D. M. Dacey. Parallel ON and OFF cone bipolar inputs establish spatially coextensive receptive field structure of blue-yellow ganglion cells in primate retina. *The Journal of neuroscience : the official journal of the Society for Neuroscience*, 29(26):8372–8387, July 2009.

[37] D. Dacey. Origins of Perception: Retinal Ganglion Cell Diversity and the Creation of Parallel Visual Pathways. *The Cognitive Neurosciences III*, page 281, 2004.

[38] D. M. Dacey. Parallel pathways for spectral coding in primate retina. *Annual review of neuroscience*, 23(1):743–775, 2000.

[39] D. M. Dacey and B. B. Lee. The 'blue-on' opponent pathway in primate retina originates from a distinct bistratified ganglion cell type. *Nature*, 367(6465):731–735, Feb. 1994.

[40] B. de Gelder, J. van Honk, and M. Tamietto. Emotion in the brain: of low roads, high roads and roads less travelled. *Nat Rev Neurosci*, 12(7):425, July 2011.

[41] P. Dean, P. Redgrave, and G. W. Westby. Event or emergency? Two response systems in the mammalian superior colliculus. *Trends in neurosciences*, 12(4):137–147, Apr. 1989.

[42] A. Delorme, L. Perrinet, and S. J. Thorpe. Networks of integrate-and-fire neurons using Rank Order Coding B: Spike timing dependent plasticity and emergence of orientation selectivity. *Neurocomputing*, 38-40:539–545, June 2001.

[43] J. T. DesJardin, A. L. Holmes, P. A. Forcelli, C. E. Cole, J. T. Gale, L. L. Wellman, K. Gale, and L. Malkova. Defense-Like Behaviors Evoked by Pharmacological Disinhibition of the Superior Colliculus in the Primate. *The Journal of Neuroscience*, 33(1):150–155, Jan. 2013.

[44] M. C. Dorris, M. Paré, and D. P. Munoz. Neuronal activity in monkey superior colliculus related to the initiation of saccadic eye movements. *The Journal of neuroscience : the official journal of the Society for Neuroscience*, 17(21):8566–8579, Nov. 1997.

[45] J. Dowling. Retina. *Scholarpedia*, 2(12):3487+, 2007.

[46] G. Drion, A. Franci, V. Seutin, and R. Sepulchre. A Novel Phase Portrait for Neuronal Excitability. *PLoS ONE*, 7(8):e41806+, Aug. 2012.

[47] M. J. Escobar. Bio-Inspired Models for Motion Estimation and Analysis: Human action recognition and motion integration. 2009.

[48] D. J. Felleman and D. C. Van Essen. Distributed hierarchical processing in the primate cerebral cortex. *Cerebral cortex (New York, N.Y. : 1991)*, 1(1):1–47, Jan. 1991.

[49] G. D. Field, A. Sher, J. L. Gauthier, M. Greschner, J. Shlens, A. M. Litke, and E. J. Chichilnisky. Spatial properties and functional organization of small bistratified ganglion cells in primate retina. *The Journal of neuroscience : the official journal of the Society for Neuroscience*, 27(48):13261–13272, Nov. 2007.

[50] D. Fitzpatrick, J. S. Lund, and G. G. Blasdel. Intrinsic connections of macaque striate cortex: afferent and efferent connections of lamina 4C. *The Journal of neuroscience : the official journal of the Society for Neuroscience*, 5(12):3329–3349, Dec. 1985.

[51] A. Franci, G. Drion, and R. Sepulchre. An Organizing Center in a Planar Model of Neuronal Excitability. *SIAM Journal on Applied Dynamical Systems*, 11(4):1698–1722, Jan. 2012.

[52] A. Franci, G. Drion, V. Seutin, and R. Sepulchre. A Balance Equation Determines a Switch in Neuronal Excitability. *PLoS Comput Biol*, 9(5):e1003040+, May 2013.

[53] H. R. Friedman and P. S. Goldman-Rakic. Activation of the hippocampus and dentate gyrus by working-memory: a 2-deoxyglucose study of behaving rhesus monkeys. *The Journal of neuroscience : the official journal of the Society for Neuroscience*, 8(12):4693–4706, Dec. 1988.

[54] K. Friston. Functional integration and inference in the brain. *Progress in neurobiology*, 68(2):113–143, Oct. 2002.

[55] K. J. Friston and C. J. Price. Generative models, brain function and neuroimaging. *Scandinavian Journal of Psychology*, 42(3):167–177, July 2001.

[56] Fuensanta and N. Doble. *The Human Eye and Adaptive Optics*, chapter 8. InTech, Jan. 2012.

[57] N. J. Gandhi and H. A. Katnani. Motor Functions of the Superior Colliculus. *Annual Review of Neuroscience*, 34(1):205–231, 2011.

[58] J. L. Gauthier, G. D. Field, A. Sher, M. Greschner, J. Shlens, A. M. Litke, and E. J. Chichilnisky. Receptive fields in primate retina are coordinated to sample visual space more uniformly. *PLoS biology*, 7(4):e63+, Apr. 2009.

[59] M. S. Gazzaniga. *Cognitive neuroscience : the biology of the mind*. Norton, Mar. 2002.

[60] P. Girard and J. Bullier. Visual activity in area V2 during reversible inactivation of area 17 in the macaque monkey. *Journal of neurophysiology*, 62(6):1287–1302, Dec. 1989.

[61] T. Gollisch and M. Meister. Rapid neural coding in the retina with relative spike latencies. *Science (New York, N.Y.)*, 319(5866):1108–1111, Feb. 2008.

[62] T. Gollisch and M. Meister. Eye Smarter than Scientists Believed: Neural Computations in Circuits of the Retina. *Neuron*, 65(2):150–164, Jan. 2010.

[63] M. A. Goodale and Milner. Separate visual pathways for perception and action. *Trends in Neurosciences*, 15(1):20–25, Jan. 1992.

[64] R. Granger and R. Hearn. Models of thalamocortical system. *Scholarpedia*, 2(11):1796+, 2007.

[65] M. Greschner, J. Shlens, C. Bakolitsa, G. D. Field, J. L. Gauthier, L. H. Jepson, A. Sher, A. M. Litke, and E. J. Chichilnisky. Correlated firing among major ganglion cell types in primate retina.

[66] F. Grimbert. *Mesoscopic models of cortical structures*. PhD thesis, University of Nice Sophia-Antipolis, Feb. 2008.

[67] S. Grossberg and M. Versace. Spikes, synchrony, and attentive learning by laminar thalamocortical circuits. *Brain research*, 1218:278–312, July 2008.

[68] R. W. Guillery and J. K. Harting. Structure and connections of the thalamic reticular nucleus: Advancing views over half a century. *The Journal of comparative neurology*, 463(4):360–371, Sept. 2003.

[69] D. E. Hannula, D. J. Simons, and N. J. Cohen. Imaging implicit perception: promise and pitfalls. *Nature Reviews Neuroscience*, 6(3):247–255, Mar. 2005.

[70] S. H. Hendry and R. C. Reid. The Koniocellular Pathway in Primate Vision. *Annual Review of Neuroscience*, 23(1):127–153, 2000.

[71] S. H. Hendry and T. Yoshioka. A neurochemically distinct third channel in the macaque dorsal lateral geniculate nucleus. *Science (New York, N.Y.)*, 264(5158):575–577, Apr. 1994.

[72] J. L. Hindmarsh and R. M. Rose. A model of neuronal bursting using three coupled first order differential equations. *Proceedings of the Royal Society of London. Series B, Containing papers of a Biological character. Royal Society (Great Britain)*, 221(1222):87–102, Mar. 1984.

[73] S. Hochstein and R. M. Shapley. Quantitative analysis of retinal ganglion cell classifications. *The Journal of physiology*, 262(2):237–264, Nov. 1976.

[74] D. H. Hubel and T. N. Wiesel. Receptive fields, binocular interaction and functional architecture in the cat's visual cortex. *The Journal of physiology*, 160:106–154, Jan. 1962.

[75] A. Hutt and F. M. Atay. Effects of distributed transmission speeds on propagating activity in neural populations. *Physical review. E, Statistical, nonlinear, and soft matter physics*, 73(2 Pt 1), Feb. 2006.

[76] A. Hyvärinen, J. Hurri, and P. O. Hoyer. *Natural Image Statistics.* Springer-Verlag, 2009.

[77] G. E. Irvin, T. T. Norton, M. A. Sesma, and V. A. Casagrande. W-like response properties of interlaminar zone cells in the lateral geniculate nucleus of a primate (Galago crassicaudatus). *Brain research*, 362(2):254–270, Jan. 1986.

[78] L. A. Isbell. Snakes as agents of evolutionary change in primate brains. *Journal of human evolution*, 51(1):1–35, July 2006.

[79] E. Izhikevich and R. FitzHugh. FitzHugh-Nagumo model. *Scholarpedia*, 1(9):1349+, 2006.

[80] E. G. Jones. Viewpoint: the core and matrix of thalamic organization. *Neuroscience*, 85(2):331–345, July 1998.

[81] E. G. Jones. The thalamic matrix and thalamocortical synchrony. *Trends in neurosciences*, 24(10):595–601, Oct. 2001.

[82] E. G. Jones. Thalamic circuitry and thalamocortical synchrony. *Philosophical transactions of the Royal Society of London. Series B, Biological sciences*, 357(1428):1659–1673, Dec. 2002.

[83] E. Kandel, J. Schwartz, and T. Jessell. *Principles of Neural Science.* McGraw-Hill Medical, 4 edition, Jan. 2000.

[84] E. Kaplan and E. Benardete. The dynamics of primate retinal ganglion cells. *Progress in brain research*, 134:17–34, 2001.

[85] H. Kirchner and S. J. Thorpe. Ultra-rapid object detection with saccadic eye movements: Visual processing speed revisited. *Vision Research*, 46(11):1762–1776, May 2006.

[86] M. Koivisto, H. Railo, A. Revonsuo, S. Vanni, and N. Salminen-Vaparanta. Recurrent Processing in V1/V2 Contributes to Categorization of Natural Scenes. *The Journal of Neuroscience*, 31(7):2488–2492, Feb. 2011.

[87] C. I. Kolmac and J. Mitrofanis. Organisation of the reticular thalamic projection to the intralaminar and midline nuclei in rats. *J. Comp. Neurol.*, 377(2):165–178, Jan. 1997.

[88] R. J. Krauzlis. The Control of Voluntary Eye Movements: New Perspectives. *The Neuroscientist*, 11(2):124–137, Apr. 2005.

[89] J. Kremers, B. B. Lee, J. Pokorny, and V. C. Smith. Responses of macaque ganglion cells and human observers to compound periodic waveforms. *Vision Research*, 33(14):1997–2011, Sept. 1993.

[90] Y.-W. W. Lam and S. M. Sherman. Functional organization of the thalamic input to the thalamic reticular nucleus. *The Journal of neuroscience : the official journal of the Society for Neuroscience*, 31(18):6791–6799, May 2011.

[91] V. Lamme and P. R. Roelfsema. The distinct modes of vision offered by feedforward and recurrent processing. *Trends in Neurosciences*, 23(11):571–579, Nov. 2000.

[92] V. A. Lamme. Blindsight: the role of feedforward and feedback corticocortical connections. *Acta psychologica*, 107(1-3):209–228, Apr. 2001.

[93] V. A. F. Lamme, H. Super, and H. Spekreijse. Feedforward, horizontal, and feedback processing in the visual cortex. *Current Opinion in Neurobiology*, 8(4):529–535, Aug. 1998.

[94] C. E. Landisman, M. A. Long, M. Beierlein, M. R. Deans, D. L. Paul, and B. W. Connors. Electrical synapses in the thalamic reticular nucleus. *The Journal of neuroscience : the official journal of the Society for Neuroscience*, 22(3):1002–1009, Feb. 2002.

[95] L. Lapicque. Recherches quantitatives sur l'excitation electrique des nerfs traitee comme une polarization. *J Physiol Pathol Gen*, 9:620–635, 1907.

[96] J. LeDoux. The amygdala. *Current biology : CB*, 17(20):R868–R874, Oct. 2007.

[97] C. Lee, W. H. Rohrer, and D. L. Sparks. Population coding of saccadic eye movements by neurons in the superior colliculus. *Nature*, 332(6162):357–360, Mar. 1988.

[98] R. J. Leigh and D. S. Zee. *The neurology of eye movements*. Oxford University Press, 4 edition, Apr. 2006.

[99] J. Lettvin, H. Maturana, W. McCulloch, and W. Pitts. What the Frog's Eye Tells the Frog's Brain. *Proceedings of the IRE*, 47(11):1940–1951, Nov. 1959.

[100] J. Y. Lin, S. O. Murray, and G. M. Boynton. Capture of Attention to Threatening Stimuli without Perceptual Awareness. *Current Biology*, 19(13):1118–1122, Sept. 2014.

[101] L. Lünenburger, W. Lindner, and K.-P. Hoffmann. *Neural activity in the primate superior colliculus and saccadic reaction times in double-step experiments*, volume 142, pages 91–107. Elsevier, 2003.

[102] D. C. Lyon, J. J. Nassi, and E. M. Callaway. A Disynaptic Relay from Superior Colliculus to Dorsal Stream Visual Cortex in Macaque Monkey. *Neuron*, 65(2):270–279, Jan. 2010.

[103] H. Markram, M. Toledo-Rodriguez, Y. Wang, A. Gupta, G. Silberberg, and C. Wu. Interneurons of the neocortical inhibitory system. *Nature reviews. Neuroscience*, 5(10):793–807, Oct. 2004.

[104] D. Marr. *Vision*. W.H.Freeman & Co Ltd, first edition edition, July 1982.

[105] R. H. Masland. Neuronal diversity in the retina. *Current opinion in neurobiology*, 11(4):431–436, Aug. 2001.

[106] R. H. Masland. The fundamental plan of the retina. *Nature neuroscience*, 4(9):877–886, Sept. 2001.

[107] R. H. Masland and P. R. Martin. The unsolved mystery of vision. *Current Biology*, 17(15):R577–R582, Aug. 2007.

[108] J. H. Maunsell, G. M. Ghose, J. A. Assad, C. J. McAdams, C. E. Boudreau, and B. D. Noerager. Visual response latencies of magnocellular and parvocellular LGN neurons in macaque monkeys. *Visual neuroscience*, 16(1):1–14, 1999.

[109] P. J. May. *The mammalian superior colliculus: laminar structure and connections*, volume 151, pages 321–378. Elsevier, 2006.

[110] K. McAlonan and V. J. Brown. The thalamic reticular nucleus: more than a sensory nucleus? *The Neuroscientist : a review journal bringing neurobiology, neurology and psychiatry*, 8(4):302–305, Aug. 2002.

[111] K. McAlonan, J. Cavanaugh, and R. H. Wurtz. Attentional modulation of thalamic reticular neurons. *The Journal of neuroscience : the official journal of the Society for Neuroscience*, 26(16):4444–4450, Apr. 2006.

[112] B. A. McGuire, C. D. Gilbert, P. K. Rivlin, and T. N. Wiesel. Targets of horizontal connections in macaque primary visual cortex. *The Journal of comparative neurology*, 305(3):370–392, Mar. 1991.

[113] M. Meister and M. J. Berry. The Neural Code of the Retina. *Neuron*, 22(3):435–450, Jan. 2015.

[114] B. K. Min. A thalamic reticular networking model of consciousness. *Theoretical Biology and Medical Modelling*, 7(1):10+, Mar. 2010.

[115] J. J. Nassi and E. M. Callaway. Parallel processing strategies of the primate visual system. *Nat. Rev. Neurosci.*, 10(5):360–372, 2009.

[116] L. G. Nowak and J. Bullier. The Timing of Information Transfer in the Visual System. In K. S. Rockland, J. H. Kaas, and A. Peters, editors, *Extrastriate Cortex in Primates*, volume 12 of *Cerebral Cortex*, pages 205–241. Plenum, New York, 1997.

[117] B. P. Olveczky, S. A. Baccus, and M. Meister. Segregation of object and background motion in the retina. *Nature*, 423(6938):401–408, May 2003.

[118] G. Osterberg. *Topography of the Layer of Rods and Cones in the Human Retina*. Acta ophthalmologica. Supplementum. A. Busck, 1935.

[119] P.-Y. Oudeyer. *Aux sources de la parole : auto-organisation et évolution*. O. Jacob, 2013.

[120] L. Perrinet, A. Delorme, M. Samuelides, and S. J. Thorpe. Networks of integrate-and-fire neuron using rank order coding A: How to implement spike time dependent Hebbian plasticity. *Neurocomputing*, 38-40:817–822, June 2001.

[121] S. E. Petersen, D. L. Robinson, and W. Keys. Pulvinar nuclei of the behaving rhesus monkey: visual responses and their modulation. *Journal of neurophysiology*, 54(4):867–886, Oct. 1985.

[122] J. W. Pillow, L. Paninski, V. J. Uzzell, E. P. Simoncelli, and E. J. Chichilnisky. Prediction and Decoding of Retinal Ganglion Cell Responses with a Probabilistic Spiking Model. *The Journal of Neuroscience*, 25(47):11003–11013, Nov. 2005.

[123] D. Purves. *Neuroscience*. Sinauer Associates, 2001.

[124] R. D. Raizada and S. Grossberg. Towards a theory of the laminar architecture of cerebral cortex: computational clues from the visual system. *Cerebral cortex (New York, N.Y. : 1991)*, 13(1):100–113, Jan. 2003.

[125] R. P. N. Rao and D. H. Ballard. Predictive coding in the visual cortex: a functional interpretation of some extra-classical receptive-field effects. *Nature Neuroscience*, 2(1):79–87, Jan. 1999.

[126] P. Redgrave. Basal ganglia. *Scholarpedia*, 2(6):1825+, 2007.

[127] F. Rieke. *Spikes : exploring the neural code*. MIT, June 1999.

[128] D. L. Robinson and J. W. McClurkin. The visual superior colliculus and pulvinar. *Reviews of oculomotor research*, 3:337–360, 1989.

[129] O. Rochel. *Une approche événementielle pour la modélisation et la simulation de réseaux de neurones impulsionnels*. PhD thesis, 2004. Thèse de doctorat dirigée par Alexandre, Frédéric Informatique Nancy 1 2004.

[130] K. S. Rockland and D. N. Pandya. Laminar origins and terminations of cortical connections of the occipital lobe in the rhesus monkey. *Brain research*, 179(1):3–20, Dec. 1979.

[131] K. S. Rockland and A. Virga. Terminal arbors of individual " Feedback" axons projecting from area V2 to V1 in the macaque monkey: A study using immunohisto-

chemistry of anterogradely transported Phaseolus vulgaris-leucoagglutinin. *J. Comp. Neurol.*, 285(1):54–72, July 1989.

[132] N. Rougier and J. Fix. DANA: Distributed numerical and adaptive modelling framework. *Network*, 23(4):237–253, Sept. 2012.

[133] N. P. Rougier. Dynamic neural field with local inhibition. *Biological cybernetics*, 94(3):169–179, Mar. 2006.

[134] N. P. Rougier and A. Hutt. Synchronous and asynchronous evaluation of dynamic neural fields. *Journal of Difference Equations and Applications*, 17(8):1119–1133, Jan. 2010.

[135] N. P. Rougier and J. Vitay. Emergence of attention within a neural population. *Neural networks : the official journal of the International Neural Network Society*, 19(5):573–581, June 2006.

[136] G. A. Rousselet, S. J. Thorpe, and M. Fabre-Thorpe. How parallel is visual processing in the ventral pathway? *Trends in cognitive sciences*, 8(8):363–370, Aug. 2004.

[137] N. F. Rulkov. Modeling of spiking-bursting neural behavior using two-dimensional map. *Physical review. E, Statistical, nonlinear, and soft matter physics*, 65(4 Pt 1), Apr. 2002.

[138] Y. B. Saalmann and S. Kastner. Gain control in the visual thalamus during perception and cognition. *Current Opinion in Neurobiology*, 19(4):408–414, Aug. 2009.

[139] P. Sah, E. S. L. Faber, M. L. de Armentia, and J. Power. The Amygdaloid Complex: Anatomy and Physiology. *Physiological Reviews*, 83(3):803–834, July 2003.

[140] P. A. Salin and J. Bullier. Corticocortical connections in the visual system: structure and function. *Physiological reviews*, 75(1):107–154, Jan. 1995.

[141] J. H. Sandell and P. H. Schiller. Effect of cooling area 18 on striate cortex cells in the squirrel monkey. *Journal of Neurophysiology*, 48(1):38–48, July 1982.

[142] K. E. Schmidt, R. Goebel, S. Löwel, and W. Singer. The perceptual grouping criterion of colinearity is reflected by anisotropies of connections in the primary visual cortex. *The European journal of neuroscience*, 9(5):1083–1089, May 1997.

[143] M. T. Schmolesky, Y. Wang, D. P. Hanes, K. G. Thompson, S. Leutgeb, J. D. Schall, and A. G. Leventhal. Signal timing across the macaque visual system. *Journal of neurophysiology*, 79(6):3272–3278, June 1998.

[144] G. Schwartz and M. J. Berry. Sophisticated temporal pattern recognition in retinal ganglion cells. *Journal of neurophysiology*, 99(4):1787–1798, Apr. 2008.

[145] K. Sergerie, C. Chochol, and J. L. Armony. The role of the amygdala in emotional processing: a quantitative meta-analysis of functional neuroimaging studies. *Neuroscience and biobehavioral reviews*, 32(4):811–830, 2008.

[146] S. Sherman. Thalamus. *Scholarpedia*, 1(9):1583+, 2006.

[147] S. M. Sherman. Dual response modes in lateral geniculate neurons: mechanisms and functions. *Visual neuroscience*, 13(2):205–213, 1996.

[148] S. M. Sherman. Tonic and burst firing: dual modes of thalamocortical relay. *Trends in neurosciences*, 24(2):122–126, Feb. 2001.

[149] S. M. Sherman. The thalamus is more than just a relay. *Current opinion in neurobiology*, 17(4):417–422, Aug. 2007.

[150] S. M. Sherman and R. W. Guillery. Functional organization of thalamocortical relays. *J. Neurophysiol.*, 76:1367–1395, 1996.

[151] S. M. Sherman and R. W. Guillery. On the actions that one nerve cell can have on another: Distinguishing " drivers" from " modulators". *Proceedings of the National Academy of Sciences*, 95(12):7121–7126, June 1998.

[152] S. M. Sherman and R. W. Guillery. *Exploring the thalamus*. Academic Press, 2001.

[153] S. M. Sherman and R. W. Guillery. The role of the thalamus in the flow of information to the cortex. *Philosophical Transactions of the Royal Society B: Biological Sciences*, 357(1428):1695–1708, Dec. 2002.

[154] S. M. Sherman and R. W. Guillery. *Exploring the thalamus and its role in cortical function*. MIT Press, 2006.

[155] J. Shlens, F. Rieke, and E. Chichilnisky. Synchronized firing in the retina. *Current Opinion in Neurobiology*, Oct. 2008.

[156] A. M. Sillito, H. E. Jones, G. L. Gerstein, and D. C. West. Feature-linked synchronization of thalamic relay cell firing induced by feedback from the visual cortex. *Nature*, 369(6480):479–482, June 1994.

[157] V. S. Sohal and J. R. Huguenard. Inhibitory interconnections control burst pattern and emergent network synchrony in reticular thalamus. *The Journal of neuroscience : the official journal of the Society for Neuroscience*, 23(26):8978–8988, Oct. 2003.

[158] L. H. Somerville, H. Kim, T. Johnstone, A. L. Alexander, and P. J. Whalen. Human amygdala responses during presentation of happy and neutral faces: correlations with state anxiety. *Biological psychiatry*, 55(9):897–903, May 2004.

[159] F. S. Soo, G. W. Schwartz, K. Sadeghi, and M. J. Berry. Fine Spatial Information Represented in a Population of Retinal Ganglion Cells. *The Journal of Neuroscience*, 31(6):2145–2155, Feb. 2011.

[160] P. Sterling. *How retinal circuits optimize the transfer of visual information*, chapter 17, pages 234–259. MIT Press, Cambridge MA, 2004.

[161] K. J. Stratford, K. Tarczy-Hornoch, K. A. Martin, N. J. Bannister, and J. J. Jack. Excitatory synaptic inputs to spiny stellate cells in cat visual cortex. *Nature*, 382(6588):258–261, July 1996.

[162] M. Subbarao. Bounds on Time-to-Collision and Rotational Component from First-Order Derivatives of Image Flow. *Computer Vision, Graphics, And Image Processing*, 52(3):329–341, June 1990.

[163] G. Tamás, P. Somogyi, and E. H. Buhl. Differentially interconnected networks of GABAergic interneurons in the visual cortex of the cat. *The Journal of neuroscience : the official journal of the Society for Neuroscience*, 18(11):4255–4270, June 1998.

[164] M. Tamietto and B. de Gelder. Neural bases of the non-conscious perception of emotional signals. *Nature reviews. Neuroscience*, 11(10):697–709, Oct. 2010.

[165] W. Taouali, F. Alexandre, A. Hutt, and N. P. Rougier. Asynchronous Evaluation as an Efficient and Natural Way to Compute Neural Networks. In *7th International Conference of Numerical Analysis and Applied Mathematics - ICNAAM 2009*, volume 1168, pp. 554-558 of *AIP Conference Proceedings*, Rethymno, Greece, 2009.

[166] J. G. Taylor. Towards the networks of the brain: from brain imaging to consciousness. *Neural Networks*, 12:943–959, 1999.

[167] E. Teftef, C. Carvajal, T. Viéville, and F. Alexandre. When early vision in the retina attempts to take decisions about visual motion events : the role of konio cells. In *Third International Symposium on Biology of Decision Making*, Paris, France, May 2013. Université Pierre et Marie Curie (Paris 6).

[168] E. Teftef, M.-J. Escobar, A. Astudillo, C. Carvajal, B. Cessac, A. Palacios, T. Viéville, and F. Alexandre. Modeling non-standard retinal in/out function using computer vision variational methods. Technical Report RR-8217, Inria, Jan. 2013.

[169] W. M. Thorburn. The Myth of Occam's Razor. *Mind*, 27(107):345–353, 1918.

[170] S. Thorpe, D. Fize, and C. Marlot. Speed of processing in the human visual system. *Nature*, 381(6582):520–522, June 1996.

[171] S. J. Thorpe and M. Fabre-Thorpe. Neuroscience. Seeking categories in the brain. *Science (New York, N.Y.)*, 291(5502):260–263, Jan. 2001.

[172] A. M. Treisman. Selective Attention In Man. *British medical bulletin*, 20(1):12–16, Jan. 1964.

[173] Y. D. Van der Werf, M. P. Witter, and H. J. Groenewegen. The intralaminar and midline nuclei of the thalamus. Anatomical and functional evidence for participation in processes of arousal and awareness. *Brain research. Brain research reviews*, 39(2-3):107–140, Sept. 2002.

[174] D. C. Van Essen, C. H. Anderson, and D. J. Felleman. Information processing in the primate visual system: an integrated systems perspective. *Science (New York, N.Y.)*, 255(5043):419–423, Jan. 1992.

[175] D. C. Van Essen, W. T. Newsome, J. H. Maunsell, and J. L. Bixby. The projections from striate cortex (V1) to areas V2 and V3 in the macaque monkey: asymmetries, areal boundaries, and patchy connections. *The Journal of comparative neurology*, 244(4):451–480, Feb. 1986.

[176] Q. Van Le, L. A. Isbell, J. Matsumoto, M. Nguyen, E. Hori, R. S. Maior, C. Tomaz, A. H. Tran, T. Ono, and H. Nishijo. Pulvinar neurons reveal neurobiological evidence

of past selection for rapid detection of snakes. *Proceedings of the National Academy of Sciences*, 110(47):19000–19005, Nov. 2013.

[177] R. VanRullen and S. J. Thorpe. The time course of visual processing: from early perception to decision-making. *Journal of cognitive neuroscience*, 13(4):454–461, May 2001.

[178] F. J. Varela. *Invitation aux sciences cognitives*. Seuil, 1996.

[179] T. Viéville and S. Crahay. Using an Hebbian Learning Rule for Multi-Class SVM Classifiers. 17(3):271–287, 2004.

[180] T. Vieville and P. Kornprobst. Modeling Cortical Maps with Feed-Backs. In *Neural Networks, 2006. IJCNN '06. International Joint Conference on*, pages 110–117. IEEE.

[181] S. Vijayan and N. J. Kopell. Thalamic model of awake alpha oscillations and implications for stimulus processing. *Proceedings of the National Academy of Sciences*, 109(45):18553–18558, Nov. 2012.

[182] P. Vuilleumier. How brains beware: neural mechanisms of emotional attention. *Trends in cognitive sciences*, 9(12):585–594, Dec. 2005.

[183] M. Wechselberger. Canards. *Scholarpedia*, 2(4):1356+, 2007.

[184] F. S. Werblin. The retinal hypercircuit: a repeating synaptic interactive motif underlying visual function. *The Journal of physiology*, 589(Pt 15):3691–3702, Aug. 2011.

[185] H. R. Wilson and J. D. Cowan. A mathematical theory of the functional dynamics of cortical and thalamic nervous tissue. *Kybernetik*, 13(2):55–80, Sept. 1973.

[186] A. Wohrer. *Model and large-scale simulator of a biological retina, with contrast gain control*. PhD thesis, 2008. Thèse de doctorat dirigée par Kornprobst, Pierre Automatique, traitement du signal et des images Nice 2008.

[187] A. Wohrer and P. Kornprobst. Virtual Retina: A biological retina model and simulator, with contrast gain control. *Journal of Computational Neuroscience*, 26(2):219–249, Apr. 2009.

[188] R. H. Wurtz and J. E. Albano. Visual-motor function of the primate superior colliculus. *Annual review of neuroscience*, 3:189–226, 1980.

[189] X. Xu, J. M. Ichida, J. D. Allison, J. D. Boyd, A. B. Bonds, and V. A. Casagrande. A comparison of koniocellular, magnocellular and parvocellular receptive field properties in the lateral geniculate nucleus of the owl monkey (Aotus trivirgatus). *The Journal of physiology*, 531(Pt 1):203–218, Feb. 2001.

[190] A. L. Yarbus. *Eye Movements and Vision*. New York: Plenum Press, 1967.

[191] S. Zeki and S. Shipp. The functional logic of cortical connections. *Nature*, 335(6188):311–317, Sept. 1988.